

Lepton Mixing in A_5 Family Symmetry and Generalized CP

Cai-Chang Li*, Gui-Jun Ding†

*Department of Modern Physics, University of Science and Technology of China,
Hefei, Anhui 230026, China*

Abstract

We study lepton mixing patterns which can be derived from the A_5 family symmetry and generalized CP. We find five phenomenologically interesting mixing patterns for which one column of the PMNS matrix is $(\sqrt{\frac{5+\sqrt{5}}{10}}, \frac{1}{\sqrt{5+\sqrt{5}}}, \frac{1}{\sqrt{5+\sqrt{5}}})^T$ (the first column of the golden ratio mixing), $(\sqrt{\frac{5-\sqrt{5}}{10}}, \frac{1}{\sqrt{5-\sqrt{5}}}, \frac{1}{\sqrt{5-\sqrt{5}}})^T$ (the second column of the golden ratio mixing), $(1, 1, 1)^T/\sqrt{3}$ or $(\sqrt{5}+1, -2, \sqrt{5}-1)^T/4$. The three lepton mixing angles are determined in terms of a single real parameter θ , and agreement with experimental data can be achieved for certain values of θ . The Dirac CP violating phase is predicted to be trivial or maximal while Majorana phases are trivial. We construct a supersymmetric model based on A_5 family symmetry and generalized CP. The lepton mixing is exactly the golden ratio pattern at leading order, and the mixing patterns of case III and case IV are reproduced after higher order corrections are considered.

*E-mail: lcc0915@mail.ustc.edu.cn

†E-mail: dinggj@ustc.edu.cn

1 Introduction

In the standard three flavor neutrino oscillation paradigm, lepton flavor mixing is described by the so-called Pontecorvo-Maki-Nakagawa-Sakata (PMNS) matrix U_{PMNS} which is a 3×3 unitary matrix [1]. U_{PMNS} contains three mixing angles θ_{12} , θ_{13} , θ_{23} and one Dirac CP violating phase δ_{CP} . There are two more Majorana CP phases if neutrinos are Majorana particles. With the measurement of the last mixing angle θ_{13} by Daya Bay [2], RENO [3] and Double Chooz [4], all three lepton mixing angles have been measured with good accuracy in neutrino oscillation experiments [5–7]. Recently T2K has reported a slight preference for δ_{CP} close to $3\pi/2$ [8], when the data are combined with the measurements of the reactor experiments. The present global fit to neutrino data also indicates nontrivial values of δ_{CP} [5–7]. However, the values of the both Majorana phases are unknown so far. Search for leptonic CP violation via the determination of δ_{CP} is one of the major goals of future long-baseline experiments such as the proposed LBNE [9], LBNO [10] and HyperKamiokande [11].

Now it is established that both neutrino and charged lepton mass matrices have residual flavor symmetries determined by lepton flavor mixing, and vice versa residual flavor symmetries in the mass matrices can determine the lepton mixing matrix up to Majorana phases and permutations of rows and columns [12]. Inspired by the fact, it is assumed that the residual flavor symmetries arise from a underlying flavor symmetry group G_f which is usually chosen to be a finite and non-abelian subgroup of $U(3)$. In the past years, much effort has been devoted to the discussion of lepton flavor mixing from a discrete flavor symmetry G_f and its breaking [13]. It is surprising that the mixing patterns achievable in this way are quite limited, the PMNS matrix can only be of the trimaximal form to accommodate the experimental data and the Dirac phase is trivial [14].

Beside residual flavor symmetries, neutrino and charged lepton mass matrices have residual CP symmetries [15,16]. Analogous to residual flavor symmetries, residual CP symmetries also impose strong constraints on the mass matrices and therefore allow us to reconstruct the lepton mixing matrix [15]. A simple example is the well-known $\mu - \tau$ reflection symmetry [17] which predicts maximal atmospheric mixing angle θ_{23} and maximal Dirac CP phase. It is natural to conjecture that there is a CP symmetry H_{CP} (also called generalized CP symmetry) at high energy scale, which is broken down to the residual CP symmetries at low energy. Note that the effects of CP symmetry on the fermion mass matrix have been discussed several decades ago [18,19].

Recently it is proposed to predict the lepton mixing angles and CP phases by combining a discrete flavor symmetry G_f with a CP symmetry H_{CP} [20,21]. H_{CP} has to be compatible with G_f such that the possible forms of the CP transformations are strongly constrained. It has been proved that the mathematical structure of the group comprising G_f and H_{CP} is in general a semi-direct product $G_f \rtimes H_{CP}$ [20]. In this framework, the flavor symmetry G_f is broken down to different abelian subgroups G_ν and G_l in the neutrino and charged lepton sectors respectively, and H_{CP} is broken into residual CP symmetry H_{CP}^ν and H_{CP}^l respectively. The mismatch between the remnant symmetries $G_\nu \rtimes H_{CP}^\nu$ and $G_l \rtimes H_{CP}^l$ generates the PMNS matrix. Neutrinos are generically assumed to be Majorana particles. As a consequence, G_ν can only be a K_4 or Z_2 subgroup of G_f . In the case that $G_\nu = K_4$ and G_l is capable of distinguishing the three generations (i.e., G_l can not be smaller than Z_3), all lepton mixing parameters including the Majorana phases would be completely fixed by residual symmetries once the CP symmetry is considered. In this way, both Dirac and Majorana CP violating phases are found to be conserved in the context of $\Delta(6n^2)$ family symmetry combined with generalized CP [22]. Recently a bottom up analysis of the remnant K_4 flavor symmetry and CP symmetry in the neutrino sector has been performed [16]. On the other hand, if $G_\nu = Z_2$ and a CP symmetry is preserved in the neutrino sector, only

one column of the PMNS matrix can be fixed and all lepton mixing parameters depend on one single real parameter θ . Along this line, the family symmetries A_4 [23], S_4 [20, 24–28], T' [29], $\Delta(48)$ [30], $\Delta(96)$ [31], $\Delta(3n^2)$ [32] and $\Delta(6n^2)$ [32, 33] which are combined with the corresponding generalized CP symmetries have been investigated already. It is found that CP phases can only be trivial or maximal in simple family symmetries A_4 [23] and S_4 [20, 24–28] while $\Delta(48)$ [30] and $\Delta(96)$ [31] (also $\Delta(3n^2)$ and $\Delta(6n^2)$ [32, 33]) family symmetries admit mixing patterns in which all CP phases nontrivially depend on the parameter θ . In addition, some models with both flavor and CP symmetries have been constructed [24–28, 30]. Last but not least, if remnant symmetries in the neutrino and charged lepton sectors are $K_4 \rtimes H_{CP}^\nu$ and $Z_2 \times H_{CP}^l$ respectively, then the PMNS matrix is also predicted in terms of the parameter θ and one row instead of one column would be fixed [28, 33].

It is known that the flavor symmetry group should be of the von Dyck type [34]. The finite von Dyck groups include S_3 , A_4 , S_4 , A_5 and dihedral groups [35]. Since S_3 and dihedral groups don't have irreducible three dimensional representations, they are not suitable as flavor symmetry otherwise two mixing angles would vanish. The phenomenological consequences of A_4 and S_4 flavor symmetries combined with generalized CP have been studied [20, 23–28]. In the present work, we shall investigate the A_5 flavor symmetry and CP symmetry. We shall perform a model independent analysis of possible lepton flavor mixing obtained from breaking of the original symmetry $A_5 \rtimes H_{CP}$. We find five phenomenologically interesting mixing patterns summarized in Table 1. The three mixing angles turn out to depend on only one free parameter θ and good agreement with their measured values can be achieved for certain values of θ , the Dirac CP phase is conserved or maximal and the Majorana CP phases are trivial. Furthermore, we construct a model based on $A_5 \rtimes H_{CP}$. The lepton mixing is exactly the golden ratio (GR) texture at leading order (LO). A non-zero θ_{13} is generated by the next-to-leading-order (NLO) corrections, and the mixing patterns of cases III and IV discussed in the model independent analysis are generated.

The layout of the rest of this paper is as follows. In section 2, the physical CP transformations compatible with the A_5 family symmetry are found. In section 3, we perform a model independent analysis of possible lepton mixing patterns achievable from the underlying symmetry group $A_5 \rtimes H_{CP}$. In section 4, we present our $A_5 \rtimes H_{CP}$ model, the LO structure, vacuum alignment and the NLO corrections are discussed. Section 5 concludes the paper. In Appendix A, we review the group theory of A_5 and the Clebsch-Gordan coefficients in our working basis are reported. In Appendix B, we present the possible mixing patterns arising from the A_5 flavor symmetry without CP symmetry, where the residual flavor symmetry in the neutrino sector is either Klein or Z_2 subgroup of A_5 . Compared with section 3, we see that generalized CP is really a powerful method of predicting CP phases as well as lepton mixing angles.

2 Approach

Both family symmetry and CP symmetry acts on the flavor space in a non-trivial way, and the interplay between them should be carefully treated. In order to consistently combine a family symmetry G_f with a CP symmetry which is represented by unitary CP transformation matrix X , X must be related to an automorphism $u : G_f \rightarrow G_f$. To be precise, the CP transformation X should be a solution to the consistency equation [20, 21]

$$X\rho^*(g)X^{-1} = \rho(u(g)), \quad \forall g \in G_f, \quad (2.1)$$

where ρ is a representation of G_f with $\rho : G \rightarrow GL(N, \mathbb{C})$, and it is generally reducible. We can easily check that the automorphism associated with $\rho(h)X$ for any $h \in G_f$ is an

composition of u and an inner automorphism $\mu_h : g \rightarrow hgh^{-1}$ with $h, g \in G_f$ [28, 31]. Therefore the effects of inner automorphism can be easily included, and it is equivalent to a family symmetry transformation. As a consequence, we could firstly focus on the the outer automorphism of G_f . Furthermore, it has been shown that u has to a class-inverting automorphism for X to be a physical CP transformation [36]. In other words, u should map each irreducible representation \mathbf{r} of G_f into its own complex conjugate. Hence the consistency condition in Eq. (2.1) takes a more restricted form:

$$X_{\mathbf{r}} \rho_{\mathbf{r}}^*(g) X_{\mathbf{r}}^{-1} = \rho_{\mathbf{r}}(u(g)), \quad \forall g \in G_f, \quad (2.2)$$

where the subscript “ \mathbf{r} ” refers to the representation space acted on. The CP transformation X in Eq. (2.1) is given by the direct sum of the $X_{\mathbf{r}}$ corresponding to the particle content of the model. Notice that the consistency conditions of Eq. (2.2) can also be derived from the requirement that the Lagrangian is invariant under both CP symmetry and flavor symmetry [37].

In the present work, we are interested in the family symmetry $G_f = A_5$. The group theory of A_5 , its representation and all the Clebsch-Gordan coefficients are reported in Appendix A. The structure of the automorphism group of A_5 is quite simple and is very clear in mathematica.

$$\begin{aligned} Z(A_5) &\cong Z_1, & \text{Aut}(A_5) &\cong S_5, \\ \text{Inn}(A_5) &\cong A_5, & \text{Out}(A_5) &\cong Z_2, \end{aligned} \quad (2.3)$$

where $Z(A_5)$, $\text{Aut}(A_5)$, $\text{Inn}(A_5)$ and $\text{Out}(A_5)$ denote the center, automorphism group, inner automorphism group and outer automorphism group of A_5 respectively. We see that the outer automorphism group of A_5 is isomorphic to Z_2 . Consequently there is only one non-trivial outer automorphism \mathbf{u} with

$$S \xrightarrow{\mathbf{u}} S, \quad T \xrightarrow{\mathbf{u}} (ST^3)^2. \quad (2.4)$$

The order of \mathbf{u} is really 2, i.e., $\mathbf{u}^2 = id$, where id represents the trivial automorphism $id(g) = g, \forall g \in A_5$. One can straightforwardly check that \mathbf{u} acts on the A_5 conjugacy classes as follows

$$1C_1 \xrightarrow{\mathbf{u}} 1C_1, \quad 15C_2 \xrightarrow{\mathbf{u}} 15C_2, \quad 20C_3 \xrightarrow{\mathbf{u}} 20C_3, \quad 12C_5 \xleftarrow{\mathbf{u}} 12C'_5. \quad (2.5)$$

It interchanges the classes $12C_5$ and $12C'_5$. Since the inverse of each A_5 conjugacy class is equal to itself, \mathbf{u} is not a class-inverting automorphism, and the corresponding CP transformation is unphysical. In terms of representations, the two different three-dimensional irreducible representations $\mathbf{3}$ and $\mathbf{3}'$ are exchanged not mapped into their conjugate under the action of \mathbf{u} . The generalized CP symmetry related with \mathbf{u} can only be consistently defined if fields transforming as $\mathbf{3}$ and $\mathbf{3}'$ are absent in a model. As a result, we conclude that only the CP transformation associated with the trivial outer automorphism (i.e., the inner automorphism) can be compatibly imposed on the theory with A_5 family symmetry.

Now we consider the representative inner automorphism $\mu_{T^3ST^2ST^3S} : (S, T) \rightarrow (S, T^4)$. The corresponding generalized CP transformation $X_{\mathbf{r}}^0$ is fixed by the consistency equations:

$$\begin{aligned} X_{\mathbf{r}}^0 \rho_{\mathbf{r}}^*(S) (X_{\mathbf{r}}^0)^{-1} &= \rho_{\mathbf{r}}(S), \\ X_{\mathbf{r}}^0 \rho_{\mathbf{r}}^*(T) (X_{\mathbf{r}}^0)^{-1} &= \rho_{\mathbf{r}}(T^4). \end{aligned} \quad (2.6)$$

From the representation matrices given in Appendix A, we see that for any representation

$$\rho_{\mathbf{r}}^*(S) = \rho_{\mathbf{r}}(S), \quad \rho_{\mathbf{r}}^*(T) = \rho_{\mathbf{r}}(T^4). \quad (2.7)$$

Therefore $X_{\mathbf{r}}^0$ is an identity matrix up to an overall phase, i.e.,

$$X_{\mathbf{r}}^0 = 1. \quad (2.8)$$

Including the contribution of the remaining inner automorphisms in the manner stated below Eq. (2.1), the most general CP transformation consistent with A_5 family symmetry is of the form

$$X_{\mathbf{r}} = \rho_{\mathbf{r}}(g)X_{\mathbf{r}}^0 = \rho_{\mathbf{r}}(g), \quad g \in A_5. \quad (2.9)$$

This means that the generalized CP transformation consistent with A_5 is of the same form as the family group transformation in our working basis while they act on the a field multiplet in different ways: $\varphi(x) \xrightarrow{g} \rho_{\mathbf{r}}(g)\varphi(x)$, $g \in A_5$ versus $\varphi(x) \xrightarrow{CP} X_{\mathbf{r}}\varphi^*(x_P) = \rho_{\mathbf{r}}(g)\varphi^*(x_P)$, where $x_P = (t, -\vec{x})$.

In this work, the phenomenological implications of A_5 family symmetry combined with the generalized CP symmetry would be investigated in a systematical and comprehensive way. The parent symmetry is $A_5 \rtimes H_{CP}$ at high energy scale, where the element of H_{CP} is the CP transformation compatible with A_5 and its explicit form is given by Eq. (2.9). In this setup, lepton mixing can be predicted from $A_5 \rtimes H_{CP}$ breaking into different remnant symmetries $G_l \rtimes H_{CP}^l$ and $G_\nu \rtimes H_{CP}^\nu$ in the charged lepton and neutrino masses respectively, where G_l , G_ν and H_{CP}^l , H_{CP}^ν denote residual family symmetries and residual CP symmetries respectively. It is notable that the predictions for the lepton flavor mixing only depend on the assumed symmetry breaking patterns and are independent of the details of a specific implementation scheme, such as the possible additional symmetries of the model and the involved flavon fields and their assignments etc. In practice, the three generations of left-handed leptons doublets are embedded into the faithful three-dimensional representation $\mathbf{3}$ of A_5 . Since $\mathbf{3}'$ is related to $\mathbf{3}$ by the outer automorphism \mathbf{u} , the results would be the same and no additional results would be found, if we assign the three left-handed leptons to the representation $\mathbf{3}'$ instead. The requirement that $G_l \rtimes H_{CP}^l$ is preserved by the charged lepton mass term implies that the hermitian combination $m_l^\dagger m_l$ must be invariant under the remnant symmetry $G_l \rtimes H_{CP}^l$, i.e.,

$$\rho_{\mathbf{3}}^\dagger(g_l)m_l^\dagger m_l \rho_{\mathbf{3}}(g_l) = m_l^\dagger m_l, \quad g_l \in G_l, \quad (2.10a)$$

$$X_{l\mathbf{3}}^\dagger m_l^\dagger m_l X_{l\mathbf{3}} = (m_l^\dagger m_l)^*, \quad X_{l\mathbf{3}} \in H_{CP}^l, \quad (2.10b)$$

where the mass matrix m_l is defined in the convention $\bar{l}_R m_l l_L$. Once G_l and H_{CP}^l are specified, the most general form of $m_l^\dagger m_l$ can be straightforwardly constructed from Eqs. (2.10a, 2.10b). In the present work, we shall assume neutrinos are Majorana particles. In the same fashion, requiring that $G_\nu \rtimes H_{CP}^\nu$ is a symmetry of the neutrino mass matrix m_ν implies that m_ν should be invariant under the action of $G_\nu \rtimes H_{CP}^\nu$,

$$\rho_{\mathbf{3}}^T(g_\nu)m_\nu \rho_{\mathbf{3}}(g_\nu) = m_\nu, \quad g_\nu \in G_\nu, \quad (2.11a)$$

$$X_{\nu\mathbf{3}}^T m_\nu X_{\nu\mathbf{3}} = m_\nu^*, \quad X_{\nu\mathbf{3}} \in H_{CP}^\nu, \quad (2.11b)$$

which allow us to derive the explicit form of m_ν . Since both remnant family symmetry and remnant CP symmetries are still preserved after symmetry breaking, they should be compatible with each other. That is to say consistency equation similar to Eq. (2.2) has to be fulfilled,

$$X_\nu \rho^*(g_{\nu_i}) X_\nu^{-1} = \rho(g_{\nu_j}), \quad g_{\nu_i}, g_{\nu_j} \in G_\nu, \quad (2.12a)$$

$$X_l \rho^*(g_{l_i}) X_l^{-1} = \rho(g_{l_j}), \quad g_{l_i}, g_{l_j} \in G_l. \quad (2.12b)$$

The prediction for the PMNS matrix can be obtained by further diagonalizing the reconstructed mass matrices $m_l^\dagger m_l$ and m_ν . Please see Ref. [15] for an alternative way of directly

extracting the PMNS matrix from the representation matrices of the remnant symmetries without resorting to the mass matrices. As the order of neutrino and charged lepton masses is indeterminate in our framework, it is only possible to determine the PMNS matrix up to independent row and column permutations.

From the remnant symmetry invariant conditions of Eqs. (2.10a, 2.10b), we can see that $X_{l\mathbf{r}}$ and $\rho_{\mathbf{r}}(g_l)X_{l\mathbf{r}}$ with $g_l \in G_l$ lead to the same constraint on $m_l^\dagger m_l$. Furthermore, the residual CP transformation $X_{l\mathbf{r}}$ should be a symmetric matrix otherwise the charged lepton masses would be restricted to be partially degenerate [15, 28]. The same comments apply to $X_{\nu\mathbf{r}}$ and $\rho_{\mathbf{r}}(g_\nu)X_{\nu\mathbf{r}}$ with $g_\nu \in G_\nu$. Notice that the same result for PMNS matrix would be obtained [23, 28, 31], if a pair of subgroups $\{G'_l, G'_\nu\}$ is conjugated to the pair of subgroups $\{G_l, G_\nu\}$ under an element of A_5 , i.e.,

$$G'_l = gG_lg^{-1}, \quad G'_\nu = gG_\nu g^{-1}, \quad g \in A_5. \quad (2.13)$$

The reason is that remnant CP symmetries determined by restricted consistency condition of Eqs. (2.12a, 2.12b) are strongly correlated in the two cases such that lepton mass matrices $\{m_l^\dagger m'_l, m'_\nu\}$ for the new primed residual symmetry are related to $\{m_l^\dagger m_l, m_\nu\}$ by a similarity transformation $\rho_3(g)$ [23, 28, 31]. In this way, it is sufficient to only discuss the independent pairs of $\{G_l, G_\nu\}$ which are not related by group conjugation and subsequently all possible residual CP compatible with the residual family symmetry should be included.

3 Lepton mixing from remnant symmetries of $A_5 \rtimes H_{CP}$

Neutrino are assumed to be Majorana particles here, therefore the remnant flavor symmetry G_ν must be a Klein four $K_4 \cong Z_2 \times Z_2$ subgroup or a single Z_2 subgroup of A_5 . G_l can be any abelian subgroups of A_5 with order equal or greater than 3. A complete or partial degeneracy of the charged lepton mass spectrum would be produced if G_l had a non-abelian character. In the case of $G_\nu = K_4$, the lepton mixing matrix U_{PMNS} is fully determined by the mismatch between the remnant family symmetry G_l and G_ν . As shown in Appendix B, U_{PMNS} can take four possible forms such as the golden ratio mixing, democratic mixing and so on. However, none of them is compatible with experimental data. Then we turn to the scenario of $G_\nu = Z_2$. With this setting, U_{PMNS} is partially constrained, and only one column of the lepton mixing matrix is fixed up to reordering and rephasing of the elements. The explicit forms of the fixed column vectors for all the independent residual flavor symmetries are summarized in Table 4. We find that four cases are viable: $(G_l, G_\nu) = (Z_5^T, Z_2^S)$, $(Z_5^T, Z_2^{T^3ST^2ST^3})$, $(Z_3^{T^3ST^2S}, Z_2^{ST^2ST^3S})$ and $(K_4^{(ST^2ST^3S, TST^4)}, Z_2^S)$ lead to the mixing column vectors $(-\sqrt{\frac{\kappa}{\sqrt{5}}}, \frac{1}{\sqrt{2\sqrt{5}\kappa}}, \frac{1}{\sqrt{2\sqrt{5}\kappa}})^T$, $(\sqrt{\frac{1}{\sqrt{5}\kappa}}, \sqrt{\frac{\kappa}{2\sqrt{5}}}, \sqrt{\frac{\kappa}{2\sqrt{5}}})^T$, $(\frac{1}{\sqrt{3}}, \frac{1}{\sqrt{3}}, \frac{1}{\sqrt{3}})^T$ and $(\frac{\kappa}{2}, -\frac{1}{2}, \frac{\kappa-1}{2})^T$ respectively, where $\kappa = (1 + \sqrt{5})/2$ is the golden ratio. The phenomenological implications of each case are explored in Appendix B, and the lepton mixing matrix U_{PMNS} turns out to depend on two free parameters up to indeterminant Majorana phases. We see that the measured values of the three mixing angles can be accommodated very well, but the allowed values of Dirac CP phase δ_{CP} scatter in a quite large range. Furthermore, the breaking patterns with $(G_l, G_\nu) = (Z_2, K_4)$ are studied as well. Accordingly a row of the lepton mixing matrix U_{PMNS} is determined to be $\frac{1}{2}(\kappa, 1, \kappa - 1)$ or $(1, 0, 0)$ which are not in the experimentally preferred regions.

In order to be able to predict the values of CP phases, we extend the A_5 family symmetry to include the generalized CP. In the following, we shall perform a thorough analysis of lepton mixing patterns for the possible residual symmetries $G_l \rtimes H_{CP}^l$ and $G_\nu \rtimes H_{CP}^\nu$ in the charged lepton and neutrino sectors, where the remnant family symmetries G_l and G_ν would be

restricted to the four viable cases listed in Table 4, and the remnant CP symmetries H_{CP}^l and H_{CP}^ν are determined by consistency condition of Eqs. (2.12a, 2.12b). In this setup, U_{PMNS} as well as all mixing angles and all CP phases generically depend on a free parameters θ whose value can be fixed by the measured value of θ_{13} . As a consequence, all observables are strongly correlated. For the concerned A_5 family symmetry, the Dirac phase would be predicted to be trivial or maximal while both Majorana phases are trivial after generalized CP symmetry is imposed. In order to evaluate how well the predicted mixing patterns agree with the experimental data on mixing angles, we shall perform a usual χ^2 analysis which uses the global fit results of Ref. [5]. We begin to discuss all possible cases one by one.

3.1 $G_l = Z_5^T, G_\nu = Z_2^S$

In this case, the parent symmetry $A_5 \rtimes H_{CP}$ is broken down to $Z_5^T \rtimes H_{CP}^l$ and $Z_2^S \rtimes H_{CP}^\nu$ subgroups in the charged lepton and neutrino sectors, respectively. The residual CP symmetry H_{CP}^l must be consistent with the residual flavor symmetry Z_5^T in the charged lepton sector. That is to say the element X_{lr} of H_{CP}^l should fulfill the consistency equation of Eq. (2.12b),

$$X_{lr}\rho_{\mathbf{r}}^*(T)X_{lr}^{-1} = \rho_{\mathbf{r}}(g'), \quad g' \in Z_5^T. \quad (3.1)$$

Then we find only 10 choices out of the 60 CP transformations of H_{CP} listed in Eq. (2.9) are acceptable

$$H_{CP}^l = \{ \rho_{\mathbf{r}}(1), \rho_{\mathbf{r}}(T), \rho_{\mathbf{r}}(T^2), \rho_{\mathbf{r}}(T^3), \rho_{\mathbf{r}}(T^4), \rho_{\mathbf{r}}(ST^2ST^3S), \rho_{\mathbf{r}}((T^2S)^2T^3S), \\ \rho_{\mathbf{r}}(T^3ST^2ST^3S), \rho_{\mathbf{r}}(T^4ST^2ST^3S), \rho_{\mathbf{r}}(ST^3ST^2S) \}. \quad (3.2)$$

As shown in Eq. (2.10a), the residual family symmetry Z_5^T impose the following constraint on the charged lepton mass matrix:

$$\rho_{\mathbf{3}}^\dagger(T)m_l^\dagger m_l \rho_{\mathbf{3}}(T) = m_l^\dagger m_l. \quad (3.3)$$

In our working basis, the representation matrix of the generator T is diagonal with $\rho_{\mathbf{3}}(T) = \text{diag}(1, \omega_5, \omega_5^4)$. Consequently the hermitian combination $m_l^\dagger m_l$ of charged lepton mass matrix is also diagonal, i.e.,

$$m_l^\dagger m_l = \text{diag}(m_e^2, m_\mu^2, m_\tau^2), \quad (3.4)$$

where m_e , m_μ and m_τ represent the electron, muon and tau masses respectively. Furthermore, we can check that the remnant CP invariant condition of Eq. (2.10b) is automatically satisfied for $X_{lr} = \rho_{\mathbf{r}}(1), \rho_{\mathbf{r}}(T), \rho_{\mathbf{r}}(T^2), \rho_{\mathbf{r}}(T^3), \rho_{\mathbf{r}}(T^4)$. However, the mass degeneracy $m_\mu = m_\tau$ arises for the remaining values $X_{lr} = \rho_{\mathbf{r}}(ST^2ST^3S), \rho_{\mathbf{r}}((T^2S)^2T^3S), \rho_{\mathbf{r}}(T^3ST^2ST^3S), \rho_{\mathbf{r}}(T^4ST^2ST^3S), \rho_{\mathbf{r}}(ST^3ST^2S)$. The reason is that all remnant CP transformations except $\rho_{\mathbf{r}}(T^3ST^2ST^3S)$ are not symmetric. Generally speaking, any remnant CP transformation must be a symmetric matrix to avoid degenerate masses [15, 28]. This case is obviously not viable, and will be disregarded hereafter.

Now we turn to the neutrino sector. The residual CP transformations $X_{\nu\mathbf{r}}$ of H_{CP}^ν is specified by the consistency condition:

$$X_{\nu\mathbf{r}}\rho_{\mathbf{r}}^*(S)X_{\nu\mathbf{r}}^{-1} = \rho_{\mathbf{r}}(S), \quad (3.5)$$

which can be easily obtained by applying the general consistency condition of Eq. (2.12a). We see that the CP transformation $X_{\nu\mathbf{r}}$ commutes with flavor symmetry transformation $\rho_{\mathbf{r}}(S)$, and therefore remnant symmetry is $Z_2^S \rtimes H_{CP}^\nu$ in the neutrino sector in this case. Notice that the semi-direct product structure between residual flavor and CP symmetries

generally reduces to a direct product if the residual flavor symmetry is a Z_2 subgroup [23,24]. It is easy to check that $X_{\nu\mathbf{r}}$ can only take 4 possible values,

$$H_{CP}^\nu = \{\rho_{\mathbf{r}}(1), \rho_{\mathbf{r}}(S), \rho_{\mathbf{r}}(T^3ST^2ST^3), \rho_{\mathbf{r}}(T^3ST^2ST^3S)\}. \quad (3.6)$$

The neutrino mass matrix m_ν respects the residual symmetry $Z_2^S \times H_{CP}^\nu$, satisfying

$$\begin{aligned} \rho_{\mathbf{3}}^T(S)m_\nu\rho_{\mathbf{3}}(S) &= m_\nu, \\ X_{\nu\mathbf{3}}^T m_\nu X_{\nu\mathbf{3}} &= m_\nu^*, \quad X_{\nu\mathbf{3}} \in H_{CP}^\nu. \end{aligned} \quad (3.7)$$

We find that the most general neutrino mass matrix invariant under the residual family symmetry Z_2^S , takes the following form

$$m_\nu = \alpha \begin{pmatrix} 1 & 0 & 0 \\ 0 & 0 & 1 \\ 0 & 1 & 0 \end{pmatrix} + \frac{\beta}{\sqrt{2}} \begin{pmatrix} -2\sqrt{2} & 3 & 3 \\ 3 & 0 & \sqrt{2} \\ 3 & \sqrt{2} & 0 \end{pmatrix} + \gamma \begin{pmatrix} 2 & 0 & 0 \\ 0 & 3 & -1 \\ 0 & -1 & 3 \end{pmatrix} + \delta \begin{pmatrix} 0 & -\sqrt{2} & \sqrt{2} \\ -\sqrt{2} & -2\kappa & 0 \\ \sqrt{2} & 0 & 2\kappa \end{pmatrix}, \quad (3.8)$$

where α , β , γ and δ are generally complex parameters, and they are further constrained to be real or pure imaginary by residual CP. This neutrino mass matrix m_ν can be simplified into a quite simple form by performing a golden ratio transformation,

$$m'_\nu = U_{GR}^T m_\nu U_{GR} = \begin{pmatrix} \alpha - (3\kappa - 1)\beta + 2\gamma & 0 & 0 \\ 0 & \alpha + (3\kappa - 2)\beta + 2\gamma & 2\sqrt{2 + \kappa} \delta \\ 0 & 2\sqrt{2 + \kappa} \delta & -\alpha - \beta + 4\gamma \end{pmatrix}, \quad (3.9)$$

where

$$U_{GR} = \begin{pmatrix} -\sqrt{\frac{\kappa}{\sqrt{5}}} & \sqrt{\frac{1}{\sqrt{5}\kappa}} & 0 \\ \sqrt{\frac{1}{2\sqrt{5}\kappa}} & \sqrt{\frac{\kappa}{2\sqrt{5}}} & -\frac{1}{\sqrt{2}} \\ \sqrt{\frac{1}{2\sqrt{5}\kappa}} & \sqrt{\frac{\kappa}{2\sqrt{5}}} & \frac{1}{\sqrt{2}} \end{pmatrix}, \quad (3.10)$$

is the golden ratio mixing pattern [38] which can be naturally derived in A_5 models [39]. The neutrino mass matrix m'_ν is further diagonalized by a unitary rotation U'_ν in the (2,3)-plane,

$$U_\nu'^T m'_\nu U'_\nu = \text{diag}(m_1, m_2, m_3). \quad (3.11)$$

The next step is to explore the constraint of remnant CP on m_ν . Two different phenomenological predictions arise for the four possible $X_{\nu\mathbf{r}}$ shown in Eq. (3.6), as $\rho_{\mathbf{r}}(S)X_{\nu\mathbf{r}}$ and $X_{\nu\mathbf{r}}$ lead to the same predictions.

(I) $X_{\nu\mathbf{r}} = \rho_{\mathbf{r}}(1), \rho_{\mathbf{r}}(S)$

Obviously we have $m_\nu = m_\nu^*$ such that all the four parameters α , β , γ and δ are real. As a consequence, the neutrino mass matrix m'_ν is a real symmetric matrix. The unitary transformation U'_ν is of the form:

$$U'_\nu = \begin{pmatrix} 1 & 0 & 0 \\ 0 & \cos\theta & \sin\theta \\ 0 & -\sin\theta & \cos\theta \end{pmatrix} K_\nu. \quad (3.12)$$

where K_ν is a diagonal phase matrix with elements equal to ± 1 or $\pm i$ which makes the neutrino masses $m_{1,2,3}$ positive. The effect of K_ν is a possible change of the Majorana

phases by π , and it would be omitted hereinafter for the other cases. The parameter θ is given by

$$\tan 2\theta = -\frac{4\sqrt{2+\kappa}\delta}{2(\alpha-\gamma)+(3\kappa-1)\beta}. \quad (3.13)$$

The light neutrino mass eigenvalues are

$$\begin{aligned} m_1 &= |\alpha - (3\kappa - 1)\beta + 2\gamma|, \\ m_2 &= \frac{1}{2} \left| 3(\kappa - 1)\beta + 6\gamma + \frac{2(\alpha - \gamma) + (3\kappa - 1)\beta}{\cos 2\theta} \right|, \\ m_3 &= \frac{1}{2} \left| 3(\kappa - 1)\beta + 6\gamma - \frac{2(\alpha - \gamma) + (3\kappa - 1)\beta}{\cos 2\theta} \right|. \end{aligned} \quad (3.14)$$

Given the diagonal charged lepton mass matrix, the lepton mixing matrix takes the form

$$U_{PMNS} = U_{GR} U'_\nu = \begin{pmatrix} -\sqrt{\frac{\kappa}{\sqrt{5}}} & \sqrt{\frac{1}{\sqrt{5}\kappa}} \cos \theta & \sqrt{\frac{1}{\sqrt{5}\kappa}} \sin \theta \\ \sqrt{\frac{1}{2\sqrt{5}\kappa}} & \sqrt{\frac{\kappa}{2\sqrt{5}}} \cos \theta + \frac{\sin \theta}{\sqrt{2}} & \sqrt{\frac{\kappa}{2\sqrt{5}}} \sin \theta - \frac{\cos \theta}{\sqrt{2}} \\ \sqrt{\frac{1}{2\sqrt{5}\kappa}} & \sqrt{\frac{\kappa}{2\sqrt{5}}} \cos \theta - \frac{\sin \theta}{\sqrt{2}} & \sqrt{\frac{\kappa}{2\sqrt{5}}} \sin \theta + \frac{\cos \theta}{\sqrt{2}} \end{pmatrix} K_\nu. \quad (3.15)$$

One can straightforwardly extract the lepton mixing angles and CP phases as follows,

$$\begin{aligned} \sin^2 \theta_{13} &= \frac{3-\kappa}{5} \sin^2 \theta, \quad \sin^2 \theta_{12} = \frac{1+\cos 2\theta}{3+2\kappa+\cos 2\theta}, \\ \sin^2 \theta_{23} &= \frac{1}{2} - \frac{\sqrt{2+\kappa} \sin 2\theta}{3\kappa-1+(\kappa-1)\cos 2\theta}, \quad \sin \delta_{CP} = \sin \alpha_{21} = \sin \alpha_{31} = 0, \end{aligned} \quad (3.16)$$

where δ_{CP} is the Dirac CP phase, α_{21} and α_{31} are the Majorana CP phases in the standard parameterization [1]. There is no CP violation in this case as the neutrino mass matrix is real. Expressing θ in terms of θ_{13} , correlations among the three mixing angles follow immediately,

$$\begin{aligned} \sin^2 \theta_{12} &= \frac{3-\kappa}{5} - \frac{2+\kappa}{5} \tan^2 \theta_{13}, \\ \sin^2 \theta_{23} &= \frac{1}{2} \pm \kappa \tan \theta_{13} \sqrt{1 - (1+\kappa) \tan^2 \theta_{13}}. \end{aligned} \quad (3.17)$$

For the measured reactor mixing angles $\sin^2 \theta_{13} \simeq 0.0234$ [5], we have $\sin^2 \theta_{23} \simeq 0.258$ or 0.742 which is outside of the experimentally favored 3σ region [5] although $\sin^2 \theta_{12} \simeq 0.259$ is acceptable. As a consequence, this mixing pattern isn't viable. This point remains even after permutation of rows and columns is considered.

(II) $X_{\nu\mathbf{r}} = \rho_{\mathbf{r}}(T^3 S T^2 S T^3), \rho_{\mathbf{r}}(T^3 S T^2 S T^3 S)$

Solving the residual CP invariant condition in Eq. (3.7), we find α, β and γ are real while δ is pure imaginary. The unitary diagonalization matrix U'_ν is

$$U'_\nu = \begin{pmatrix} 1 & 0 & 0 \\ 0 & \cos \theta & \sin \theta \\ 0 & -i \sin \theta & i \cos \theta \end{pmatrix}, \quad (3.18)$$

where the diagonal matrix K_ν multiplied from the right-hand side has been omitted, and the rotation angle θ fulfills

$$\tan 2\theta = -\frac{4i\sqrt{2+\kappa}\delta}{3(\kappa-1)\beta+6\gamma}. \quad (3.19)$$

The three neutrino masses are given by

$$\begin{aligned} m_1 &= |\alpha - (3\kappa - 1)\beta + 2\gamma|, \\ m_2 &= \frac{1}{2} \left| 2\alpha + (3\kappa - 1)\beta - 2\gamma + \frac{3((\kappa - 1)\beta + 2\gamma)}{\cos 2\theta} \right|, \\ m_3 &= \frac{1}{2} \left| 2\alpha + (3\kappa - 1)\beta - 2\gamma - \frac{3((\kappa - 1)\beta + 2\gamma)}{\cos 2\theta} \right|. \end{aligned} \quad (3.20)$$

All the four parameters α , β , γ and δ are involved in the three neutrino masses. As a result, the measured mass squared differences $\delta m^2 \equiv m_2^2 - m_1^2$ and $\Delta m^2 \equiv m_3^2 - (m_1^2 + m_2^2)/2$ can be easily accommodated [5], the absolute neutrino mass scale can not be fixed, and the neutrino mass spectrum can be either normal ordering (NO) or inverted ordering (IO). The PMNS matrix takes the following form:

$$U_{PMNS} = \begin{pmatrix} -\sqrt{\frac{\kappa}{\sqrt{5}}} & \sqrt{\frac{1}{\sqrt{5}\kappa}} \cos \theta & \sqrt{\frac{1}{\sqrt{5}\kappa}} \sin \theta \\ \sqrt{\frac{1}{2\sqrt{5}\kappa}} & \sqrt{\frac{\kappa}{2\sqrt{5}}} \cos \theta + \frac{i \sin \theta}{\sqrt{2}} & \sqrt{\frac{\kappa}{2\sqrt{5}}} \sin \theta - \frac{i \cos \theta}{\sqrt{2}} \\ \sqrt{\frac{1}{2\sqrt{5}\kappa}} & \sqrt{\frac{\kappa}{2\sqrt{5}}} \cos \theta - \frac{i \sin \theta}{\sqrt{2}} & \sqrt{\frac{\kappa}{2\sqrt{5}}} \sin \theta + \frac{i \cos \theta}{\sqrt{2}} \end{pmatrix}. \quad (3.21)$$

Note that the first column vector of this mixing pattern coincides with the first column of the GR mixing. The lepton mixing angles and CP phases can be read out as¹

$$\begin{aligned} \sin^2 \theta_{13} &= \frac{3 - \kappa}{5} \sin^2 \theta, & \sin^2 \theta_{12} &= \frac{1 + \cos 2\theta}{3 + 2\kappa + \cos 2\theta}, \\ \sin^2 \theta_{23} &= \frac{1}{2}, & |\sin \delta_{CP}| &= 1, & \sin \alpha_{21} &= \sin \alpha_{31} = 0. \end{aligned} \quad (3.22)$$

Here we present the absolute value of $\sin \delta_{CP}$, since the sign of $\sin \delta_{CP}$ depends on the ordering of rows and columns. We see that both atmospheric angle θ_{23} and Dirac CP phase δ_{CP} are maximal while Majorana phases are conserved. Given the weak evidence of $\delta_{CP} \sim 3\pi/2$ from T2K [8], this pattern is slightly preferred. The prediction of maximal Dirac CP can be tested by next generation long-baseline neutrino oscillation experiments such as the proposed LBNE [9], LBNO [10] and HyperKamiokande [11], which aim to search for leptonic CP violation. Moreover, the correlation between θ_{13} and θ_{12} is of the same form as that of case I, and it is plotted in Fig. 1. The results of the χ^2 analysis are reported in Table 1. We see that the experimental data [5] on lepton mixing angles can be accommodated very well. Notice that the solar mixing angle θ_{12} is predicted to be around the present 3σ lower bound. As far as we known, the JUNO experiment can measure θ_{12} with high accuracy [44]. If significant deviations $\sin^2 \theta_{12}$ from 0.259 was detected, this mixing pattern would be excluded. It is well-known that leptonic CP phases can play a crucial role in the rare process neutrinoless double beta $((\beta\beta)_{0\nu}-)$ decay. The dependence of the $(\beta\beta)_{0\nu}-$ decay amplitude on the neutrino mixing parameters is characterized by the effective Majorana mass $|m_{ee}|$ [1] with the definition:

$$|m_{ee}| = |m_1 \cos^2 \theta_{12} \cos^2 \theta_{13} + m_2 \sin^2 \theta_{12} \cos^2 \theta_{13} e^{i\alpha_{21}} + m_3 \sin^2 \theta_{13} e^{i(\alpha_{31} - 2\delta_{CP})}|. \quad (3.23)$$

For the predicted mixing parameters in Eq. (3.22), we have

$$|m_{ee}| = \frac{1}{\sqrt{5}} |\kappa m_1 + \kappa^{-1} k_2 m_2 \cos^2 \theta + \kappa^{-1} k_3 m_3 \sin^2 \theta|, \quad (3.24)$$

¹In the case of $\sin 2\theta = 0$, either θ_{12} or θ_{13} vanishes, consequently the value of δ_{CP} can not be determined uniquely.

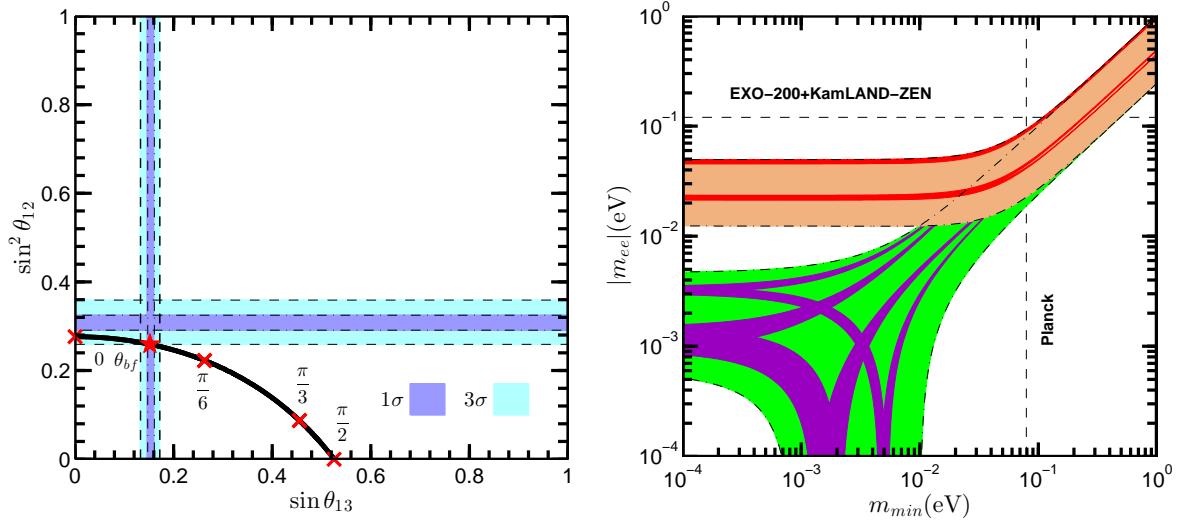


Figure 1: The correlation between $\sin^2 \theta_{12}$ and $\sin \theta_{13}$ (left panel) and the allowed values of the effective mass $|m_{ee}|$ (right panel) in case II. On the left panel, the best fitting value is labelled with a red pentagram, and the points for $\theta = 0, \pi/6, \pi/3$ and $\pi/2$ are marked with a cross to guide the eye. The 1σ and 3σ ranges of the mixing angles are taken from Ref. [5]. On the right panel, the orange and green bands denote the 3σ regions for normal ordering and inverted ordering mass spectrum respectively. The red and purple areas are the predictions for the lepton mixing matrix in Eq. (3.21). The present most strict bound $|m_{ee}| < (0.120 - 0.250)$ eV from EXO-200 [40, 41] combined with KamLAND-ZEN [42] is represented by the horizontal dashed line, and the upper limit on m_{min} from the latest Planck result $m_1 + m_2 + m_3 < 0.230$ eV at 95% confidence level [43] is shown by vertical dashed line.

where $k_2, k_3 = \pm 1$ originates from the ambiguity of the matrix K_ν . The prediction for the effective mass $|m_{ee}|$ with respect to the lightest neutrino mass is shown Fig. 1. We find that $|m_{ee}|$ is close to 0.022 eV or the upper bound 0.045 eV in case of IO neutrino mass spectrum, which are within the future sensitivity of planned $(\beta\beta)_{0\nu}$ -decay experiments. However, in case of NO spectrum, $|m_{ee}|$ strongly depends on lightest neutrino mass m_{min} , and it can even be approximately vanishing for particular value of m_{min} .

3.2 $G_l = Z_5^T, G_\nu = Z_2^{T^3 ST^2 ST^3}$

The charged lepton sector preserves the same remnant symmetry $Z_5^T \rtimes H_{CP}^l$ as that discussed in section 3.1. Therefore the charged lepton mass is subject to the same constraint, and $m_l^\dagger m_l$ should be diagonal as well. In neutrino sector, the residual CP symmetry H_{CP}^ν has to be compatible with the residual family symmetry $G_\nu = Z_2^{T^3 ST^2 ST^3}$, i.e.,

$$X_{\nu\mathbf{r}} \rho_{\mathbf{r}}^* (T^3 ST^2 ST^3) X_{\nu\mathbf{r}}^{-1} = \rho_{\mathbf{r}} (T^3 ST^2 ST^3). \quad (3.25)$$

It is easy to check that only 4 generalized CP transformations are acceptable,

$$H_{CP}^\nu = \{ \rho_{\mathbf{r}}(1), \rho_{\mathbf{r}}(S), \rho_{\mathbf{r}}(T^3 ST^2 ST^3), \rho_{\mathbf{r}}(T^3 ST^2 ST^3 S) \}. \quad (3.26)$$

Straightforward calculations demonstrate that the most general neutrino mass matrix invariant under $Z_2^{T^3 ST^2 ST^3}$ is of the form

$$m_\nu = \alpha \begin{pmatrix} 1 & 0 & 0 \\ 0 & 0 & 1 \\ 0 & 1 & 0 \end{pmatrix} + \frac{\beta}{\sqrt{2}} \begin{pmatrix} -2\sqrt{2} & 3 & 3 \\ 3 & 0 & \sqrt{2} \\ 3 & \sqrt{2} & 0 \end{pmatrix} + \gamma \begin{pmatrix} 2 & 0 & 0 \\ 0 & 3 & -1 \\ 0 & -1 & 3 \end{pmatrix} + \delta \begin{pmatrix} 0 & \sqrt{2}\kappa & -\sqrt{2}\kappa \\ \sqrt{2}\kappa & -2 & 0 \\ -\sqrt{2}\kappa & 0 & 2 \end{pmatrix}, \quad (3.27)$$

		Analytic expression			Best fitting				
		$\sin^2 \theta_{13}$	$\sin^2 \theta_{12}$	$\sin^2 \theta_{23}$	θ_{bf}	χ^2_{min}	$\sin^2 \theta_{13}$	$\sin^2 \theta_{12}$	$\sin^2 \theta_{23}$
II	IO	$\frac{3-\kappa}{5} \sin^2 \theta$	$\frac{2 \cos^2 \theta}{3+2\kappa+\cos 2\theta}$	$\frac{1}{2}$	0.295	8.468	0.0234	0.259	0.5
	NO			$\frac{1}{2}$	0.292	11.88	0.0229	0.259	0.5
III	IO	$\frac{\kappa}{\sqrt{5}} \sin^2 \theta$	$\frac{4-2\kappa}{5-2\kappa+\cos 2\theta}$	$\frac{1}{2} - \frac{\sqrt{3-\kappa} \sin 2\theta}{3\kappa-2+\kappa \cos 2\theta}$	0.182	4.851	0.0236	0.283	0.404 ($\theta_{23} < 45^\circ$)
					2.958	3.165	0.0240	0.283	0.597 ($\theta_{23} > 45^\circ$)
	0.179				4.087	0.0230	0.283	0.406 ($\theta_{23} < 45^\circ$)	
	2.965				24.88	0.0224	0.283	0.593 ($\theta_{23} > 45^\circ$)	
IV	IO			$\frac{1}{2}$	0.183	2.232	0.0241	0.283	0.5
	NO			$\frac{1}{2}$	0.181	5.802	0.0235	0.283	0.5
V	IO	$\frac{1-\sin 2\theta}{3}$	$\frac{1}{2+\sin 2\theta}$	$\frac{1}{2}$	0.976	3.987	0.0238	0.341	0.5
	NO			$\frac{1}{2}$	0.973	7.480	0.0233	0.341	0.5
VII	IO	$\frac{(\cos \theta - \kappa \sin \theta)^2}{4\kappa^2}$	$\frac{(\kappa \cos \theta + \sin \theta)^2}{4\kappa^2 - (\cos \theta - \kappa \sin \theta)^2}$	$\frac{(\kappa^2 \cos \theta - \sin \theta)^2}{4\kappa^2 - (\cos \theta - \kappa \sin \theta)^2}$	0.286	1.626	0.0242	0.329	0.486 ($\theta_{23} < 45^\circ$)
				$\frac{\kappa^2 (\cos \theta + \kappa \sin \theta)^2}{4\kappa^2 - (\cos \theta - \kappa \sin \theta)^2}$	0.286	1.751	0.0242	0.329	0.513 ($\theta_{23} > 45^\circ$)
	NO			$\frac{(\kappa^2 \cos \theta - \sin \theta)^2}{4\kappa^2 - (\cos \theta - \kappa \sin \theta)^2}$	0.293	3.503	0.0229	0.330	0.480 ($\theta_{23} < 45^\circ$)
				$\frac{\kappa^2 (\cos \theta + \kappa \sin \theta)^2}{4\kappa^2 - (\cos \theta - \kappa \sin \theta)^2}$	0.282	6.958	0.0248	0.329	0.510 ($\theta_{23} > 45^\circ$)

Table 1: Summary of the predictions for the lepton mixing angles and their best fitting values for all viable cases in the framework of $A_5 \rtimes H_{CP}$. In case VII, the mixing patterns for θ_{23} in the first and second octant are related through the exchange of the second and third rows of the PMNS matrix. Notice that all the three CP phases are independent of θ in all cases: Dirac phase is trivial or maximal, and both Majorana phases are trivial.

where the parameters α , β , γ and δ are generically complexes, and they are further constrained by the remnant CP. After performing a GR transformation, m_ν becomes

$$m'_\nu = U_{GR}^T m_\nu U_{GR} = \begin{pmatrix} \alpha - (3\kappa - 1)\beta + 2\gamma & 0 & 2\sqrt{2 + \kappa} \delta \\ 0 & \alpha + (3\kappa - 2)\beta + 2\gamma & 0 \\ 2\sqrt{2 + \kappa} \delta & 0 & -\alpha - \beta + 4\gamma \end{pmatrix}. \quad (3.28)$$

In the following, we proceed to investigate the constraints imposed by the remnant CP transformations shown in Eq. (3.26). The four possible $X_{\nu\mathbf{r}}$ can be divided into two classes.

(III) $X_{\nu\mathbf{r}} = \rho_{\mathbf{r}}(1), \rho_{\mathbf{r}}(T^3 S T^2 S T^3)$

In this case, the residual flavor and residual CP transformations are of the same form. As a result, the four parameters α , β , γ and δ are all real. The neutrino mass matrix m'_ν can be diagonalized by a unitary transformation

$$U'_\nu = \begin{pmatrix} \cos \theta & 0 & \sin \theta \\ 0 & 1 & 0 \\ -\sin \theta & 0 & \cos \theta \end{pmatrix}, \quad (3.29)$$

with

$$\tan 2\theta = -\frac{4\sqrt{2 + \kappa} \delta}{2(\alpha - \gamma) - (3\kappa - 2)\beta}, \quad (3.30)$$

The three neutrino masses are

$$m_1 = \frac{1}{2} \left| -3\kappa\beta + 6\gamma + \frac{2(\alpha - \gamma) - (3\kappa - 2)\beta}{\cos 2\theta} \right|,$$

$$\begin{aligned}
m_2 &= |\alpha + (3\kappa - 2)\beta + 2\gamma|, \\
m_3 &= \frac{1}{2} \left| -3\kappa\beta + 6\gamma - \frac{2(\alpha - \gamma) - (3\kappa - 2)\beta}{\cos 2\theta} \right|.
\end{aligned} \tag{3.31}$$

The absolute neutrino mass scale can not be predicted. Then the PMNS matrix reads

$$U_{PMNS} = U_{GR} U'_\nu = \begin{pmatrix} -\sqrt{\frac{\kappa}{\sqrt{5}}} \cos \theta & \sqrt{\frac{1}{\sqrt{5}\kappa}} & -\sqrt{\frac{\kappa}{\sqrt{5}}} \sin \theta \\ \frac{\cos \theta}{\sqrt{2\sqrt{5}\kappa}} + \frac{\sin \theta}{\sqrt{2}} & \sqrt{\frac{\kappa}{2\sqrt{5}}} & \frac{\sin \theta}{\sqrt{2\sqrt{5}\kappa}} - \frac{\cos \theta}{\sqrt{2}} \\ \frac{\cos \theta}{\sqrt{2\sqrt{5}\kappa}} - \frac{\sin \theta}{\sqrt{2}} & \sqrt{\frac{\kappa}{2\sqrt{5}}} & \frac{\sin \theta}{\sqrt{2\sqrt{5}\kappa}} + \frac{\cos \theta}{\sqrt{2}} \end{pmatrix}. \tag{3.32}$$

Note that the second column vector is $\left(\sqrt{\frac{1}{\sqrt{5}\kappa}}, \sqrt{\frac{\kappa}{2\sqrt{5}}}, \sqrt{\frac{\kappa}{2\sqrt{5}}} \right)^T$ which coincides with the second column of the GR mixing. The lepton mixing parameters are predicted to be

$$\begin{aligned}
\sin^2 \theta_{13} &= \frac{\kappa}{\sqrt{5}} \sin^2 \theta, \quad \sin^2 \theta_{12} = \frac{4 - 2\kappa}{5 - 2\kappa + \cos 2\theta}, \\
\sin^2 \theta_{23} &= \frac{1}{2} - \frac{\sqrt{3 - \kappa} \sin 2\theta}{3\kappa - 2 + \kappa \cos 2\theta}, \quad \sin \delta_{CP} = \sin \alpha_{21} = \sin \alpha_{31} = 0.
\end{aligned} \tag{3.33}$$

We see that θ_{23} deviates from maximal mixing and all the three CP violating phases are trivial due to a common CP transformation $\rho_r(1)$ of the charged lepton and neutrino sectors. The mixing angles θ_{12} , θ_{13} and θ_{23} only depend on the parameter θ , and they fulfill the following relations,

$$\sin^2 \theta_{12} \cos^2 \theta_{13} = \frac{3 - \kappa}{5}, \quad \sin^2 \theta_{23} = \frac{1}{2} \pm (\kappa - 1) \tan \theta_{13} \sqrt{1 + (\kappa - 2) \tan^2 \theta_{13}}, \tag{3.34}$$

which are plotted in Fig. 2. Obviously the mixing angles can be very close to the their measured values for certain values of the parameter θ . The global minimum of the χ^2 function is rather small, as shown in Table 1. The predictions for the effective mass $|m_{ee}|$ are also displayed in Fig. 2.

(IV) $X_{\nu r} = \rho_r(S), \rho_r(T^3 S T^2 S T^3 S)$

Invariance of the neutrino mass matrix m_ν under the action of these residual CP transformations implies that α, β, γ are real while δ is pure imaginary. The diagonalization matrix of m'_ν is

$$U'_\nu = \begin{pmatrix} i \cos \theta & 0 & i \sin \theta \\ 0 & 1 & 0 \\ -\sin \theta & 0 & \cos \theta \end{pmatrix}, \tag{3.35}$$

where

$$\tan 2\theta = -\frac{4i\sqrt{2 + \kappa} \delta}{3(\kappa\beta - 2\gamma)}. \tag{3.36}$$

The neutrino masses are given by

$$\begin{aligned}
m_1 &= \frac{1}{2} \left| -2\alpha + (3\kappa - 2)\beta + 2\gamma + \frac{3(\kappa\beta - 2\gamma)}{\cos 2\theta} \right|, \\
m_2 &= |\alpha + (3\kappa - 2)\beta + 2\gamma|, \\
m_3 &= \frac{1}{2} \left| -2\alpha + (3\kappa - 2)\beta + 2\gamma - \frac{3(\kappa\beta - 2\gamma)}{\cos 2\theta} \right|.
\end{aligned} \tag{3.37}$$

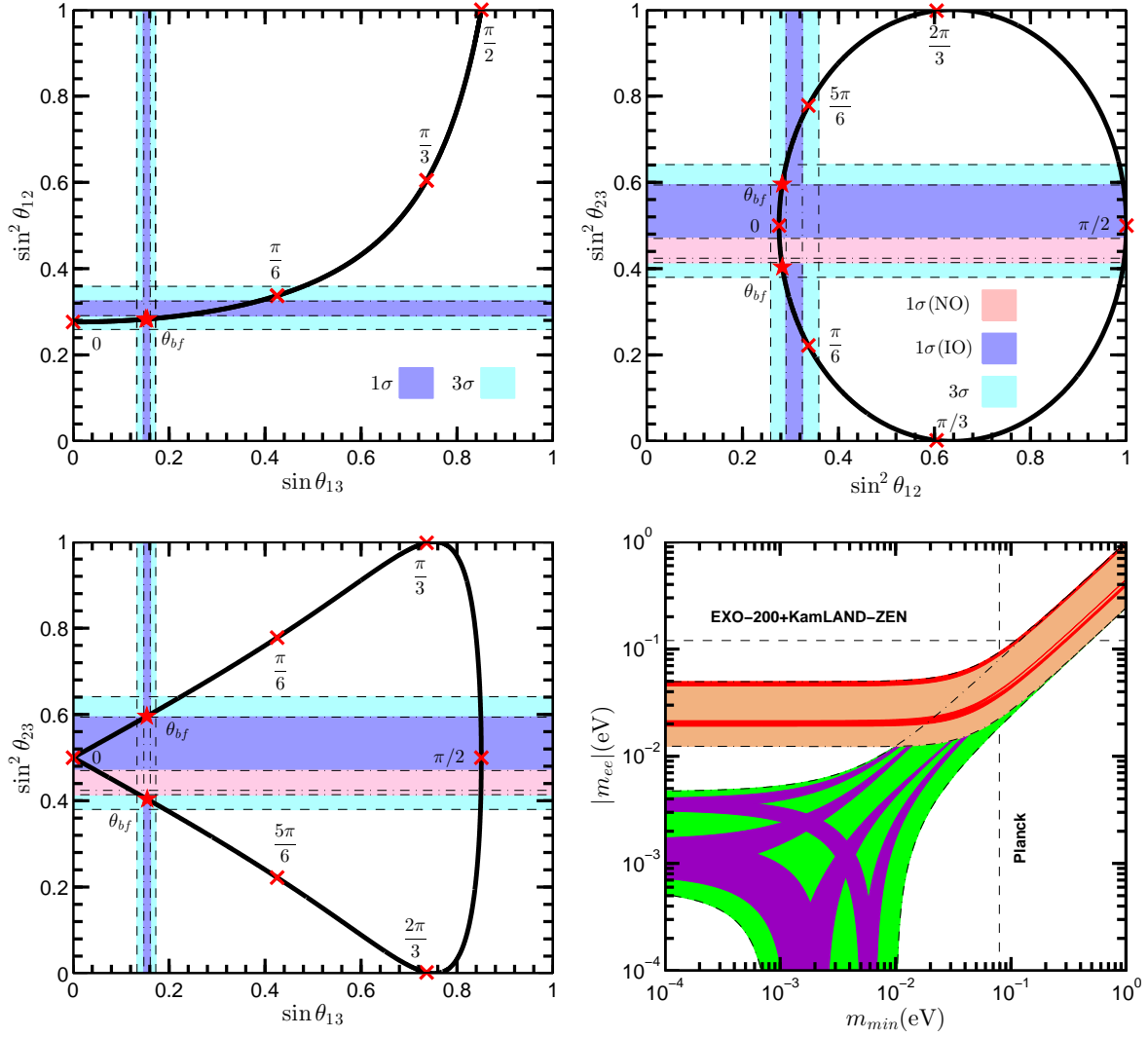


Figure 2: The correlation among $\sin^2 \theta_{12}$, $\sin^2 \theta_{23}$ and $\sin \theta_{13}$ (the former three panels) and the allowed values of the effective mass $|m_{ee}|$ (the last panel) in case III. The global minimum of the χ^2 function is labelled with a red pentagram, and the points for $\theta = 0, \pi/6, \pi/3, \pi/2, 2\pi/3$ and $5\pi/6$ are marked with a cross to guide the eye. The 1σ and 3σ ranges of the mixing angles are taken from Ref. [5]. In the last panel, the orange and green bands denote the 3σ regions for normal ordering and inverted ordering mass spectrum respectively. The red and purple areas are the predictions for the lepton mixing matrix in Eq. (3.32). The present most strict bound $|m_{ee}| < (0.120 - 0.250)$ eV from EXO-200 [40, 41] combined with KamLAND-ZEN [42] is represented by the horizontal dashed line, and the upper limit on m_{min} from the latest Planck result $m_1 + m_2 + m_3 < 0.230$ eV at 95% confidence level [43] is shown by vertical dashed line.

The PMNS matrix is of the form

$$U_{PMNS} = U_{GR} U'_\nu = \begin{pmatrix} -i\sqrt{\frac{\kappa}{\sqrt{5}}} \cos \theta & \sqrt{\frac{1}{\sqrt{5}\kappa}} & -i\sqrt{\frac{\kappa}{\sqrt{5}}} \sin \theta \\ \frac{i \cos \theta}{\sqrt{2\sqrt{5}\kappa}} + \frac{\sin \theta}{\sqrt{2}} & \sqrt{\frac{\kappa}{2\sqrt{5}}} & \frac{i \sin \theta}{\sqrt{2\sqrt{5}\kappa}} - \frac{\cos \theta}{\sqrt{2}} \\ \frac{i \cos \theta}{\sqrt{2\sqrt{5}\kappa}} - \frac{\sin \theta}{\sqrt{2}} & \sqrt{\frac{\kappa}{2\sqrt{5}}} & \frac{i \sin \theta}{\sqrt{2\sqrt{5}\kappa}} + \frac{\cos \theta}{\sqrt{2}} \end{pmatrix}. \quad (3.38)$$

The second column has the same form as for the GR mixing. The lepton mixing angles and CP phases are determined to be

$$\sin^2 \theta_{13} = \frac{\kappa}{\sqrt{5}} \sin^2 \theta, \quad \sin^2 \theta_{12} = \frac{4 - 2\kappa}{5 - 2\kappa + \cos 2\theta},$$

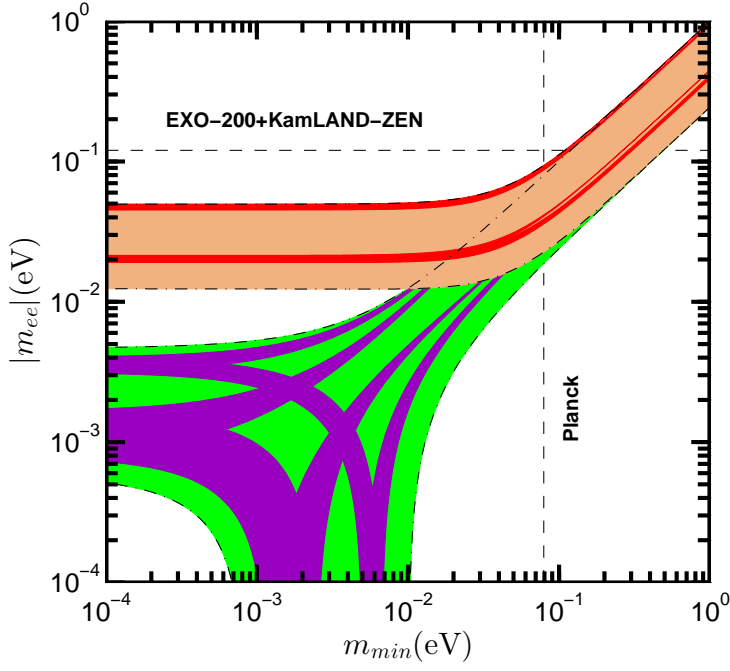


Figure 3: The $(\beta\beta)_{0\nu}$ -decay effective mass $|m_{ee}|$ with respect the lightest neutrino mass m_{min} in case IV. The orange and green bands denote the 3σ regions for normal ordering and inverted ordering mass spectrum respectively. The red and purple areas are the predictions for the lepton mixing matrix in Eq. (3.38). The present most strict bound $|m_{ee}| < (0.120 - 0.250)$ eV from EXO-200 [40, 41] combined with KamLAND-ZEN [42] is represented by the horizontal dashed line, and the upper limit on m_{min} from the latest Planck result $m_1 + m_2 + m_3 < 0.230$ eV at 95% confidence level [43] is shown by vertical dashed line. Note that the correlation between $\sin^2 \theta_{12}$ and $\sin \theta_{13}$ is the same as that of case III and can be found in Fig. 2.

$$\sin^2 \theta_{23} = \frac{1}{2}, \quad |\sin \delta_{CP}| = 1, \quad \sin \alpha_{21} = \sin \alpha_{31} = 0. \quad (3.39)$$

We see that both θ_{23} and δ_{CP} are maximal and the two Majorana CP phases α_{21} and α_{31} are trivial. Similar to case III, the relation $\sin^2 \theta_{12} \cos^2 \theta_{13} = (3 - \kappa)/5$ is satisfied as well. The best fitting results for the three mixing angles are listed in Table 1. The predictions for the $(\beta\beta)_{0\nu}$ -decay effective mass $|m_{ee}|$ are shown in Fig. 3.

3.3 $G_l = Z_3^{T^3 ST^2 S}$, $G_\nu = Z_2^{ST^2 ST^3 S}$

In the charged lepton sector, the remnant CP transformation H_{CP}^l is determined by the consistency condition

$$X_{l\mathbf{r}} \rho_{\mathbf{r}}^* (T^3 ST^2 S) X_{l\mathbf{r}}^{-1} = \rho_{\mathbf{r}}(g'), \quad g' \in Z_3^{T^3 ST^2 S}. \quad (3.40)$$

We find that there are 6 possible solutions for $X_{l\mathbf{r}}$, i.e.,

$$H_{CP}^l = \{\rho_{\mathbf{r}}(ST^3), \rho_{\mathbf{r}}(ST^3 S), \rho_{\mathbf{r}}(T^3), \rho_{\mathbf{r}}(T^3 S), \rho_{\mathbf{r}}(T^3 ST^2 ST^3), \rho_{\mathbf{r}}(T^3 ST^2 ST^3 S)\}. \quad (3.41)$$

The charged lepton mass matrix should respect both the remnant family symmetry $Z_3^{T^3 ST^2 S}$ and the remnant CP symmetry H_{CP}^l :

$$\rho_{\mathbf{3}}^\dagger (T^3 ST^2 S) m_l^\dagger m_l \rho_{\mathbf{3}} (T^3 ST^2 S) = m_l^\dagger m_l, \quad X_{l\mathbf{3}}^\dagger m_l^\dagger m_l X_{l\mathbf{3}} = (m_l^\dagger m_l)^*, \quad X_{l\mathbf{3}} \in H_{CP}^l. \quad (3.42)$$

Notice that the three residual CP transformations $X_{l\mathbf{r}} = \rho_{\mathbf{r}}(ST^3)$, $\rho_{\mathbf{r}}(T^3 S)$, $\rho_{\mathbf{r}}(T^3 ST^2 ST^3 S)$ lead to degenerate charged lepton masses since both $\rho_{\mathbf{r}}(ST^3)$ and $\rho_{\mathbf{r}}(T^3 S)$ are not symmetric.

For the remaining ones $X_{lr} = \rho_r(ST^3S)$, $\rho_r(T^3)$, $\rho_r(T^3ST^2ST^3)$, the hermitian combination $m_l^\dagger m_l$ is constrained to take the following form

$$m_l^\dagger m_l = \begin{pmatrix} a & 2(\kappa b + \sqrt{2}(2\kappa - 3)c) e^{-\frac{3\pi i}{5}} & 2\kappa b e^{-\frac{2\pi i}{5}} \\ 2(\kappa b + \sqrt{2}(2\kappa - 3)c) e^{\frac{3\pi i}{5}} & a + \frac{\sqrt{2}}{\kappa} b + (8\kappa - 14)c & 2(\kappa - 1) c e^{\frac{\pi i}{5}} \\ 2\kappa b e^{\frac{2\pi i}{5}} & 2(\kappa - 1) c e^{-\frac{\pi i}{5}} & a - \frac{\sqrt{2}}{\kappa} (b + \sqrt{2}c) \end{pmatrix}, \quad (3.43)$$

where a , b and c are real parameters. It can be diagonalized by the unitary matrix

$$U_l = \begin{pmatrix} \sqrt{\frac{7-4\kappa}{15}} e^{-\frac{2\pi i}{5}} & \sqrt{\frac{2\sqrt{5}\kappa}{15}} e^{\frac{3\pi i}{5}} & \sqrt{\frac{2\sqrt{5}\kappa}{15}} e^{-\frac{2\pi i}{5}} \\ \sqrt{\frac{2\sqrt{5}\kappa}{15}} e^{-\frac{4\pi i}{5}} & \frac{1}{2} \left(1 - \sqrt{\frac{7-4\kappa}{15}}\right) e^{\frac{\pi i}{5}} & \frac{1}{2} \left(1 + \sqrt{\frac{7-4\kappa}{15}}\right) e^{\frac{\pi i}{5}} \\ \sqrt{\frac{2\sqrt{5}\kappa}{15}} & \frac{1}{2} \left(1 + \sqrt{\frac{7-4\kappa}{15}}\right) & \frac{1}{2} \left(1 - \sqrt{\frac{7-4\kappa}{15}}\right) \end{pmatrix}, \quad (3.44)$$

with $U_l^\dagger m_l^\dagger m_l U_l = \text{diag}(m_e^2, m_\mu^2, m_\tau^2)$, where the charged lepton masses are

$$\begin{aligned} m_e^2 &= a - 4(\kappa - 1)c, & m_\mu^2 &= a - \sqrt{6(2 + \kappa)} b - \left(8 - 5\kappa + \sqrt{3(47 - 29\kappa)}\right) c, \\ m_\tau^2 &= a + \sqrt{6(2 + \kappa)} b + \left(5\kappa - 8 + \sqrt{3(47 - 29\kappa)}\right) c. \end{aligned} \quad (3.45)$$

The symmetry group $A_5 \rtimes H_{CP}$ is broken into $Z_2^{ST^2ST^3S} \times H_{CP}^\nu$ in the neutrino sector. By solving the restricted consistency equation of Eq. (2.12a), we find

$$H_{CP}^\nu = \{\rho_r(T^2), \rho_r(TST), \rho_r(T^3ST^2ST^3S), \rho_r((ST^2)^2S)\}. \quad (3.46)$$

The neutrino mass matrix preserving the remnant family symmetry $G_\nu = Z_2^{ST^2ST^3S}$ is of the form

$$m_\nu = \alpha \begin{pmatrix} 1 & 0 & 0 \\ 0 & 0 & 1 \\ 0 & 1 & 0 \end{pmatrix} + \beta \begin{pmatrix} 2 & 0 & 0 \\ 0 & 3e^{-\frac{4\pi i}{5}} & -1 \\ 0 & -1 & 3e^{\frac{4\pi i}{5}} \end{pmatrix} + \gamma \begin{pmatrix} 0 & e^{\frac{3\pi i}{5}} & e^{-\frac{3\pi i}{5}} \\ e^{\frac{3\pi i}{5}} & \sqrt{2}e^{\frac{\pi i}{5}} & 0 \\ e^{-\frac{3\pi i}{5}} & 0 & \sqrt{2}e^{-\frac{\pi i}{5}} \end{pmatrix} + \delta \begin{pmatrix} 2\sqrt{2} & e^{-\frac{2\pi i}{5}} & e^{\frac{2\pi i}{5}} \\ e^{-\frac{2\pi i}{5}} & \sqrt{2}e^{\frac{\pi i}{5}} & -\sqrt{2} \\ e^{\frac{2\pi i}{5}} & -\sqrt{2} & \sqrt{2}e^{-\frac{\pi i}{5}} \end{pmatrix}, \quad (3.47)$$

where parameters α , β , γ and δ are generally complex, and they are further constrained to be either real or imaginary by CP symmetry. It is convenient to firstly perform a constant unitary transformation U_{GRP} and yield

$$\begin{aligned} m'_\nu &= U_{GRP}^T m_\nu U_{GRP} \\ &= \begin{pmatrix} \alpha + 2\beta - \sqrt{2(1 + \kappa)} \gamma & 0 & -\sqrt{10} \delta \\ 0 & -\alpha + 4\beta - \sqrt{2} \gamma & 0 \\ -\sqrt{10} \delta & 0 & \alpha + 2\beta + \sqrt{2(2 - \kappa)} \gamma \end{pmatrix}, \end{aligned} \quad (3.48)$$

where

$$U_{GRP} = \begin{pmatrix} \sqrt{\frac{1}{\sqrt{5}\kappa}} & 0 & -\sqrt{\frac{\kappa}{\sqrt{5}}} \\ \sqrt{\frac{\kappa}{2\sqrt{5}}} e^{\frac{2\pi i}{5}} & \frac{1}{\sqrt{2}} e^{-\frac{3\pi i}{5}} & \frac{1}{\sqrt{2\sqrt{5}\kappa}} e^{\frac{2\pi i}{5}} \\ \sqrt{\frac{\kappa}{2\sqrt{5}}} e^{-\frac{2\pi i}{5}} & \frac{1}{\sqrt{2}} e^{-\frac{2\pi i}{5}} & \frac{1}{\sqrt{2\sqrt{5}\kappa}} e^{-\frac{2\pi i}{5}} \end{pmatrix}. \quad (3.49)$$

Next we discuss the constraints of the residual CP symmetry on the neutrino mass matrix m_ν .

(V) $X_{\nu\mathbf{r}} = \rho_{\mathbf{r}}(T^2), \rho_{\mathbf{r}}(T^3ST^2ST^3S)$

In this case, α, β, γ and δ are determined to be real. Then neutrino mass matrix m'_ν is a real symmetric matrix, and it can be diagonalized by a rotation matrix U'_ν in the (2,3) sector,

$$U'_\nu = \begin{pmatrix} \cos \theta & 0 & -\sin \theta \\ 0 & 1 & 0 \\ \sin \theta & 0 & \cos \theta \end{pmatrix}, \quad (3.50)$$

with

$$\tan 2\theta = 2\delta/\gamma. \quad (3.51)$$

The three light neutrino masses are given by

$$\begin{aligned} m_1 &= \frac{1}{2} \left| 2\alpha + 4\beta - \sqrt{2}\gamma - \frac{\sqrt{10}\gamma}{\cos 2\theta} \right|, \\ m_2 &= \left| -\alpha + 4\beta - \sqrt{2}\gamma \right|, \\ m_3 &= \frac{1}{2} \left| 2\alpha + 4\beta - \sqrt{2}\gamma + \frac{\sqrt{10}\gamma}{\cos 2\theta} \right|. \end{aligned} \quad (3.52)$$

The lepton mixing matrix is of the form

$$U_{PMNS} = U_l^\dagger U_{GRP} U'_\nu = \frac{1}{\sqrt{3}} \begin{pmatrix} \cos \theta + \sin \theta & 1 & \cos \theta - \sin \theta \\ e^{\frac{2\pi i}{3}} \cos \theta - e^{\frac{\pi i}{3}} \sin \theta & 1 & e^{\frac{4\pi i}{3}} \cos \theta - e^{\frac{2\pi i}{3}} \sin \theta \\ e^{\frac{4\pi i}{3}} \cos \theta + e^{\frac{2\pi i}{3}} \sin \theta & 1 & e^{\frac{2\pi i}{3}} \cos \theta + e^{\frac{\pi i}{3}} \sin \theta \end{pmatrix}. \quad (3.53)$$

We see that the second column of the PMNS matrix is $(1, 1, 1)^T / \sqrt{3}$, which frequently appears in discrete flavor symmetry models. The leptonic mixing parameters read as²

$$\begin{aligned} \sin^2 \theta_{13} &= \frac{1}{3}(1 - \sin 2\theta), \quad \sin^2 \theta_{12} = \frac{1}{2 + \sin 2\theta}, \quad \sin^2 \theta_{23} = \frac{1}{2}, \\ |\sin \delta_{CP}| &= 1, \quad \sin \alpha_{21} = \sin \alpha_{31} = 0. \end{aligned} \quad (3.54)$$

Both Dirac CP phase and θ_{23} are maximal while Majorana CP phases are conserved in this case. In common with all trimaximal mixings, θ_{12} and θ_{13} are related with each other by

$$3 \sin^2 \theta_{12} \cos^2 \theta_{13} = 1. \quad (3.55)$$

The measured 3σ range $0.0176 \leq \sin^2 \theta_{13} \leq 0.0295$ [5] gives rise to $0.339 \leq \sin^2 \theta_{12} \leq 0.343$ which can be directly tested by JUNO in near future [44]. The correlation between θ_{12} and θ_{13} and the predictions for the $(\beta\beta)_{0\nu}$ -decay are displayed in Fig. 4. All the three mixing angles can agree within 3σ with the experimental data for certain values of θ . The best fitting results are listed in Table 1, and the minimum values of the χ^2 functions are 3.987 and 7.480 for IO and NO, respectively.

(VI) $X_{\nu\mathbf{r}} = \rho_{\mathbf{r}}(TST), \rho_{\mathbf{r}}((ST^2)^2S)$

The requirement of real α, β, γ and pure imaginary δ follows immediately from the remnant CP invariant condition. In the same way as previous cases, the PMNS mixing matrix is found to be

$$U_{PMNS} = \frac{1}{\sqrt{3}} \begin{pmatrix} e^{\frac{5\pi i}{6}} \cos \theta + e^{\frac{2\pi i}{3}} \sin \theta & 1 & e^{\frac{2\pi i}{3}} \cos \theta - e^{\frac{5\pi i}{6}} \sin \theta \\ e^{\frac{\pi i}{6}} \cos \theta - e^{\frac{\pi i}{3}} \sin \theta & 1 & e^{\frac{4\pi i}{3}} \cos \theta + e^{\frac{7\pi i}{6}} \sin \theta \\ \sin \theta - i \cos \theta & 1 & \cos \theta + i \sin \theta \end{pmatrix}, \quad (3.56)$$

²For $\cos 2\theta = 0$, we have $\sin \theta_{13} = 0$ or $\cos \theta_{12} = 0$ so that δ_{CP} cannot be determined uniquely.

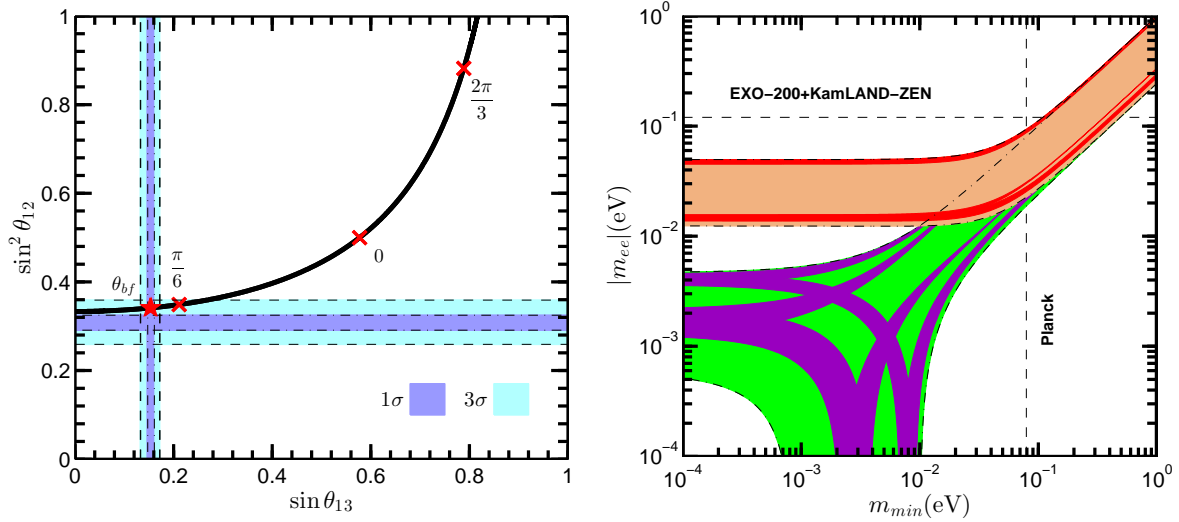


Figure 4: Results for $\sin^2 \theta_{12}$ and $\sin \theta_{13}$ (left panel) and the allowed values of the effective mass $|m_{ee}|$ (right panel) in case V. On the left panel, the best fitting value is labelled with a red pentagram, and the points for $\theta = 0, \pi/6$ and $2\pi/3$ are marked with a cross to guide the eye. The 1σ and 3σ ranges of the mixing angles are taken from Ref. [5]. On the right panel, the orange and green bands denote the 3σ regions for normal ordering and inverted ordering mass spectrum respectively. The red and purple areas are the predictions for the lepton mixing matrix in Eq. (3.53). The present most strict bound $|m_{ee}| < (0.120 - 0.250)$ eV from EXO-200 [40, 41] combined with KamLAND-ZEN [42] is represented by the horizontal dashed line, and the upper limit on m_{min} from the latest Planck result $m_1 + m_2 + m_3 < 0.230$ eV at 95% confidence level [43] is shown by vertical dashed line.

The expressions for the lepton mixing parameters are as follows,

$$\begin{aligned} \sin^2 \theta_{13} &= \frac{1}{3} - \frac{\sqrt{3} \sin 2\theta}{6}, \quad \sin^2 \theta_{12} = \frac{2}{4 + \sqrt{3} \sin 2\theta}, \\ \sin^2 \theta_{23} &= \frac{2 + \sqrt{3} \sin 2\theta}{4 + \sqrt{3} \sin 2\theta}, \quad |\sin \delta_{CP}| = \left| \frac{8 \cos 2\theta + \sqrt{3} \sin 4\theta}{2(2 + \sqrt{3} \sin 2\theta) \sqrt{4 - 2\sqrt{3} \sin 2\theta}} \right|, \\ |\sin \alpha_{21}| &= \left| \frac{2 \sin 2\theta + \sqrt{3}}{2 + \sqrt{3} \sin 2\theta} \right|, \quad |\sin \alpha'_{31}| = \left| \frac{4\sqrt{3} \cos 2\theta}{5 + 3 \cos 4\theta} \right|, \end{aligned} \quad (3.57)$$

where $\alpha'_{31} = \alpha_{31} - 2\delta_{CP}$. It is remarkable that all the three CP violating phases nontrivially depend on the parameter θ . However, we see that in case of $\theta = \pi/4$ the minimum value of θ_{13} is obtained with $\sin^2 \theta_{13}|_{\theta=\pi/4} = (2 - \sqrt{3})/6 \simeq 0.0447$ which is outside the 3σ range [5]. Furthermore, we note that the atmospheric angle θ_{23} is the complementary angle of θ_{12} or is equal to θ_{12} if the second and the third rows of the PMNS matrix is interchanged. As a result, this mixing pattern is not compatible with experimental data and consequently we don't included it in Table 1.

3.4 $G_l = K_4^{(ST^2 ST^3 S, TST^4)}, G_\nu = Z_2^S$

In the last case, the residual symmetries are assumed to be $K_4^{(ST^2 ST^3 S, TST^4)} \rtimes H_{CP}^l$ in the charged lepton sector and $Z_2^S \times H_{CP}^\nu$ in the neutrino sector. For the remnant family symmetry $K_4^{(ST^2 ST^3 S, TST^4)}$ to hold, the mass matrix $m_l^\dagger m_l$ has to fulfill

$$\rho_3^\dagger(ST^2 ST^3 S)m_l^\dagger m_l \rho_3(ST^2 ST^3 S) = m_l^\dagger m_l, \quad \rho_3^\dagger(TST^4)m_l^\dagger m_l \rho_3(TST^4) = m_l^\dagger m_l. \quad (3.58)$$

Then $m_l^\dagger m_l$ is constrained to take the form

$$m_l^\dagger m_l = \begin{pmatrix} a & 2\kappa b e^{-\frac{2\pi i}{5}} & 2\kappa b e^{\frac{2\pi i}{5}} \\ 2\kappa b e^{\frac{2\pi i}{5}} & a + 2\sqrt{2}\kappa b + 2(\kappa - 1)c & 2(\kappa - 1)ce^{-\frac{\pi i}{5}} \\ 2\kappa b e^{-\frac{2\pi i}{5}} & 2(\kappa - 1)ce^{\frac{\pi i}{5}} & a + 2\sqrt{2}\kappa b + 2(\kappa - 1)c \end{pmatrix}, \quad (3.59)$$

where a , b and c are real. It is diagonalized by the unitary matrix

$$U_l = \begin{pmatrix} \sqrt{\frac{\kappa}{\sqrt{5}}} & 0 & \sqrt{\frac{1}{\sqrt{5}\kappa}} \\ \frac{1}{\sqrt{2\sqrt{5}\kappa}}e^{-\frac{3\pi i}{5}} & \frac{1}{\sqrt{2}}e^{-\frac{\pi i}{10}} & \sqrt{\frac{\kappa}{2\sqrt{5}}}e^{\frac{2\pi i}{5}} \\ \frac{1}{\sqrt{2\sqrt{5}\kappa}}e^{\frac{3\pi i}{5}} & \frac{1}{\sqrt{2}}e^{\frac{\pi i}{10}} & \sqrt{\frac{\kappa}{2\sqrt{5}}}e^{-\frac{2\pi i}{5}} \end{pmatrix}, \quad (3.60)$$

with $U_l^\dagger m_l^\dagger m_l U_l = \text{diag}(m_e^2, m_\mu^2, m_\tau^2)$ where

$$m_e^2 = a - 2\sqrt{2}b, \quad m_\mu^2 = a + 2\sqrt{2}\kappa b + 4(\kappa - 1)c, \quad m_\tau^2 = a + 2\sqrt{2}\kappa^2 b. \quad (3.61)$$

The mass matrix $m_l^\dagger m_l$ is also subject to the constraint of the residual CP symmetry H_{CP}^l . It is straightforward to determine that H_{CP}^l can take the value

$$H_{CP}^l = \{ \rho_{\mathbf{r}}(ST^2ST), \rho_{\mathbf{r}}((ST^2)^2S), \rho_{\mathbf{r}}(ST^3), \rho_{\mathbf{r}}(T^2), \rho_{\mathbf{r}}((T^2S)^2T^3), \rho_{\mathbf{r}}(T^2ST^4), \rho_{\mathbf{r}}(T^3S), \\ \rho_{\mathbf{r}}(T^3(ST^2)^2), \rho_{\mathbf{r}}(T^3ST^2ST^3S), \rho_{\mathbf{r}}(T^4ST^2), \rho_{\mathbf{r}}(TST^2S), \rho_{\mathbf{r}}(TST) \}. \quad (3.62)$$

The twelve CP transformations can be classified into two categories. For $X_{l\mathbf{r}} = \rho_{\mathbf{r}}((ST^2)^2S)$, $\rho_{\mathbf{r}}(T^2)$, $\rho_{\mathbf{r}}(T^3ST^2ST^3S)$, $\rho_{\mathbf{r}}(TST)$, the remnant CP invariant condition $X_{l\mathbf{3}}^\dagger m_l^\dagger m_l X_{l\mathbf{3}} = (m_l^\dagger m_l)^*$ is automatically satisfied, and therefore no additional constraint is produced. Nevertheless, the remaining eight CP transformations $X_{l\mathbf{r}} = \rho_{\mathbf{r}}(ST^2ST)$, $\rho_{\mathbf{r}}(ST^3)$, $\rho_{\mathbf{r}}((T^2S)^2T^3)$, $\rho_{\mathbf{r}}(T^2ST^4)$, $\rho_{\mathbf{r}}(T^3S)$, $\rho_{\mathbf{r}}(T^3(ST^2)^2)$, $\rho_{\mathbf{r}}(T^4ST^2)$ and $\rho_{\mathbf{r}}(TST^2S)$ are not viable, as they require $b = c = 0$ so that the charged lepton mass spectrum is completely degenerate with $m_e^2 = m_\mu^2 = m_\tau^2 = a$. In neutrino sector, the remnant symmetry $Z_2^S \times H_{CP}^\nu$ and its phenomenological implications have been studied in section 3.1. The neutrino mass matrix m_ν is found to be given by Eq. (3.8), where the parameters α , β and γ are real while δ is real or pure imaginary depending on the residual CP transformation $X_{\nu\mathbf{r}}$.

(VII) $X_{\nu\mathbf{r}} = \rho_{\mathbf{r}}(T^3ST^2ST^3)$, $\rho_{\mathbf{r}}(T^3ST^2ST^3S)$

In this case, the neutrino mass matrix is diagonalized by the unitary matrix in Eq. (3.21). Combining the unitary transformation U_l in Eq. (3.60) from the charged lepton sector, we obtain the lepton flavor mixing matrix:

$$U_{PMNS} = \frac{1}{2} \begin{pmatrix} \kappa & \cos \theta + (\kappa - 1) \sin \theta & (\kappa - 1) \cos \theta - \sin \theta \\ -1 & (\kappa - 1) \cos \theta + \kappa \sin \theta & \kappa \cos \theta - (\kappa - 1) \sin \theta \\ \kappa - 1 & \sin \theta - \kappa \cos \theta & \cos \theta + \kappa \sin \theta \end{pmatrix}, \quad (3.63)$$

where the parameter θ is specified by Eq. (3.19). The lepton mixing parameters are predicted to be

$$\sin^2 \theta_{13} = \frac{(\cos \theta - \kappa \sin \theta)^2}{4\kappa^2}, \quad \sin^2 \theta_{12} = \frac{(\kappa \cos \theta + \sin \theta)^2}{4\kappa^2 - (\cos \theta - \kappa \sin \theta)^2}, \\ \sin^2 \theta_{23} = \frac{(\kappa^2 \cos \theta - \sin \theta)^2}{4\kappa^2 - (\cos \theta - \kappa \sin \theta)^2}, \quad \sin \delta_{CP} = \sin \alpha_{21} = \sin \alpha_{31} = 0. \quad (3.64)$$

We find all the three CP violating phases δ_{CP} , α_{21} and α_{31} are conserved, this is because that a common CP transformation $\rho_{\mathbf{r}}(T^3 S T^2 S T^3 S)$ is shared by the neutrino and charged lepton sectors. In addition, θ_{23} deviates from maximal value. After some tedious calculations, we find the following relations between the mixing angles

$$4 \cos^2 \theta_{12} \cos^2 \theta_{13} = 1 + \kappa, \quad 5 \sin^2 \theta_{23} = 3 - \kappa + (1 + 2\kappa) \tan^2 \theta_{13} \pm 2\kappa \tan \theta_{13} \sqrt{2 + \kappa - (2 + 3\kappa) \tan^2 \theta_{13}}, \quad (3.65)$$

which is plotted in Fig. 5. For the 3σ interval $0.0176 \leq \sin^2 \theta_{13} \leq 0.0295$ [5], we have $0.326 \leq \sin^2 \theta_{12} \leq 0.334$ and $0.454 \leq \sin^2 \theta_{23} \leq 0.511$, which are in the experimentally favored ranges [5]. The global minimum of the χ^2 function is rather small 3.503 (1.626) for NO (IO) neutrino mass spectrum, therefore this mixing pattern can describe the experimental data very well. Moreover, we note that the best fitting value of θ_{23} is in the first octant with $\sin^2 \theta_{23}(\theta_{bf}) = 0.480$ (0.486) for NO (IO) spectrum. Agreement with experimental data can also be achieved if the second and third rows of the PMNS matrix in Eq. (3.63) are exchanged. Then the atmospheric mixing angle θ_{23} changes to

$$\sin^2 \theta_{23} = \frac{\kappa^2 (\cos \theta + \kappa \sin \theta)^2}{4\kappa^2 - (\cos \theta - \kappa \sin \theta)^2}, \quad (3.66)$$

and the predictions for the other mixing parameters remain as Eq. (3.64). The allowed region of $\sin^2 \theta_{23}$ becomes $0.489 \leq \sin^2 \theta_{23} \leq 0.546$ with the best fitting value $\sin^2 \theta_{23}(\theta_{bf}) = 0.510$ (0.513) for NO (IO) spectrum. Obviously $\theta_{23}(\theta_{bf})$ is in the second octant. Comparing with other mixing patterns shown in Table 1, we see that this case gives rise to the smallest χ_{min}^2 for both NO and IO. The above predictions for solar and atmospheric mixing angles could be tested directly in near future, since the next generation neutrino oscillation experiments are expected to reduce the experimental error on θ_{12} and θ_{23} to few degrees. The theoretical results for the $(\beta\beta)_{0\nu}$ -decay effective mass $|m_{ee}|$ are displayed in Fig. 5. Note that interchanging the second and third rows doesn't matter since $|m_{ee}|$ is independent of θ_{23} . Again, the predictions for IO neutrino spectrum are within the sensitivity of forthcoming experiments.

(VIII) $X_{\nu\mathbf{r}} = \rho_{\mathbf{r}}(1), \rho_{\mathbf{r}}(S)$

The neutrino mass matrix is diagonalized by the unitary transformation in Eq. (3.15). The PMNS matrix is found to take the following form

$$U_{PMNS} = \frac{1}{2} \begin{pmatrix} \sin \theta - i\kappa \cos \theta & \cos \theta + i\kappa \sin \theta & \kappa - 1 \\ i \cos \theta + (\kappa - 1) \sin \theta & (\kappa - 1) \cos \theta - i \sin \theta & \kappa \\ i(\kappa - 1) \cos \theta + \kappa \sin \theta & \kappa \cos \theta - i(\kappa - 1) \sin \theta & -1 \end{pmatrix}, \quad (3.67)$$

up to permutations of rows and columns. The lepton mixing angles and CP phases can be read off as

$$\sin^2 \theta_{13} = \frac{3 - \sqrt{5}}{8} \simeq 0.0955, \quad \sin^2 \theta_{12} = \frac{1}{2} - \frac{\sqrt{5}}{10} \cos 2\theta, \quad \sin^2 \theta_{23} = \frac{5 + \sqrt{5}}{10} \simeq 0.724, \\ |\sin \delta_{CP}| = \left| \frac{\sqrt{10} \sin 2\theta}{\sqrt{9 - \cos 4\theta}} \right|, \quad |\sin \alpha_{21}| = \left| \frac{8 \sin 2\theta}{9 - \cos 4\theta} \right|, \quad |\sin \alpha'_{31}| = \left| \frac{2 \sin 2\theta}{\sqrt{5} + \cos 2\theta} \right|. \quad (3.68)$$

We see that the solar mixing angle θ_{12} has a lower bound given by $\sin^2 \theta_{12} \geq (5 - \sqrt{5})/10 \simeq 0.276$, and the experimental data on θ_{12} can be accommodated for particular values of θ . Both θ_{13} and θ_{23} are independent of θ , and they are outside the 3σ ranges [5]. Furthermore, $6 \times 6 = 36$ possible permutations of rows and columns of this mixing pattern are considered. However, none of them can give rise to three mixing angles in the experimentally preferred 3σ range [5].

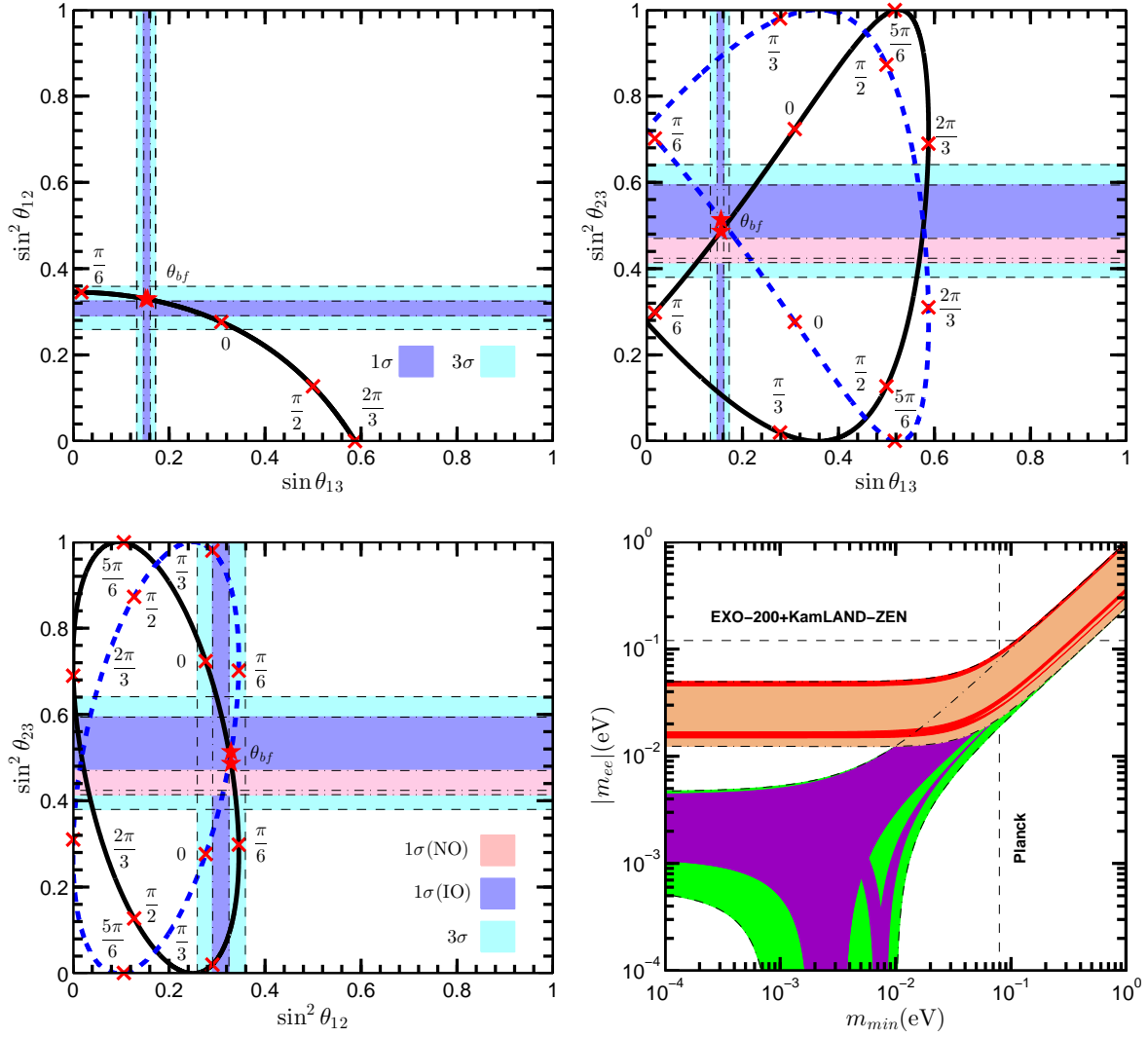


Figure 5: The results for $\sin^2 \theta_{12}$, $\sin^2 \theta_{23}$ and $\sin \theta_{13}$ (the former three panels) and the allowed values of the effective mass $|m_{ee}|$ (the last panel) in case VII. The global minimum of the χ^2 function is labelled with a red pentagram, and the points for $\theta = 0, \pi/6, \pi/3, \pi/2, 2\pi/3$ and $5\pi/6$ are marked with a cross to guide the eye. The black solid lines and blue dashed lines in the upper-right and lower-left panels represent the two solutions for θ_{23} shown in Eq. (3.64) and Eq. (3.66) respectively. The corresponding PMNS matrices are related through a exchange of the second and third rows. The 1σ and 3σ ranges of the mixing angles are taken from Ref. [5]. In the last panel, the orange and green bands denote the 3σ regions for normal ordering and inverted ordering mass spectrum respectively. The red and purple areas are the predictions for the lepton mixing matrix in Eq. (3.63). The present most strict bound $|m_{ee}| < (0.120 - 0.250)$ eV from EXO-200 [40,41] combined with KamLAND-ZEN [42] is represented by the horizontal dashed line, while the upper limit on m_{min} from the latest Planck result $m_1 + m_2 + m_3 < 0.230$ eV at 95% confidence level [43] is shown by dashed line.

4 Model building

In previous section, we have performed a model-independent analysis of the lepton mixing patterns which can be derived from $A_5 \rtimes H_{CP}$. As summarized in Table 1, we find five new mixing patterns which are compatible with current experimental data. In this section, we shall construct a concrete model with both A_5 family symmetry and generalized CP symmetry, the symmetry breaking patterns studied in section 3.2 are implemented, and therefore the lepton flavor mixings given by Eqs. (3.32, 3.38) in case III and case IV are realized. Note that it would be also interesting to implement other cases such as case VII in

Field	l	ν^c	e^c	μ^c	τ^c	$h_{u,d}$	φ	ϕ	ψ	ξ	ζ	χ	ρ	Δ	σ^0	ϕ^0	ψ^0	ξ^0	χ^0	ρ^0	Δ^0
A_5	3	3	1	1	1	1	3	3'	5	1	1	3	3'	5	1	4	5	1	3	3	5
Z_3	ω_3	1	ω_3^2	ω_3^2	ω_3^2	1	1	1	ω_3^2	ω_3	ω_3	ω_3	ω_3	ω_3^2	1	1	1	ω_3	1	1	ω_3
Z_4	-1	1	-1	-1	-1	1	1	1	-1	i	i	- i	-1	1	1	1	-1	i	- i	-1	-1
Z_6	1	1	ω_6	ω_6^2	ω_6^5	1	ω_6	ω_6^2	ω_6^2	1	1	1	1	1	ω_6^4	ω_6^3	ω_6^4	1	1	1	1
$U(1)_R$	1	1	1	1	1	0	0	0	0	0	0	0	0	0	2	2	2	2	2	2	2

Table 2: The matter fields, flavon fields, driving fields and their transformation properties under the family symmetry $A_5 \times Z_3 \times Z_4 \times Z_6$ and $U(1)_R$, where the phase $\omega_3 = e^{\frac{2i\pi}{3}}$ and $\omega_6 = e^{\frac{i\pi}{3}}$.

a model. In the present model, both the three generations of left-handed lepton doublets l and the three generations of right-handed neutrinos ν^c are assigned to transform as A_5 triplet **3**, while the right-handed charged leptons e^c , μ^c and τ^c are all invariant under A_5 . In discrete flavor symmetry model building, either cyclic Z_n or continuous $U(1)$ symmetry is frequently introduced to eliminate unwanted operators, to ensure the required vacuum alignment and to reproduce the observed charged lepton mass hierarchies. The auxiliary symmetry is taken to be $Z_3 \times Z_4 \times Z_6$ in this model. The A_5 family symmetry and CP symmetry are broken by some flavons in a proper manner. All the flavon fields are standard model gauge singlets. As anticipated, we formulate our model in the framework of supersymmetry (SUSY). A $U(1)_R$ symmetry related to R -parity and the presence of driving fields in the flavon superpotential are common features of supersymmetric formulations. The field content of the model and their classification under the symmetry are listed in Table 2. In the following, we first discuss the vacuum alignment of the model, then specify the structure of the model at leading order and next-to-leading order. As we shall show, the lepton mixing is exactly the GR at LO, and a non-vanishing value of the reactor mixing angle θ_{13} is generated by higher order corrections. Consequently θ_{13} is naturally of the correct order in our model.

4.1 Vacuum alignment

We utilize the standard supersymmetric driving field mechanism [45] to solve the vacuum alignment problem. A global $U(1)_R$ continuous symmetry is assumed in this approach, and the usual R -parity is a discrete group of this $U(1)_R$. The matter fields have R -charge equal to one, both flavon fields and Higgs are chargeless and the driving fields carry two units of R -charge. At LO the most general driving superpotential w_d invariant under $A_5 \times Z_3 \times Z_4 \times Z_6$ with $R = 2$ can be written as

$$w_d = w_d^l + w_d^\nu, \quad (4.1)$$

with

$$w_d^l = f_1 \sigma^0 (\varphi \varphi)_1 + f_2 (\phi^0 (\varphi \phi)_4)_1 + f_3 (\phi^0 (\varphi \psi)_4)_1 + M_\psi (\psi^0 \psi)_1 + f_4 (\psi^0 (\varphi \varphi)_5)_1, \quad (4.2)$$

$$w_d^\nu = M_\xi \xi^0 \xi + g_1 \xi^0 \zeta^2 + g_2 \xi^0 (\chi \chi)_1 + g_3 \xi^0 (\rho \rho)_1 + g_4 \xi (\chi^0 \chi)_1 + g_5 (\chi^0 (\chi \Delta)_3)_1 \\ + g_6 (\rho^0 (\rho \Delta)_3)_1 + M_\Delta (\Delta^0 \Delta)_1 + g_7 (\Delta^0 (\chi \chi)_5)_1 + g_8 (\Delta^0 (\rho \rho)_5)_1, \quad (4.3)$$

where $(\dots)_\mathbf{R}$ denotes a contraction into the A_5 irreducible representation \mathbf{R} according to the Clebsch-Gordan coefficients listed in Appendix A. Notice that all the couplings f_i ($i = 1, \dots, 4$), g_i ($i = 1, \dots, 8$) and the mass parameters M_ψ , M_ξ , M_Δ are real, since the theory is invariant under the generalized CP defined in Eq. (2.9). In the SUSY limit, the vacuum alignment is achieved via the requirement of vanishing F -terms of the driving fields. In the

charged lepton sector, the equations for the vanishing of the derivatives of w_d^l with respect to each component of the driving fields are:

$$\begin{aligned}
\frac{\partial w_d^l}{\partial \sigma^0} &= f_1(\varphi_1^2 + 2\varphi_2\varphi_3) = 0, \\
\frac{\partial w_d^l}{\partial \phi_1^0} &= f_2(\varphi_2\phi_3 + \sqrt{2}\varphi_3\phi_1) - f_3(2\sqrt{2}\varphi_1\psi_5 + \varphi_2\psi_4 - \sqrt{6}\varphi_3\psi_1) = 0, \\
\frac{\partial w_d^l}{\partial \phi_2^0} &= -f_2(\sqrt{2}\varphi_1\phi_3 + \varphi_2\phi_2) + f_3(\sqrt{2}\varphi_1\psi_4 + 3\varphi_2\psi_3 - 2\varphi_3\psi_5) = 0, \\
\frac{\partial w_d^l}{\partial \phi_3^0} &= -f_2(\sqrt{2}\varphi_1\phi_2 + \varphi_3\phi_3) - f_3(\sqrt{2}\varphi_1\psi_3 - 2\varphi_2\psi_2 + 3\varphi_3\psi_4) = 0, \\
\frac{\partial w_d^l}{\partial \phi_4^0} &= f_2(\sqrt{2}\varphi_2\phi_1 + \varphi_3\phi_2) + f_3(2\sqrt{2}\varphi_1\psi_2 - \sqrt{6}\varphi_2\psi_1 + \varphi_3\psi_3) = 0, \\
\frac{\partial w_d^l}{\partial \psi_1^0} &= M_\psi\psi_1 + 2f_4(\varphi_1^2 - \varphi_2\varphi_3) = 0, \\
\frac{\partial w_d^l}{\partial \psi_2^0} &= M_\psi\psi_5 - 2\sqrt{3}f_4\varphi_1\varphi_3 = 0, \\
\frac{\partial w_d^l}{\partial \psi_3^0} &= M_\psi\psi_4 + \sqrt{6}f_4\varphi_3^2 = 0, \\
\frac{\partial w_d^l}{\partial \psi_4^0} &= M_\psi\psi_3 + \sqrt{6}f_4\varphi_2^2 = 0, \\
\frac{\partial w_d^l}{\partial \psi_5^0} &= M_\psi\psi_2 - 2\sqrt{3}f_4\varphi_1\varphi_2 = 0,
\end{aligned} \tag{4.4}$$

We find one solution to those equations,

$$\langle \varphi \rangle = \begin{pmatrix} 0 \\ 1 \\ 0 \end{pmatrix} v_\varphi, \quad \langle \phi \rangle = \begin{pmatrix} 0 \\ 1 \\ 0 \end{pmatrix} v_\phi, \quad \langle \psi \rangle = \begin{pmatrix} 0 \\ 0 \\ 1 \\ 0 \\ 0 \end{pmatrix} v_\psi, \tag{4.5}$$

up to A_5 family symmetry transformations, where the vacuum expectation values (VEVs) v_φ , v_ϕ and v_ψ are related by

$$v_\phi = -\frac{3\sqrt{6}f_3f_4}{M_\psi f_2}v_\varphi^2, \quad v_\psi = -\frac{\sqrt{6}f_4}{M_\psi}v_\varphi^2, \tag{4.6}$$

with v_φ undetermined. A common order of magnitude for the VEVs (scaled by the cutoff Λ) is expected. In order to generate the mass hierarchies among the charged lepton, we assume

$$\frac{v_\varphi}{\Lambda} \sim \frac{v_\phi}{\Lambda} \sim \frac{v_\psi}{\Lambda} \sim \mathcal{O}(\lambda_c^2), \tag{4.7}$$

where $\lambda_c \simeq 0.23$ is the Cabibbo angle [1]. In the neutrino sector, the minimization equations for the vacuum are

$$\begin{aligned}
\frac{\partial w_d^\nu}{\partial \xi^0} &= M_\xi\xi + g_1\zeta^2 + g_2(\chi_1^2 + 2\chi_2\chi_3) + g_3(\rho_1^2 + 2\rho_2\rho_3) = 0, \\
\frac{\partial w_d^\nu}{\partial \chi_1^0} &= g_4\xi\chi_1 - g_5(2\chi_1\Delta_1 - \sqrt{3}\chi_2\Delta_5 - \sqrt{3}\chi_3\Delta_2) = 0,
\end{aligned}$$

$$\begin{aligned}
\frac{\partial w_d^\nu}{\partial \chi_2^0} &= g_4 \xi \chi_3 + g_5 (\sqrt{3} \chi_1 \Delta_5 - \sqrt{6} \chi_2 \Delta_4 + \chi_3 \Delta_1) = 0, \\
\frac{\partial w_d^\nu}{\partial \chi_3^0} &= g_4 \xi \chi_2 + g_5 (\sqrt{3} \chi_1 \Delta_2 + \chi_2 \Delta_1 - \sqrt{6} \chi_3 \Delta_3) = 0, \\
\frac{\partial w_d^\nu}{\partial \rho_1^0} &= g_6 (\sqrt{3} \rho_1 \Delta_1 + \rho_2 \Delta_4 + \rho_3 \Delta_3) = 0, \\
\frac{\partial w_d^\nu}{\partial \rho_2^0} &= g_6 (\rho_1 \Delta_5 - \sqrt{2} \rho_2 \Delta_3 - \sqrt{2} \rho_3 \Delta_2) = 0, \\
\frac{\partial w_d^\nu}{\partial \rho_3^0} &= g_6 (\rho_1 \Delta_2 - \sqrt{2} \rho_2 \Delta_5 - \sqrt{2} \rho_3 \Delta_4) = 0, \\
\frac{\partial w_d^\nu}{\partial \Delta_1^0} &= M_\Delta \Delta_1 + 2g_7 (\chi_1^2 - \chi_2 \chi_3) + 2g_8 (\rho_1^2 - \rho_2 \rho_3) = 0, \\
\frac{\partial w_d^\nu}{\partial \Delta_2^0} &= M_\Delta \Delta_5 - 2\sqrt{3} g_7 \chi_1 \chi_3 + \sqrt{6} g_8 \rho_2^2 = 0, \\
\frac{\partial w_d^\nu}{\partial \Delta_3^0} &= M_\Delta \Delta_4 + \sqrt{6} g_7 \chi_3^2 - 2\sqrt{3} g_8 \rho_1 \rho_3 = 0, \\
\frac{\partial w_d^\nu}{\partial \Delta_4^0} &= M_\Delta \Delta_3 + \sqrt{6} g_7 \chi_2^2 - 2\sqrt{3} g_8 \rho_1 \rho_2 = 0, \\
\frac{\partial w_d^\nu}{\partial \Delta_5^0} &= M_\Delta \Delta_2 - 2\sqrt{3} g_7 \chi_1 \chi_2 + \sqrt{6} g_8 \rho_3^2 = 0.
\end{aligned} \tag{4.8}$$

A solution to those equations with each flavon acquiring non-zero VEV is given by

$$\langle \xi \rangle = v_\xi, \quad \langle \zeta \rangle = v_\zeta, \quad \langle \chi \rangle = \begin{pmatrix} \frac{\sqrt{2}}{\kappa} \\ 1 \\ 1 \end{pmatrix} v_\chi, \quad \langle \rho \rangle = \begin{pmatrix} -\sqrt{2}\kappa \\ 1 \\ 1 \end{pmatrix} v_\rho, \quad \langle \Delta \rangle = \begin{pmatrix} -\sqrt{\frac{2}{3}}\kappa v_1 \\ v_1 \\ -(1+\kappa)v_1 \\ -(1+\kappa)v_1 \\ v_1 \end{pmatrix}. \tag{4.9}$$

These VEVs are related through

$$\begin{aligned}
v_\xi &= \frac{10(\kappa-3)g_5g_7}{g_4M_\Delta} v_\chi^2, \quad v_\zeta^2 = \frac{2(\kappa-3)[(g_2g_8+g_3g_7)g_4M_\Delta-5g_5g_7g_8M_\xi]}{g_1g_4g_8M_\Delta} v_\chi^2, \\
v_\rho^2 &= \frac{(2-\kappa)g_7}{g_8} v_\chi^2, \quad v_1 = \frac{\sqrt{30}(2-\kappa)g_7}{M_\Delta} v_\chi^2,
\end{aligned} \tag{4.10}$$

where v_χ is undetermined. It is easy to check that the VEVs of ξ , ζ and Δ break the A_5 family symmetry down to $K_4^{(S,T^3ST^2ST^3)}$ while the subgroup $Z_2^{T^3ST^2ST^3}$ is preserved by vacuum of χ and ρ . Furthermore, Eq. (4.10) implies that v_ζ^2 , v_χ^2 , v_ρ^2 , v_ξ and v_1 have the same phase up to π , since all couplings are real. In our model, the GR mixing is reproduced exactly and a non-zero reactor mixing angle θ_{13} is generated after subleading order contributions are included. In order to obtain the correct size of θ_{13} , we could choose

$$\frac{v_\xi}{\Lambda} \sim \frac{v_\zeta}{\Lambda} \sim \frac{v_\chi}{\Lambda} \sim \frac{v_\rho}{\Lambda} \sim \frac{v_1}{\Lambda} \sim \mathcal{O}(\lambda_c). \tag{4.11}$$

4.2 Leading order results

The charged lepton mass terms, which are invariant under the imposed family symmetry $A_5 \times Z_3 \times Z_4 \times Z_6$, can be written as

$$w_l = \frac{y_\tau}{\Lambda} \tau^c (l\varphi)_1 h_d + \frac{y_{\mu 1}}{\Lambda^2} \mu^c (l(\phi\psi)_3)_1 h_d + \frac{y_{\mu 2}}{\Lambda^2} \mu^c (l(\psi\psi)_3)_1 h_d + \frac{y_{e 1}}{\Lambda^3} e^c (l\varphi)_1 (\phi\phi)_1 h_d$$

$$\begin{aligned}
& + \frac{y_{e2}}{\Lambda^3} e^c ((l\varphi)_5 (\phi\phi)_5)_1 h_d + \frac{y_{e3}}{\Lambda^3} e^c ((l\varphi)_3 (\phi\psi)_3)_1 h_d + \frac{y_{e4}}{\Lambda^3} e^c ((l\varphi)_5 (\phi\psi)_5)_1 h_d \\
& + \frac{y_{e5}}{\Lambda^3} e^c (l\varphi)_1 (\psi\psi)_1 h_d + \frac{y_{e6}}{\Lambda^3} e^c ((l\varphi)_3 (\psi\psi)_3)_1 h_d + \frac{y_{e7}}{\Lambda^3} e^c ((l\varphi)_5 (\psi\psi)_5)_1 h_d \\
& + \frac{y_{e8}}{\Lambda^3} e^c ((l\varphi)_5 (\psi\psi)_5)_1 h_d + \dots,
\end{aligned} \tag{4.12}$$

where dots stand for higher dimensional operators which will be discussed later. Note that all couplings here are real due to the generalized CP symmetry. After the electroweak and flavor symmetries breaking by the VEVs shown in Eq. (4.5), we obtain a diagonal charged lepton mass matrix, and the three charged lepton masses are

$$\begin{aligned}
m_e &= \sqrt{2} \left| 3y_{e2} \frac{v_\phi^2 v_\varphi}{\Lambda^3} + (y_{e3} - \sqrt{3}y_{e4}) \frac{v_\phi v_\varphi v_\psi}{\Lambda^3} + 3y_{e8} \frac{v_\varphi v_\psi^2}{\Lambda^3} \right| v_d, \\
m_\mu &= \sqrt{2} \left| y_{\mu 1} \frac{v_\phi v_\psi}{\Lambda^2} \right| v_d, \quad m_\tau = \left| y_\tau \frac{v_\varphi}{\Lambda} \right| v_d,
\end{aligned} \tag{4.13}$$

We see that the realistic mass hierarchies $m_e : m_\mu : m_\tau \simeq \lambda_c^4 : \lambda_c^2 : 1$ is generated for the order of magnitude of the flavon VEVs in Eq. (4.7). Furthermore, as both m_l and $\rho_3(T)$ are diagonal, obviously we have $\rho_3^\dagger(T) m_l^\dagger m_l \rho_3(T) = m_l^\dagger m_l$, i.e., the residual flavor symmetry of $m_l^\dagger m_l$ is Z_5^T . Next let's discuss the neutrino sector. Neutrino masses are generated by type I see-saw mechanism in this work. The LO superpotential for neutrino masses is

$$w_\nu = \frac{y_1}{\Lambda} \xi (\nu^c l)_1 h_u + \frac{y_2}{\Lambda} ((\nu^c l)_5 \Delta)_1 h_u + M (\nu^c \nu^c)_1, \tag{4.14}$$

where the coupling constants y_1, y_2 and the mass M are enforced to be real by the generalized CP symmetry. The Dirac mass matrix is obtained from the first two terms in Eq. (4.14) and it is given by

$$m_D = a \begin{pmatrix} 1 & 0 & 0 \\ 0 & 0 & 1 \\ 0 & 1 & 0 \end{pmatrix} v_u + b \begin{pmatrix} -2\sqrt{2}\kappa & -3 & -3 \\ -3 & -3\sqrt{2}(\kappa+1) & \sqrt{2}\kappa \\ -3 & \sqrt{2}\kappa & -3\sqrt{2}(\kappa+1) \end{pmatrix} v_u, \tag{4.15}$$

where $v_u = \langle h_u \rangle$, and the parameters a, b are

$$a = y_1 \frac{v_\xi}{\Lambda}, \quad b = y_2 \frac{v_1}{\sqrt{3}\Lambda}. \tag{4.16}$$

The common phase of a and b can be absorbed by field redefinition, consequently both a and b can be considered as real. The last term of Eq. (4.14) leads to the Majorana mass matrix:

$$m_M = M \begin{pmatrix} 1 & 0 & 0 \\ 0 & 0 & 1 \\ 0 & 1 & 0 \end{pmatrix}. \tag{4.17}$$

Therefore the three right-handed neutrinos are completely degenerate with mass equal to M . The light neutrino mass matrix is then given by the see-saw relation:

$$m_\nu = -m_D^T m_M^{-1} m_D = \alpha \begin{pmatrix} 1 & 0 & 0 \\ 0 & 0 & 1 \\ 0 & 1 & 0 \end{pmatrix} + \frac{\beta}{\sqrt{2}} \begin{pmatrix} -2\sqrt{2} & 3 & 3 \\ 3 & 0 & \sqrt{2} \\ 3 & \sqrt{2} & 0 \end{pmatrix} + \gamma \begin{pmatrix} 2 & 0 & 0 \\ 0 & 3 & -1 \\ 0 & -1 & 3 \end{pmatrix}, \tag{4.18}$$

where

$$\alpha = -[a^2 + 40(1 + \kappa)b^2] \frac{v_u^2}{M},$$

$$\begin{aligned}\beta &= 2 \left[\sqrt{2}ab - (3 + 4\kappa)b^2 \right] \frac{v_u^2}{M}, \\ \gamma &= \left[2\sqrt{2}(1 + \kappa)ab + (1 + 8\kappa)b^2 \right] \frac{v_u^2}{M}.\end{aligned}\quad (4.19)$$

We find that the neutrino mass matrix m_ν in Eq. (4.18) is of the same form as the general mass matrix in Eq. (3.27) with $\delta = 0$. Therefore m_ν is exactly diagonalized by the GR mixing pattern, i.e.,

$$U_{GR}^T m_\nu U_{GR} = \text{diag}(m_1, m_2, m_3), \quad (4.20)$$

where the phase matrix K_ν which encodes the CP parity of the neutrino state, has been omitted. The mass eigenvalues $m_{1,2,3}$ are

$$\begin{aligned}m_1 &= \left| a^2 - 2\sqrt{2}(3 - \kappa)ab + 10(2 - \kappa)b^2 \right| \frac{v_u^2}{M}, \\ m_2 &= \left| a^2 - 10\sqrt{2}\kappa ab + 50(1 + \kappa)b^2 \right| \frac{v_u^2}{M}, \\ m_3 &= \left| a^2 + 2\sqrt{2}(3 + 4\kappa)ab + 10(5 + 8\kappa)b^2 \right| \frac{v_u^2}{M}.\end{aligned}\quad (4.21)$$

Since the charged lepton mass matrix is diagonal in LO, the lepton mixing is exactly the GR mixing pattern. Here the reason why the GR mixing is produced is because that the flavor symmetry A_5 is broken to $K_4^{(S, T^2 ST^2 ST^3)}$ subgroup by the VEVs of ξ and Δ . Furthermore, we see that three neutrino masses $m_{1,2,3}$ only depend on two real parameters a and b which can be fixed by the measured values of the mass-squared difference $\delta m^2 \equiv m_2^2 - m_1^2$ and $\Delta m^2 \equiv m_3^2 - (m_1^2 + m_2^2)$. For the best fitting values $\delta m^2 = 7.54 \times 10^{-5} \text{eV}^2$ and $\Delta m^2 = 2.43 \times 10^{-3} \text{eV}^2$ [5], we find the neutrino mass spectrum can only be NO, and the absolute values of the neutrino masses are $m_1 = 4.81 \times 10^{-4} \text{eV}$, $m_2 = 8.70 \times 10^{-3} \text{eV}$ and $m_3 = 0.0497 \text{eV}$.

4.3 Next-to-leading-order corrections

At LO our model gives rise to the GR mixing pattern U_{GR} which predicts a vanishing reactor mixing angle ($\theta_{13} = 0^\circ$). Hence substantial next-to-leading-order corrections are needed to bring the model to agree with the experimental data on θ_{13} . We will demonstrate in the following that a non-zero θ_{13} can be obtained after the NLO contributions are included. Moreover, the LO remnant symmetry $K_4^{(S, T^3 ST^2 ST^3)}$ of neutrino sector is further broken down to $Z_2^{T^3 ST^2 ST^3}$ such that the mixing patterns of case III and case IV discussed in section 3.2 are realized. Firstly we consider the corrections to the flavon superpotential w_d^l in Eq. (4.2) which determines the vacuum alignment of the charged lepton sector. The symmetry allowed NLO operators are of the following form

$$\delta w_d^l = ((\phi^0 \varphi)_5 (\varphi \varphi)_5)_1 / \Lambda + (\Psi_l^0 \Psi_l \Psi_\nu^2 \Psi'_\nu \rho)_1 / \Lambda^3, \quad (4.22)$$

where all possible A_5 contractions should be considered, and all dimensionless coupling constants are omitted with $\Psi_l^0 \equiv \{\sigma^0, \psi^0\}$, $\Psi_l \equiv \{\phi, \psi\}$, $\Psi_\nu \equiv \{\xi, \Delta\}$ and $\Psi'_\nu \equiv \{\zeta, \chi\}$. Note that δw_d^l is suppressed by λ_c^2 with respect to the LO superpotential w_d^l in Eq. (4.2). The NLO vacuum configuration is determined by searching for the zeros of the F -terms of $w_d^l + \delta w_d^l$ with respect to the driving fields σ^0 , ϕ^0 and ψ^0 . We find that the NLO vacuum of φ , ϕ and ψ are given by

$$\langle \varphi \rangle = \begin{pmatrix} \epsilon_1 \lambda_c^2 \\ 1 \\ \epsilon_2 \lambda_c^2 \end{pmatrix} v_\varphi, \quad \langle \phi \rangle = \begin{pmatrix} \epsilon_3 \lambda_c^2 \\ 1 + \epsilon_4 \lambda_c^2 \\ \epsilon_5 \lambda_c^2 \end{pmatrix} v_\phi, \quad \langle \psi \rangle = \begin{pmatrix} \epsilon_6 \lambda_c^2 \\ \epsilon_7 \lambda_c^2 \\ 1 + \epsilon_8 \lambda_c^2 \\ \epsilon_9 \lambda_c^2 \\ \epsilon_{10} \lambda_c^2 \end{pmatrix} v_\psi, \quad (4.23)$$

where ϵ_i ($i = 1, \dots, 10$) are general complex numbers with absolute values of order one. The higher dimensional operators contributing to the charged lepton masses are:

$$\delta w_l = \mu^c (l\varphi^2\Psi_l)h_d/\Lambda^3 + e^c(l\varphi^3\Psi_l)/\Lambda^4. \quad (4.24)$$

The charged lepton mass matrix can be obtained by inserting the NLO VEVs of Eq. (4.23) into the LO mass terms plus the contribution of δw_l evaluated with the LO VEVs of Eq. (4.5). We find that the NLO charged lepton mass matrix is of the following form:

$$m_l \simeq \begin{pmatrix} m_e & \lambda_c^2 m_e & \lambda_c^2 m_e \\ \lambda_c^2 m_\mu & m_\mu & \lambda_c^2 m_\mu \\ \lambda_c^2 m_\tau & \lambda_c^2 m_\tau & m_\tau \end{pmatrix}. \quad (4.25)$$

Therefore the contributions of charged lepton sector to the lepton mixing angles is of order λ_c^2 and can be neglected.

We proceed to discuss the subleading corrections in the neutrino sector. The higher order corrections to the flavon superpotential of ξ , ζ , χ , ρ and Δ read

$$\begin{aligned} \delta w_d^\nu = & \frac{g_9}{\Lambda}\zeta^2(\chi^0\chi)_1 + \frac{g_{10}}{\Lambda}\zeta(\chi^0(\chi\chi)_3)_1 + \frac{g_{11}}{\Lambda}(\chi^0\chi)_1(\chi\chi)_1 + \frac{g_{12}}{\Lambda}((\chi^0\chi)_3(\chi\chi)_3)_1 \\ & + \frac{g_{13}}{\Lambda}((\chi^0\chi)_5(\chi\chi)_5)_1 + \frac{g_{14}}{\Lambda}(\chi^0\chi)_1(\rho\rho)_1 + \frac{g_{15}}{\Lambda}((\chi^0\chi)_5(\rho\rho)_5)_1 \\ & + \frac{g_{16}}{\Lambda}((\rho^0\rho)_5(\chi\chi)_5)_1 + \frac{g_{17}}{\Lambda}((\rho^0\rho)_5(\rho\rho)_5)_1, \end{aligned} \quad (4.26)$$

where all couplings g_i ($i = 9, \dots, 17$) are real because of the generalized CP symmetry. The resulting contributions to the F -terms of the driving fields σ^0 , ρ^0 , χ^0 and Δ^0 are suppressed by $\langle\Psi\rangle/\Lambda \sim \lambda_c$ ($\Psi \equiv \{\zeta, \chi, \rho\}$) compared to the contribution from the LO terms in Eq. (4.3). Hence they induce shifts in the VEVs of ξ , ζ , χ , ρ and Δ at relative order λ_c with respect to the LO results. After some straightforward algebra, the new vacuum configuration can be written as

$$\begin{aligned} \langle\xi\rangle &= v_\xi + \delta v_\xi, \quad \langle\zeta\rangle = v_\zeta + \delta v_\zeta, \quad \langle\chi\rangle = \begin{pmatrix} \frac{\sqrt{2}}{\kappa}v_\chi \\ v_\chi \\ v_\chi \end{pmatrix}, \\ \langle\rho\rangle &= \begin{pmatrix} -\sqrt{2}\kappa(v_\rho + \delta v_\rho) \\ v_\rho + \delta v_\rho \\ v_\rho + \delta v_\rho \end{pmatrix}, \quad \langle\Delta\rangle = \begin{pmatrix} \sqrt{\frac{2}{3}}(-\kappa v_1 + (1+2\kappa)\delta v_\Delta) \\ v_1 + \delta v_\Delta \\ -(1+\kappa)v_1 + 2\kappa\delta v_\Delta \\ -(1+\kappa)v_1 + 2\kappa\delta v_\Delta \\ v_1 + \delta v_\Delta \end{pmatrix}, \end{aligned} \quad (4.27)$$

where

$$\begin{aligned} \delta v_\xi &= -\frac{X_1 + g_5 X_2}{g_4 g_6 \Lambda}, \quad \delta v_\zeta = \frac{g_8 M_\xi X_1 + (g_5 g_8 M_\xi - g_3 g_4 M_\Delta) X_2}{2g_1 g_4 g_6 g_8 \Lambda v_\zeta}, \\ \delta v_\rho &= \frac{2(\kappa - 2)g_{16} M_\Delta v_\chi^2 + 2g_{17} M_\Delta v_\rho^2}{4g_6 g_8 \Lambda v_\rho}, \quad \delta v_\Delta = \frac{2\sqrt{6}((\kappa - 1)g_{16} v_\chi^2 - \kappa g_{17} v_\rho^2)}{g_6 \Lambda}, \end{aligned} \quad (4.28)$$

with

$$\begin{aligned} X_1 &= g_6 \left(g_9 v_\zeta^2 + 2(3 - \kappa)(g_{11} + 4g_{13})v_\chi^2 + 2\sqrt{5}\kappa(g_{14} + g_{15})v_\rho^2 \right), \\ X_2 &= 2(\kappa - 3)g_{16} v_\chi^2 + 2\sqrt{5}\kappa g_{17} v_\rho^2. \end{aligned} \quad (4.29)$$

Obviously the vacuum of χ is kept intact, $\langle \rho \rangle$ acquires $\mathcal{O}(\lambda_c)$ corrections in the same direction, while the alignment of Δ is tilted. Moreover, from the relations in Eq. (4.10), we see that the shifts δv_ξ , δv_ζ , δv_ρ and δv_Δ carry the same phase as v_ξ , v_ζ , v_ρ and v_1 up to π , respectively.

The light neutrino mass matrix receives corrections from both the modified vacuum and the higher dimensional operators in the superpotential w_ν . It is easy to check that the NLO corrections to the Majorana mass terms are suppressed by $1/\Lambda^4$ which can be safely neglected. The subleading operators contributing to the neutrino Dirac masses are as follows

$$\begin{aligned} \delta w_\nu = & \frac{y_3}{\Lambda^2} \zeta^2 (l\nu^c)_1 h_u + \frac{y_4}{\Lambda^2} \zeta ((l\nu^c)_3 \chi)_1 h_u + \frac{y_5}{\Lambda^2} (l\nu^c)_1 (\chi\chi)_1 h_u + \frac{y_6}{\Lambda^2} ((l\nu^c)_3 (\chi\chi)_3)_1 h_u \\ & + \frac{y_7}{\Lambda^2} ((l\nu^c)_5 (\chi\chi)_5)_1 h_u + \frac{y_8}{\Lambda^2} (l\nu^c)_1 (\rho\rho)_1 h_u + \frac{y_9}{\Lambda^2} ((l\nu^c)_5 (\rho\rho)_5)_1 h_u. \end{aligned} \quad (4.30)$$

As a consequence, the corrected Dirac mass matrix becomes

$$\begin{aligned} m_D = & a \begin{pmatrix} 1 & 0 & 0 \\ 0 & 0 & 1 \\ 0 & 1 & 0 \end{pmatrix} v_u + b \begin{pmatrix} 2\sqrt{2} & -3 & -3 \\ -3 & 0 & -\sqrt{2} \\ -3 & -\sqrt{2} & 0 \end{pmatrix} v_u + c \begin{pmatrix} 2\sqrt{2} & 0 & 0 \\ 0 & 3\sqrt{2} & -\sqrt{2} \\ 0 & -\sqrt{2} & 3\sqrt{2} \end{pmatrix} v_u \\ & + d \begin{pmatrix} 0 & 1 & -1 \\ -1 & 0 & \frac{\sqrt{5}-1}{\sqrt{2}} \\ 1 & \frac{1-\sqrt{5}}{\sqrt{2}} & 0 \end{pmatrix} v_u, \end{aligned} \quad (4.31)$$

where the four parameters a , b , c and d are

$$\begin{aligned} a = & y_1 \frac{v_\xi + \delta v_\xi}{\Lambda} + y_3 \frac{v_\zeta^2}{\Lambda^2} + 2(3 - \kappa) y_5 \frac{v_\chi^2}{\Lambda^2} + 2\sqrt{5} \kappa y_8 \frac{v_\rho^2}{\Lambda^2}, \\ b = & \frac{y_2}{\sqrt{3}} \frac{v_1 + \delta v_\Delta}{\Lambda} - 2\sqrt{2}(\kappa - 1) y_7 \frac{v_\chi^2}{\Lambda^2} + \sqrt{2} y_9 \frac{v_\rho^2}{\Lambda^2}, \\ c = & -\frac{y_2}{\sqrt{3}} \frac{(1 + \kappa) v_1 - 2\kappa \delta v_\Delta}{\Lambda} + \sqrt{2} y_7 \frac{v_\chi^2}{\Lambda^2} + 2\sqrt{2} \kappa y_9 \frac{v_\rho^2}{\Lambda^2}, \quad d = y_4 \frac{v_\zeta v_\chi}{\Lambda^2}. \end{aligned} \quad (4.32)$$

Notice that the three parameters a , b and c have the same phase with v_χ^2 up to π , while the phase difference between d and v_χ^2 is 0, π or $\pm\frac{\pi}{2}$ depending on the product $g_1 M_\Delta [(g_2 g_8 + g_3 g_7) g_4^2 g_8 M_\Delta - 5 g_4 g_5 g_7 g_8^2 M_\xi]$ being positive or negative. Since the phase of v_χ can be factorized out as an overall phase of the neutrino mass matrix m_ν , the VEV v_χ can be taken to be real without loss of generality. As a result, a , b and c are all real and the parameter d is real for $g_1 M_\Delta [(g_2 g_8 + g_3 g_7) g_4^2 g_8 M_\Delta - 5 g_4 g_5 g_7 g_8^2 M_\xi] < 0$ or pure imaginary for $g_1 M_\Delta [(g_2 g_8 + g_3 g_7) g_4^2 g_8 M_\Delta - 5 g_4 g_5 g_7 g_8^2 M_\xi] > 0$. In addition, we see that d are suppressed by λ_c with respect to a , b and c , i.e.,

$$a \sim b \sim c \sim \mathcal{O}(\lambda_c), \quad d \sim \mathcal{O}(\lambda_c^2). \quad (4.33)$$

Utilizing the see-saw formula, we find the light neutrino mass matrix m_ν is of the same form as Eq. (3.27) with

$$\begin{aligned} \alpha = & -[3a^2 + 24(2b^2 + bc + 2c^2) - 4(3 - \kappa)d^2] \frac{v_u^2}{3M}, \\ \beta = & [6b(\sqrt{2}a + b + 4c) - 2(\kappa - 1)d^2] \frac{v_u^2}{3M}, \\ \gamma = & -[6\sqrt{2}ac + 3(3b + 2c)(b - 2c) + d^2] \frac{v_u^2}{3M}, \end{aligned}$$

$$\delta = -3d[b + 2(\kappa - 1)c] \frac{v_u^2}{M}. \quad (4.34)$$

Note that the term proportional to δ spoils the LO GR mixing, and it is of relative order λ_c compared with α , β and γ since it is induced by the NLO corrections. Therefore the correct size of the reactor mixing angle θ_{13} can be naturally achieved in our model. After extracting the overall phase of v_χ , the parameters α , β and γ are real while δ is real or pure imaginary. In the case of $g_1 M_\Delta [(g_2 g_8 + g_3 g_7) g_4^2 g_8 M_\Delta - 5 g_4 g_5 g_7 g_8^2 M_\xi] < 0$, δ is real such that the neutrino mass matrix m_ν has the most general form compatible with the preservation of the remnant symmetry $Z_2^{T^3 ST^2 ST^3} \times H_{CP}^\nu$ with $H_{CP}^\nu = \{\rho_r(1), \rho_r(T^3 ST^2 ST^3)\}$. This is the case III investigated in the model independent analysis of section 3.2. The lepton mixing matrix U_{PMNS} and the corresponding predictions for the lepton mixing parameters are given by Eq. (3.32) and Eq. (3.33) respectively. There is no CP violation in this case.

In the case of $g_1 M_\Delta [(g_2 g_8 + g_3 g_7) g_4^2 g_8 M_\Delta - 5 g_4 g_5 g_7 g_8^2 M_\xi] > 0$, the parameter δ becomes imaginary. The origin symmetry $A_5 \rtimes H_{CP}$ is broken down to $Z_2^{T^3 ST^2 ST^3} \times H_{CP}^\nu$ with $H_{CP}^\nu = \{\rho_r(S), \rho_r(T^3 ST^2 ST^3 S)\}$ in the neutrino sector. The neutrino mass matrix m_ν has the same form as that of case IV discussed in section 3.2. Both atmospheric mixing angle and Dirac CP phase are predicted to be maximal while Majorana CP phases are conserved, as shown in Eq. (3.39). In short, our model reproduces the GR mixing at LO, and realistic value of θ_{13} is obtained after higher order contributions are taken into account. Depending on the overall sign of the product $g_1 M_\Delta [(g_2 g_8 + g_3 g_7) g_4^2 g_8 M_\Delta - 5 g_4 g_5 g_7 g_8^2 M_\xi]$, either case III or case IV can be realized.

5 Conclusions

Combining a discrete flavor symmetry with a CP symmetry is a very promising approach of predicting both lepton mixing angles and CP phases. In this work we have performed a comprehensive analysis of the A_5 family symmetry and CP symmetry. Since the inverse of each conjugacy class of A_5 is equal to itself, all the inner automorphisms of A_5 are class-inverting while the unique nontrivial outer automorphism of A_5 is not. As a result, the physical CP transformations are defined by the inner automorphisms of A_5 . In our working basis, the CP transformations are found to be of the same form as the flavor symmetry transformations.

Assuming neutrinos are Majorana particles, we have analyzed the possible symmetry breaking patterns of $A_5 \rtimes H_{CP}$ and the corresponding predictions for the PMNS matrix as well as the lepton mixing parameters in a model independent way. We find five phenomenologically interesting mixing patterns summarized in Table 1, and one column of the PMNS matrix is fixed to be $(-\sqrt{\frac{\kappa}{\sqrt{5}}}, \frac{1}{\sqrt{2\sqrt{5}\kappa}}, \frac{1}{\sqrt{2\sqrt{5}\kappa}})^T, (\sqrt{\frac{1}{\sqrt{5}\kappa}}, \sqrt{\frac{\kappa}{2\sqrt{5}}}, \sqrt{\frac{\kappa}{2\sqrt{5}}})^T, (\frac{1}{\sqrt{3}}, \frac{1}{\sqrt{3}}, \frac{1}{\sqrt{3}})^T$ or $(\frac{\kappa}{2}, -\frac{1}{2}, \frac{\kappa-1}{2})^T$, where $\kappa = (1 + \sqrt{5})/2$ is the golden ratio. All the three mixing angles are determined in terms of a single real parameter θ , and their measured values can be accommodated for certain values of θ . In particular, the Dirac CP violating phase δ_{CP} is predicted to be trivial or maximal while the Majorana phases are trivial. In contrast, δ_{CP} is quite weakly constrained and Majorana phases can not be predicted if CP symmetry is not considered, as shown in Appendix B. Our theoretical predictions can be tested by forthcoming long-baseline neutrino oscillation experiments such as LBNE, LBNO and HyperKamiokande. The predicted mixing patterns would be ruled out, if significant deviations of δ_{CP} from trivial and maximal values were detected. Furthermore, the phenomenological predictions for the $(\beta\beta)_{0\nu}$ -decay are investigated. The present experimental bounds are saturated, and the effective mass $|m_{ee}|$ is found to be within the sensitivity of future $(\beta\beta)_{0\nu}$ -decay experiments

for inverted ordering neutrino mass spectrum.

Guided by above model independent analysis, we construct a flavor model with both A_5 flavor symmetry and generalized CP symmetry. The lepton mixing is exactly the GR pattern at LO, the observed mass hierarchies among charged lepton are generated, and the three light neutrino masses effectively depend on two real parameters which can be fixed by the measured values of the mass-squared splittings. Therefore the neutrino mass spectrum can only be normal ordering and the absolute neutrino masses are predicted. The model is built in such a way that the GR mixing is modified by NLO contributions and only the second column of GR mixing matrix is kept. A non-vanishing value of θ_{13} is generated at NLO and it is naturally of the correct order λ_c in our model. In case of $g_1 M_\Delta [(g_2 g_8 + g_3 g_7) g_4^2 g_8 M_\Delta - 5 g_4 g_5 g_7 g_8^2 M_\xi] < 0$, Dirac CP phase δ_{CP} is 0 or π , consequently the mixing pattern of case III of general analysis in section 3.2 is reproduced exactly. In case of $g_1 M_\Delta [(g_2 g_8 + g_3 g_7) g_4^2 g_8 M_\Delta - 5 g_4 g_5 g_7 g_8^2 M_\xi] > 0$, Dirac CP phase δ_{CP} is maximal with $\delta_{CP} = \pm\pi/2$, the mixing pattern of case IV is generated. In other words, our model provides an explicit dynamical realization of the assumed symmetry breaking pattern in section 3.2.

It is interesting to implement any of the remaining cases II, V and VII in Table 1 in a concrete model. Moreover, the group \mathcal{I}' , which is the double cover of A_5 , may deserve to be studied in a similar fashion. Since \mathcal{I}' has doublet representations [46], quark masses and mixing should be easily reproduced.

Acknowledgements

One of the author (G.J.D.) is grateful to Stephen F. King and Alexander J. Stuart for stimulating discussions on generalized CP symmetry. The idea of combining A_5 family symmetry with generalized CP was initiated during visiting the School of Physics and Astronomy at the University of Southampton. We would like to thank Luis Lavoura for email correspondence. We acknowledge Chang-Yuan Yao for his help on plotting the figures. This work is supported by the National Natural Science Foundation of China under Grant Nos. 11275188 and 11179007.

Appendix

A Group Theory of A_5

A_5 is the group of even permutations of five objects, and it has $5!/2 = 60$ elements. Geometrically it is the symmetry group of a regular icosahedron. A_5 group can be generated by two generators S and T which satisfy the multiplication rules [47]:

$$S^2 = T^5 = (ST)^3 = 1. \quad (\text{A.1})$$

The 60 element of A_5 group are divided into 5 conjugacy classes:

$$\begin{aligned} 1C_1 : & 1 \\ 15C_2 : & ST^2ST^3S, TST^4, T^4(ST^2)^2, T^2ST^3, (T^2S)^2T^3S, ST^2ST, S, T^3ST^2ST^3, \\ & T^3ST^2ST^3S, T^3ST^2, T^4ST^2ST^3S, TST^2S, ST^3ST^2S, T^4ST, (T^2S)^2T^4 \\ 20C_3 : & ST, TS, ST^4, T^4S, TST^3, T^2ST^2, T^2ST^4, T^3ST, T^3ST^3, T^4ST^2, TST^3S, T^2ST^3S, \\ & T^3ST^2S, ST^2ST^3, ST^3ST, ST^3ST^2, (T^2S)^2T^2, T^2(T^2S)^2, (ST^2)^2S, (ST^2)^2T^2 \\ 12C_5 : & T, T^4, ST^2, T^2S, ST^3, T^3S, STS, TST, TST^2, T^2ST, T^3ST^4, T^4ST^3 \\ 12C'_5 : & T^2, T^3, ST^2S, ST^3S, (ST^2)^2, (T^2S)^2, (ST^3)^2, (T^3S)^2, (T^2S)^2T^3, \\ & T^3(ST^2)^2, T^3ST^2ST^4, T^4ST^2ST^3, \end{aligned} \quad (\text{A.2})$$

where nC_k denotes a class with n elements which have order k . The group structure of A_5 has been elaborately analyzed in Ref. [47]. Following the convention of Ref. [47], we find that A_5 group has thirty-six abelian subgroups in total: fifteen Z_2 subgroups, ten Z_3 subgroups, five K_4 subgroups and six Z_5 subgroups. In terms of the generators S and T , the concrete forms of these abelian subgroups are as follows:

- Z_2 subgroups

$$\begin{aligned} Z_2^{ST^2ST^3S} &= \{1, ST^2ST^3S\}, \quad Z_2^{TST^4} = \{1, TST^4\}, \quad Z_2^{T^4(ST^2)^2} = \{1, T^4(ST^2)^2\}, \\ Z_2^{T^2ST^3} &= \{1, T^2ST^3\}, \quad Z_2^{(T^2S)^2T^3S} = \{1, (T^2S)^2T^3S\}, \quad Z_2^{ST^2ST} = \{1, ST^2ST\}, \\ Z_2^S &= \{1, S\}, \quad Z_2^{T^3ST^2ST^3} = \{1, T^3ST^2ST^3\}, \quad Z_2^{T^3ST^2ST^3S} = \{1, T^3ST^2ST^3S\}, \\ Z_2^{T^3ST^2} &= \{1, T^3ST^2\}, \quad Z_2^{T^4ST^2ST^3S} = \{1, T^4ST^2ST^3S\}, \quad Z_2^{TST^2S} = \{1, TST^2S\}, \\ Z_2^{ST^3ST^2S} &= \{1, ST^3ST^2S\}, \quad Z_2^{T^4ST} = \{1, T^4ST\}, \quad Z_2^{(T^2S)^2T^4} = \{1, (T^2S)^2T^4\}. \end{aligned}$$

All the above fifteen Z_2 subgroups are conjugate to each other.

- Z_3 subgroups

$$\begin{aligned} Z_3^{T^3ST^2S} &= \{1, T^3ST^2S, ST^3ST^2\}, \quad Z_3^{TST^3S} = \{1, TST^3S, (ST^2)^2T^2\}, \\ Z_3^{T^3ST} &= \{1, T^3ST, T^4ST^2\}, \quad Z_3^{ST} = \{1, ST, T^4S\}, \\ Z_3^{(T^2S)^2T^2} &= \{1, (T^2S)^2T^2, (ST^2)^2S\}, \quad Z_3^{TST^3} = \{1, TST^3, T^2ST^4\}, \\ Z_3^{T^2ST^2} &= \{1, T^2ST^2, T^3ST^3\}, \quad Z_3^{TS} = \{1, TS, ST^4\}, \\ Z_3^{ST^3ST} &= \{1, ST^3ST, T^2(T^2S)^2\}, \quad Z_3^{ST^2ST^3} = \{1, ST^2ST^3, T^2ST^3S\}. \end{aligned}$$

The ten Z_3 subgroups are related with each other by group conjugation.

- K_4 subgroups

$$\begin{aligned}
K_4^{(ST^2ST^3S, TST^4)} &\equiv Z_2^{ST^2ST^3S} \times Z_2^{TST^4} = \{1, ST^2ST^3S, TST^4, T^4(ST^2)^2\}, \\
K_4^{(T^2ST^3, ST^2ST)} &\equiv Z_2^{T^2ST^3} \times Z_2^{ST^2ST} = \{1, T^2ST^3, (T^2S)^2T^3S, ST^2ST\}, \\
K_4^{(S, T^3ST^2ST^3)} &\equiv Z_2^S \times Z_2^{T^3ST^2ST^3} = \{1, S, T^3ST^2ST^3, T^3ST^2ST^3S\}, \\
K_4^{(T^3ST^2, TST^2S)} &\equiv Z_2^{T^3ST^2} \times Z_2^{TST^2S} = \{1, T^3ST^2, T^4ST^2ST^3S, TST^2S\}, \\
K_4^{(ST^3ST^2S, T^4ST)} &\equiv Z_2^{ST^3ST^2S} \times Z_2^{T^4ST} = \{1, ST^3ST^2S, T^4ST, (T^2S)^2T^4\}.
\end{aligned}$$

All the five K_4 subgroups are conjugate as well.

- Z_5 subgroups

$$\begin{aligned}
Z_5^{STS} &= \{1, STS, ST^2S, ST^3S, TST\}, \quad Z_5^{ST^3} = \{1, ST^3, T^2S, (ST^3)^2, (T^2S)^2\}, \\
Z_5^{T^2ST} &= \{1, T^2ST, T^4ST^3, T^3(ST^2)^2, T^4ST^2ST^3\}, \quad Z_5^T = \{1, T, T^2, T^3, T^4\}, \\
Z_5^{TST^2} &= \{1, TST^2, T^3ST^4, (T^2S)^2T^3, T^3ST^2ST^4\}, \quad Z_5^{ST^2} = \{1, ST^2, T^3S, (ST^2)^2, (T^3S)^2\}.
\end{aligned}$$

All the six Z_5 subgroups are related to each other under group conjugation.

Here the superscript of a subgroup denotes its generator (generators). The A_5 group has five irreducible representations: one singlet representation **1**, two three-dimensional representations **3** and **3'**, one four-dimensional representation **4** and one five-dimensional representation **5**. In the present work, we choose the same basis as that of Ref. [47]. The explicit forms of the generators S and T in the five irreducible representations are as follows

$$\begin{aligned}
\mathbf{1}: \quad & S = 1, \quad T = 1, \\
\mathbf{3}: \quad & S = \frac{1}{\sqrt{5}} \begin{pmatrix} 1 & -\sqrt{2} & -\sqrt{2} \\ -\sqrt{2} & -\kappa & \kappa-1 \\ -\sqrt{2} & \kappa-1 & -\kappa \end{pmatrix}, \quad T = \begin{pmatrix} 1 & 0 & 0 \\ 0 & \omega_5 & 0 \\ 0 & 0 & \omega_5^4 \end{pmatrix}, \\
\mathbf{3}': \quad & S = \frac{1}{\sqrt{5}} \begin{pmatrix} -1 & \sqrt{2} & \sqrt{2} \\ \sqrt{2} & 1-\kappa & \kappa \\ \sqrt{2} & \kappa & 1-\kappa \end{pmatrix}, \quad T = \begin{pmatrix} 1 & 0 & 0 \\ 0 & \omega_5^2 & 0 \\ 0 & 0 & \omega_5^3 \end{pmatrix}, \\
\mathbf{4}: \quad & S = \frac{1}{\sqrt{5}} \begin{pmatrix} 1 & \kappa-1 & \kappa & -1 \\ \kappa-1 & -1 & 1 & \kappa \\ \kappa & 1 & -1 & \kappa-1 \\ -1 & \kappa & \kappa-1 & 1 \end{pmatrix}, \quad T = \begin{pmatrix} \omega_5 & 0 & 0 & 0 \\ 0 & \omega_5^2 & 0 & 0 \\ 0 & 0 & \omega_5^3 & 0 \\ 0 & 0 & 0 & \omega_5^4 \end{pmatrix}, \\
\mathbf{5}: \quad & S = \frac{1}{5} \begin{pmatrix} -1 & \sqrt{6} & \sqrt{6} & \sqrt{6} & \sqrt{6} \\ \sqrt{6} & (\kappa-1)^2 & -2\kappa & 2(\kappa-1) & \kappa^2 \\ \sqrt{6} & -2\kappa & \kappa^2 & (\kappa-1)^2 & 2(\kappa-1) \\ \sqrt{6} & 2(\kappa-1) & (\kappa-1)^2 & \kappa^2 & -2\kappa \\ \sqrt{6} & \kappa^2 & 2(\kappa-1) & -2\kappa & (\kappa-1)^2 \end{pmatrix}, \quad T = \begin{pmatrix} 1 & 0 & 0 & 0 & 0 \\ 0 & \omega_5 & 0 & 0 & 0 \\ 0 & 0 & \omega_5^2 & 0 & 0 \\ 0 & 0 & 0 & \omega_5^3 & 0 \\ 0 & 0 & 0 & 0 & \omega_5^4 \end{pmatrix},
\end{aligned} \tag{A.3}$$

where $\omega_5 = e^{\frac{2\pi i}{5}}$. The character table of A_5 group is reported in Table 3. We can straightforwardly obtain the Kronecker products between various representations:

$$\begin{aligned}
\mathbf{1} \otimes \mathbf{R} &= \mathbf{R} \otimes \mathbf{1} = \mathbf{R}, \quad \mathbf{3} \otimes \mathbf{3} = \mathbf{1} \oplus \mathbf{3} \oplus \mathbf{5}, \quad \mathbf{3}' \otimes \mathbf{3}' = \mathbf{1} \oplus \mathbf{3}' \oplus \mathbf{5}, \quad \mathbf{3} \times \mathbf{3}' = \mathbf{4} \oplus \mathbf{5}, \\
\mathbf{3} \otimes \mathbf{4} &= \mathbf{3}' \oplus \mathbf{4} \oplus \mathbf{5}, \quad \mathbf{3}' \otimes \mathbf{4} = \mathbf{3} \oplus \mathbf{4} \oplus \mathbf{5}, \quad \mathbf{3} \otimes \mathbf{5} = \mathbf{3} \oplus \mathbf{3}' \oplus \mathbf{4} \oplus \mathbf{5}, \\
\mathbf{3}' \otimes \mathbf{5} &= \mathbf{3} \oplus \mathbf{3}' \oplus \mathbf{4} \oplus \mathbf{5}, \quad \mathbf{4} \otimes \mathbf{4} = \mathbf{1} \oplus \mathbf{3} \oplus \mathbf{3}' \oplus \mathbf{4} \oplus \mathbf{5}, \quad \mathbf{4} \otimes \mathbf{5} = \mathbf{3} \oplus \mathbf{3}' \oplus \mathbf{4} \oplus \mathbf{5}_1 \oplus \mathbf{5}_2, \\
\mathbf{5} \otimes \mathbf{5} &= \mathbf{1} \oplus \mathbf{3} \oplus \mathbf{3}' \oplus \mathbf{4}_1 \oplus \mathbf{4}_2 \oplus \mathbf{5}_1 \oplus \mathbf{5}_2.
\end{aligned} \tag{A.4}$$

	Conjugacy Classes				
	$1C_1$	$15C_2$	$20C_3$	$12C_5$	$12C'_5$
1	1	1	1	1	1
3	3	-1	0	κ	$1 - \kappa$
3'	3	-1	0	$1 - \kappa$	κ
4	4	0	1	-1	-1
5	5	1	-1	0	0

Table 3: The character table of the A_5 group, where $\kappa = \frac{1+\sqrt{5}}{2}$.

where **R** represents any irreducible representation of A_5 , and **4**₁, **4**₂, **5**₁ and **5**₂ stand for the two **4** and two **5** representations that appear in the Kronecker products.

We now list the Clebsch-Gordan coefficients for our basis. We use the notation α_i (β_i) to denote the elements of the first (second) representation. The subscript "S" ("A") refers to symmetric (antisymmetric) combinations.

$\mathbf{3} \otimes \mathbf{3} = \mathbf{1}_S \oplus \mathbf{3}_A \oplus \mathbf{5}_S$	$\mathbf{3}' \otimes \mathbf{3}' = \mathbf{1}_S \oplus \mathbf{3}'_A \oplus \mathbf{5}_S$	$\mathbf{3} \otimes \mathbf{3}' = \mathbf{4} \oplus \mathbf{5}$
$\mathbf{1}_S : \alpha_1\beta_1 + \alpha_2\beta_3 + \alpha_3\beta_2$ $\mathbf{3}_A : \begin{pmatrix} \alpha_2\beta_3 - \alpha_3\beta_2 \\ \alpha_1\beta_2 - \alpha_2\beta_1 \\ \alpha_3\beta_1 - \alpha_1\beta_3 \end{pmatrix}$ $\mathbf{5}_S : \begin{pmatrix} 2\alpha_1\beta_1 - \alpha_2\beta_3 - \alpha_3\beta_2 \\ -\sqrt{3}(\alpha_1\beta_2 + \alpha_2\beta_1) \\ \sqrt{6}\alpha_2\beta_2 \\ \sqrt{6}\alpha_3\beta_3 \\ -\sqrt{3}(\alpha_1\beta_3 + \alpha_3\beta_1) \end{pmatrix}$	$\mathbf{1}_S : \alpha_1\beta_1 + \alpha_2\beta_3 + \alpha_3\beta_2$ $\mathbf{3}'_A : \begin{pmatrix} \alpha_2\beta_3 - \alpha_3\beta_2 \\ \alpha_1\beta_2 - \alpha_2\beta_1 \\ \alpha_3\beta_1 - \alpha_1\beta_3 \end{pmatrix}$ $\mathbf{5}_S : \begin{pmatrix} 2\alpha_1\beta_1 - \alpha_2\beta_3 - \alpha_3\beta_2 \\ \sqrt{6}\alpha_3\beta_3 \\ -\sqrt{3}(\alpha_1\beta_2 + \alpha_2\beta_1) \\ -\sqrt{3}(\alpha_1\beta_3 + \alpha_3\beta_1) \\ \sqrt{6}\alpha_2\beta_2 \end{pmatrix}$	$\mathbf{4} : \begin{pmatrix} \sqrt{2}\alpha_2\beta_1 + \alpha_3\beta_2 \\ -\sqrt{2}\alpha_1\beta_2 - \alpha_3\beta_3 \\ -\sqrt{2}\alpha_1\beta_3 - \alpha_2\beta_2 \\ \sqrt{2}\alpha_3\beta_1 + \alpha_2\beta_3 \end{pmatrix}$ $\mathbf{5} : \begin{pmatrix} \sqrt{3}\alpha_1\beta_1 \\ \alpha_2\beta_1 - \sqrt{2}\alpha_3\beta_2 \\ \alpha_1\beta_2 - \sqrt{2}\alpha_3\beta_3 \\ \alpha_1\beta_3 - \sqrt{2}\alpha_2\beta_2 \\ \alpha_3\beta_1 - \sqrt{2}\alpha_2\beta_3 \end{pmatrix}$

$\mathbf{3} \otimes \mathbf{4} = \mathbf{3}' \oplus \mathbf{4} \oplus \mathbf{5}$	$\mathbf{3}' \otimes \mathbf{4} = \mathbf{3} \oplus \mathbf{4} \oplus \mathbf{5}$
$\mathbf{3}' : \begin{pmatrix} -\sqrt{2}(\alpha_2\beta_4 + \alpha_3\beta_1) \\ \sqrt{2}\alpha_1\beta_2 - \alpha_2\beta_1 + \alpha_3\beta_3 \\ \sqrt{2}\alpha_1\beta_3 + \alpha_2\beta_2 - \alpha_3\beta_4 \end{pmatrix}$ $\mathbf{4} : \begin{pmatrix} \alpha_1\beta_1 - \sqrt{2}\alpha_3\beta_2 \\ -\alpha_1\beta_2 - \sqrt{2}\alpha_2\beta_1 \\ \alpha_1\beta_3 + \sqrt{2}\alpha_3\beta_4 \\ -\alpha_1\beta_4 + \sqrt{2}\alpha_2\beta_3 \end{pmatrix}$ $\mathbf{5} : \begin{pmatrix} \sqrt{6}(\alpha_2\beta_4 - \alpha_3\beta_1) \\ 2\sqrt{2}\alpha_1\beta_1 + 2\alpha_3\beta_2 \\ -\sqrt{2}\alpha_1\beta_2 + \alpha_2\beta_1 + 3\alpha_3\beta_3 \\ \sqrt{2}\alpha_1\beta_3 - 3\alpha_2\beta_2 - \alpha_3\beta_4 \\ -2\sqrt{2}\alpha_1\beta_4 - 2\alpha_2\beta_3 \end{pmatrix}$	$\mathbf{3} : \begin{pmatrix} -\sqrt{2}(\alpha_2\beta_3 + \alpha_3\beta_2) \\ \sqrt{2}\alpha_1\beta_1 + \alpha_2\beta_4 - \alpha_3\beta_3 \\ \sqrt{2}\alpha_1\beta_4 - \alpha_2\beta_2 + \alpha_3\beta_1 \end{pmatrix}$ $\mathbf{4} : \begin{pmatrix} \alpha_1\beta_1 + \sqrt{2}\alpha_3\beta_3 \\ \alpha_1\beta_2 - \sqrt{2}\alpha_3\beta_4 \\ -\alpha_1\beta_3 + \sqrt{2}\alpha_2\beta_1 \\ -\alpha_1\beta_4 - \sqrt{2}\alpha_2\beta_2 \end{pmatrix}$ $\mathbf{5} : \begin{pmatrix} \sqrt{6}(\alpha_2\beta_3 - \alpha_3\beta_2) \\ \sqrt{2}\alpha_1\beta_1 - 3\alpha_2\beta_4 - \alpha_3\beta_3 \\ 2\sqrt{2}\alpha_1\beta_2 + 2\alpha_3\beta_4 \\ -2\sqrt{2}\alpha_1\beta_3 - 2\alpha_2\beta_1 \\ -\sqrt{2}\alpha_1\beta_4 + \alpha_2\beta_2 + 3\alpha_3\beta_1 \end{pmatrix}$

$\mathbf{3} \otimes \mathbf{5} = \mathbf{3} \oplus \mathbf{3}' \oplus \mathbf{4} \oplus \mathbf{5}$	$\mathbf{3}' \otimes \mathbf{5} = \mathbf{3} \oplus \mathbf{3}' \oplus \mathbf{4} \oplus \mathbf{5}$
$\mathbf{3} : \begin{pmatrix} -2\alpha_1\beta_1 + \sqrt{3}\alpha_2\beta_5 + \sqrt{3}\alpha_3\beta_2 \\ \sqrt{3}\alpha_1\beta_2 + \alpha_2\beta_1 - \sqrt{6}\alpha_3\beta_3 \\ \sqrt{3}\alpha_1\beta_5 - \sqrt{6}\alpha_2\beta_4 + \alpha_3\beta_1 \end{pmatrix}$	$\mathbf{3} : \begin{pmatrix} \sqrt{3}\alpha_1\beta_1 + \alpha_2\beta_4 + \alpha_3\beta_3 \\ \alpha_1\beta_2 - \sqrt{2}\alpha_2\beta_5 - \sqrt{2}\alpha_3\beta_4 \\ \alpha_1\beta_5 - \sqrt{2}\alpha_2\beta_3 - \sqrt{2}\alpha_3\beta_2 \end{pmatrix}$
$\mathbf{3}' : \begin{pmatrix} \sqrt{3}\alpha_1\beta_1 + \alpha_2\beta_5 + \alpha_3\beta_2 \\ \alpha_1\beta_3 - \sqrt{2}\alpha_2\beta_2 - \sqrt{2}\alpha_3\beta_4 \\ \alpha_1\beta_4 - \sqrt{2}\alpha_2\beta_3 - \sqrt{2}\alpha_3\beta_5 \end{pmatrix}$	$\mathbf{3}' : \begin{pmatrix} -2\alpha_1\beta_1 + \sqrt{3}\alpha_2\beta_4 + \sqrt{3}\alpha_3\beta_3 \\ \sqrt{3}\alpha_1\beta_3 + \alpha_2\beta_1 - \sqrt{6}\alpha_3\beta_5 \\ \sqrt{3}\alpha_1\beta_4 - \sqrt{6}\alpha_2\beta_2 + \alpha_3\beta_1 \end{pmatrix}$
$\mathbf{4} : \begin{pmatrix} 2\sqrt{2}\alpha_1\beta_2 - \sqrt{6}\alpha_2\beta_1 + \alpha_3\beta_3 \\ -\sqrt{2}\alpha_1\beta_3 + 2\alpha_2\beta_2 - 3\alpha_3\beta_4 \\ \sqrt{2}\alpha_1\beta_4 + 3\alpha_2\beta_3 - 2\alpha_3\beta_5 \\ -2\sqrt{2}\alpha_1\beta_5 - \alpha_2\beta_4 + \sqrt{6}\alpha_3\beta_1 \end{pmatrix}$	$\mathbf{4} : \begin{pmatrix} \sqrt{2}\alpha_1\beta_2 + 3\alpha_2\beta_5 - 2\alpha_3\beta_4 \\ 2\sqrt{2}\alpha_1\beta_3 - \sqrt{6}\alpha_2\beta_1 + \alpha_3\beta_5 \\ -2\sqrt{2}\alpha_1\beta_4 - \alpha_2\beta_2 + \sqrt{6}\alpha_3\beta_1 \\ -\sqrt{2}\alpha_1\beta_5 + 2\alpha_2\beta_3 - 3\alpha_3\beta_2 \end{pmatrix}$
$\mathbf{5} : \begin{pmatrix} \sqrt{3}(\alpha_2\beta_5 - \alpha_3\beta_2) \\ -\alpha_1\beta_2 - \sqrt{3}\alpha_2\beta_1 - \sqrt{2}\alpha_3\beta_3 \\ -2\alpha_1\beta_3 - \sqrt{2}\alpha_2\beta_2 \\ 2\alpha_1\beta_4 + \sqrt{2}\alpha_3\beta_5 \\ \alpha_1\beta_5 + \sqrt{2}\alpha_2\beta_4 + \sqrt{3}\alpha_3\beta_1 \end{pmatrix}$	$\mathbf{5} : \begin{pmatrix} \sqrt{3}(\alpha_2\beta_4 - \alpha_3\beta_3) \\ 2\alpha_1\beta_2 + \sqrt{2}\alpha_3\beta_4 \\ -\alpha_1\beta_3 - \sqrt{3}\alpha_2\beta_1 - \sqrt{2}\alpha_3\beta_5 \\ \alpha_1\beta_4 + \sqrt{2}\alpha_2\beta_2 + \sqrt{3}\alpha_3\beta_1 \\ -2\alpha_1\beta_5 - \sqrt{2}\alpha_2\beta_3 \end{pmatrix}$

$\mathbf{4} \otimes \mathbf{4} = \mathbf{1}_S \oplus \mathbf{3}_A \oplus \mathbf{3}'_A \oplus \mathbf{4}_S \oplus \mathbf{5}_S$	$\mathbf{4} \otimes \mathbf{5} = \mathbf{3} \oplus \mathbf{3}' \oplus \mathbf{4} \oplus \mathbf{5}_1 \oplus \mathbf{5}_2$
$\mathbf{1}_S : \alpha_1\beta_4 + \alpha_2\beta_3 + \alpha_3\beta_2 + \alpha_4\beta_1$	$\mathbf{3} : \begin{pmatrix} 2\sqrt{2}\alpha_1\beta_5 - \sqrt{2}\alpha_2\beta_4 + \sqrt{2}\alpha_3\beta_3 - 2\sqrt{2}\alpha_4\beta_2 \\ -\sqrt{6}\alpha_1\beta_1 + 2\alpha_2\beta_5 + 3\alpha_3\beta_4 - \alpha_4\beta_3 \\ \alpha_1\beta_4 - 3\alpha_2\beta_3 - 2\alpha_3\beta_2 + \sqrt{6}\alpha_4\beta_1 \end{pmatrix}$
$\mathbf{3}_A : \begin{pmatrix} -\alpha_1\beta_4 + \alpha_2\beta_3 - \alpha_3\beta_2 + \alpha_4\beta_1 \\ \sqrt{2}(\alpha_2\beta_4 - \alpha_4\beta_2) \\ \sqrt{2}(\alpha_1\beta_3 - \alpha_3\beta_1) \end{pmatrix}$	$\mathbf{3}' : \begin{pmatrix} \sqrt{2}\alpha_1\beta_5 + 2\sqrt{2}\alpha_2\beta_4 - 2\sqrt{2}\alpha_3\beta_3 - \sqrt{2}\alpha_4\beta_2 \\ 3\alpha_1\beta_2 - \sqrt{6}\alpha_2\beta_1 - \alpha_3\beta_5 + 2\alpha_4\beta_4 \\ -2\alpha_1\beta_3 + \alpha_2\beta_2 + \sqrt{6}\alpha_3\beta_1 - 3\alpha_4\beta_5 \end{pmatrix}$
$\mathbf{3}'_A : \begin{pmatrix} \alpha_1\beta_4 + \alpha_2\beta_3 - \alpha_3\beta_2 - \alpha_4\beta_1 \\ \sqrt{2}(\alpha_3\beta_4 - \alpha_4\beta_3) \\ \sqrt{2}(\alpha_1\beta_2 - \alpha_2\beta_1) \end{pmatrix}$	$\mathbf{4} : \begin{pmatrix} \sqrt{3}\alpha_1\beta_1 - \sqrt{2}\alpha_2\beta_5 + \sqrt{2}\alpha_3\beta_4 - 2\sqrt{2}\alpha_4\beta_3 \\ -\sqrt{2}\alpha_1\beta_2 - \sqrt{3}\alpha_2\beta_1 + 2\sqrt{2}\alpha_3\beta_5 + \sqrt{2}\alpha_4\beta_4 \\ \sqrt{2}\alpha_1\beta_3 + 2\sqrt{2}\alpha_2\beta_2 - \sqrt{3}\alpha_3\beta_1 - \sqrt{2}\alpha_4\beta_5 \\ -2\sqrt{2}\alpha_1\beta_4 + \sqrt{2}\alpha_2\beta_3 - \sqrt{2}\alpha_3\beta_2 + \sqrt{3}\alpha_4\beta_1 \end{pmatrix}$
$\mathbf{4}_S : \begin{pmatrix} \alpha_2\beta_4 + \alpha_3\beta_3 + \alpha_4\beta_2 \\ \alpha_1\beta_1 + \alpha_3\beta_4 + \alpha_4\beta_3 \\ \alpha_1\beta_2 + \alpha_2\beta_1 + \alpha_4\beta_4 \\ \alpha_1\beta_3 + \alpha_2\beta_2 + \alpha_3\beta_1 \end{pmatrix}$	$\mathbf{5}_1 : \begin{pmatrix} \sqrt{2}\alpha_1\beta_5 - \sqrt{2}\alpha_2\beta_4 - \sqrt{2}\alpha_3\beta_3 + \sqrt{2}\alpha_4\beta_2 \\ -\sqrt{2}\alpha_1\beta_1 - \sqrt{3}\alpha_3\beta_4 - \sqrt{3}\alpha_4\beta_3 \\ \sqrt{3}\alpha_1\beta_2 + \sqrt{2}\alpha_2\beta_1 + \sqrt{3}\alpha_3\beta_5 \\ \sqrt{3}\alpha_2\beta_2 + \sqrt{2}\alpha_3\beta_1 + \sqrt{3}\alpha_4\beta_5 \\ -\sqrt{3}\alpha_1\beta_4 - \sqrt{3}\alpha_2\beta_3 - \sqrt{2}\alpha_4\beta_1 \end{pmatrix}$
$\mathbf{5}_S : \begin{pmatrix} \sqrt{3}(\alpha_1\beta_4 - \alpha_2\beta_3 - \alpha_3\beta_2 + \alpha_4\beta_1) \\ -\sqrt{2}\alpha_2\beta_4 + 2\sqrt{2}\alpha_3\beta_3 - \sqrt{2}\alpha_4\beta_2 \\ -2\sqrt{2}\alpha_1\beta_1 + \sqrt{2}\alpha_3\beta_4 + \sqrt{2}\alpha_4\beta_3 \\ \sqrt{2}\alpha_1\beta_2 + \sqrt{2}\alpha_2\beta_1 - 2\sqrt{2}\alpha_4\beta_4 \\ -\sqrt{2}\alpha_1\beta_3 + 2\sqrt{2}\alpha_2\beta_2 - \sqrt{2}\alpha_3\beta_1 \end{pmatrix}$	$\mathbf{5}_2 : \begin{pmatrix} 2\alpha_1\beta_5 + 4\alpha_2\beta_4 + 4\alpha_3\beta_3 + 2\alpha_4\beta_2 \\ 4\alpha_1\beta_1 + 2\sqrt{6}\alpha_2\beta_5 \\ -\sqrt{6}\alpha_1\beta_2 + 2\alpha_2\beta_1 - \sqrt{6}\alpha_3\beta_5 + 2\sqrt{6}\alpha_4\beta_4 \\ 2\sqrt{6}\alpha_1\beta_3 - \sqrt{6}\alpha_2\beta_2 + 2\alpha_3\beta_1 - \sqrt{6}\alpha_4\beta_5 \\ 2\sqrt{6}\alpha_3\beta_2 + 4\alpha_4\beta_1 \end{pmatrix}$

$\mathbf{5} \otimes \mathbf{5} = \mathbf{1}_S \oplus \mathbf{3}_A \oplus \mathbf{3}'_A \oplus \mathbf{4}_{S,1} \oplus \mathbf{4}_{A,2} \oplus \mathbf{5}_{S,1} \oplus \mathbf{5}_{S,2}$
$ \begin{aligned} &\mathbf{1}_S : \alpha_1\beta_1 + \alpha_2\beta_5 + \alpha_3\beta_4 + \alpha_4\beta_3 + \alpha_5\beta_2 \\ &\mathbf{3}_A : \begin{pmatrix} \alpha_2\beta_5 + 2\alpha_3\beta_4 - 2\alpha_4\beta_3 - \alpha_5\beta_2 \\ -\sqrt{3}\alpha_1\beta_2 + \sqrt{3}\alpha_2\beta_1 + \sqrt{2}\alpha_3\beta_5 - \sqrt{2}\alpha_5\beta_3 \\ \sqrt{3}\alpha_1\beta_5 + \sqrt{2}\alpha_2\beta_4 - \sqrt{2}\alpha_4\beta_2 - \sqrt{3}\alpha_5\beta_1 \end{pmatrix} \\ &\mathbf{3}'_A : \begin{pmatrix} 2\alpha_2\beta_5 - \alpha_3\beta_4 + \alpha_4\beta_3 - 2\alpha_5\beta_2 \\ \sqrt{3}\alpha_1\beta_3 - \sqrt{3}\alpha_3\beta_1 + \sqrt{2}\alpha_4\beta_5 - \sqrt{2}\alpha_5\beta_4 \\ -\sqrt{3}\alpha_1\beta_4 + \sqrt{2}\alpha_2\beta_3 - \sqrt{2}\alpha_3\beta_2 + \sqrt{3}\alpha_4\beta_1 \end{pmatrix} \\ &\mathbf{4}_{S,1} : \begin{pmatrix} 3\sqrt{2}\alpha_1\beta_2 + 3\sqrt{2}\alpha_2\beta_1 - \sqrt{3}\alpha_3\beta_5 + 4\sqrt{3}\alpha_4\beta_4 - \sqrt{3}\alpha_5\beta_3 \\ 3\sqrt{2}\alpha_1\beta_3 + 4\sqrt{3}\alpha_2\beta_2 + 3\sqrt{2}\alpha_3\beta_1 - \sqrt{3}\alpha_4\beta_5 - \sqrt{3}\alpha_5\beta_4 \\ 3\sqrt{2}\alpha_1\beta_4 - \sqrt{3}\alpha_2\beta_3 - \sqrt{3}\alpha_3\beta_2 + 3\sqrt{2}\alpha_4\beta_1 + 4\sqrt{3}\alpha_5\beta_5 \\ 3\sqrt{2}\alpha_1\beta_5 - \sqrt{3}\alpha_2\beta_4 + 4\sqrt{3}\alpha_3\beta_3 - \sqrt{3}\alpha_4\beta_2 + 3\sqrt{2}\alpha_5\beta_1 \end{pmatrix} \\ &\mathbf{4}_{A,2} : \begin{pmatrix} \sqrt{2}\alpha_1\beta_2 - \sqrt{2}\alpha_2\beta_1 + \sqrt{3}\alpha_3\beta_5 - \sqrt{3}\alpha_5\beta_3 \\ -\sqrt{2}\alpha_1\beta_3 + \sqrt{2}\alpha_3\beta_1 + \sqrt{3}\alpha_4\beta_5 - \sqrt{3}\alpha_5\beta_4 \\ -\sqrt{2}\alpha_1\beta_4 - \sqrt{3}\alpha_2\beta_3 + \sqrt{3}\alpha_3\beta_2 + \sqrt{2}\alpha_4\beta_1 \\ \sqrt{2}\alpha_1\beta_5 - \sqrt{3}\alpha_2\beta_4 + \sqrt{3}\alpha_4\beta_2 - \sqrt{2}\alpha_5\beta_1 \end{pmatrix} \\ &\mathbf{5}_{S,1} : \begin{pmatrix} 2\alpha_1\beta_1 + \alpha_2\beta_5 - 2\alpha_3\beta_4 - 2\alpha_4\beta_3 + \alpha_5\beta_2 \\ \alpha_1\beta_2 + \alpha_2\beta_1 + \sqrt{6}\alpha_3\beta_5 + \sqrt{6}\alpha_5\beta_3 \\ -2\alpha_1\beta_3 + \sqrt{6}\alpha_2\beta_2 - 2\alpha_3\beta_1 \\ -2\alpha_1\beta_4 - 2\alpha_4\beta_1 + \sqrt{6}\alpha_5\beta_5 \\ \alpha_1\beta_5 + \sqrt{6}\alpha_2\beta_4 + \sqrt{6}\alpha_4\beta_2 + \alpha_5\beta_1 \end{pmatrix} \\ &\mathbf{5}_{S,2} : \begin{pmatrix} 2\alpha_1\beta_1 - 2\alpha_2\beta_5 + \alpha_3\beta_4 + \alpha_4\beta_3 - 2\alpha_5\beta_2 \\ -2\alpha_1\beta_2 - 2\alpha_2\beta_1 + \sqrt{6}\alpha_4\beta_4 \\ \alpha_1\beta_3 + \alpha_3\beta_1 + \sqrt{6}\alpha_4\beta_5 + \sqrt{6}\alpha_5\beta_4 \\ \alpha_1\beta_4 + \sqrt{6}\alpha_2\beta_3 + \sqrt{6}\alpha_3\beta_2 + \alpha_4\beta_1 \\ -2\alpha_1\beta_5 + \sqrt{6}\alpha_3\beta_3 - 2\alpha_5\beta_1 \end{pmatrix}. \end{aligned} $

B Lepton flavor mixing from A_5 family symmetry without CP

In this section, we investigate the possible lepton mixing patterns which can be derived from only A_5 family symmetry without CP symmetry imposed. As usual, the three generations of left-handed leptons are assigned to the triplet representation $\mathbf{3}$, and A_5 is broken into two different abelian subgroups G_l and G_ν in the charged lepton and neutrino sector respectively. The residual flavor symmetry G_ν can only be a Z_2 or K_4 subgroup of A_5 since we assume neutrinos are Majorana particles here. In this approach, the PMNS matrix can be obtained by simply diagonalizing the representation matrices of the generators of G_l and G_ν without resorting to the mass matrix [12, 48, 49]. For $G_\nu = K_4$ and G_l is capable of distinguishing the three generations of charged lepton, i.e., the eigenvalues of the generators of G_l aren't degenerate, the PMNS matrix would be completely fixed up to row and column permutations. However, only one column would be fixed by the remnant flavor symmetries G_l and G_ν in case of $G_\nu = Z_2$. In the following, the scenario of $G_l = Z_2$ and $G_\nu = K_4$ shall be discussed as well, and one row would be fixed instead. It is noteworthy that two pairs of subgroups (G_l, G_ν) and (G'_l, G'_ν) lead to the same result for the PMNS matrix, if they are conjugate under an element of the A_5 group.

B.1 $G_\nu = K_4$

From Appendix A, we know that G_l can be a Z_3 , Z_5 or K_4 subgroup of A_5 . In case of $G_l = Z_5$, all $6 \times 5 = 30$ possible combinations of G_l and G_ν give rise to the same mixing matrix

$$U_{PMNS} = \begin{pmatrix} -\sqrt{\frac{\kappa}{\sqrt{5}}} & \sqrt{\frac{1}{\sqrt{5}\kappa}} & 0 \\ \sqrt{\frac{1}{2\sqrt{5}\kappa}} & \sqrt{\frac{\kappa}{2\sqrt{5}}} & -\frac{1}{\sqrt{2}} \\ \sqrt{\frac{1}{2\sqrt{5}\kappa}} & \sqrt{\frac{\kappa}{2\sqrt{5}}} & \frac{1}{\sqrt{2}} \end{pmatrix} \equiv U_{GR}, \quad (\text{B.1})$$

which is the well-known golden ratio mixing pattern. The mixing angles are determined to be $\sin^2 \theta_{12} = (3 - \kappa)/5 \simeq 0.276$, $\sin^2 \theta_{23} = 1/2$ and $\sin^2 \theta_{13} = 0$. Obviously θ_{13} should acquire moderate corrections to accommodate the measured non-vanishing value of the reactor angle although θ_{12} and θ_{23} are in the experimentally favored 3σ ranges [5].

In case of $G_l = Z_3$, we find two mixing patterns can be obtained. For the representative symmetries $G_l = Z_3^{T^3 ST^2 S}$ and $G_\nu = K_4^{(ST^2 ST^3 S, TST^4)}$, the elements of G_l and G_ν generate an A_4 subgroup instead of the full flavor symmetry group A_5 . The resulting mixing matrix is given by the familiar democratic mixing in which all elements have the same absolute value [50], i.e.,

$$U_{PMNS} = \frac{1}{\sqrt{3}} \begin{pmatrix} 1 & 1 & 1 \\ e^{\frac{2\pi i}{3}} & 1 & -e^{\frac{\pi i}{3}} \\ -e^{\frac{\pi i}{3}} & 1 & e^{\frac{2\pi i}{3}} \end{pmatrix} \equiv U_{DM}. \quad (\text{B.2})$$

The mixing angles are $\sin^2 \theta_{12} = \sin^2 \theta_{23} = 1/2$ and $\sin^2 \theta_{13} = 1/3$. Large corrections to θ_{12} and θ_{13} are needed to be compatible with experimental data. For another representative symmetries $G_l = Z_3^{T^3 ST^2 S}$ and $G_\nu = K_4^{(S, T^3 ST^2 ST^3)}$, the parent group A_5 can be generated by G_l and G_ν . The mixing matrix is found to be of the form:

$$U_{PMNS} = \frac{1}{\sqrt{6}} \begin{pmatrix} \sqrt{2}\kappa & \sqrt{2}(1 - \kappa) & 0 \\ \kappa - 1 & \kappa & -\sqrt{3} \\ \kappa - 1 & \kappa & \sqrt{3} \end{pmatrix} \equiv U_{ST}, \quad (\text{B.3})$$

which leads to the following mixing angles: $\sin^2 \theta_{12} = (2 - \kappa)/3 \simeq 0.127$, $\sin^2 \theta_{23} = 1/2$ and $\sin^2 \theta_{13} = 0$. Notice that both θ_{12} and θ_{13} are outside of the 3σ ranges [5]. The same results have been obtained in Refs. [49, 51]. For the last case of $G_l = K_4$, where G_ν and G_l are not the same Klein group, only one mixing pattern can be derived,

$$U_{PMNS} = \frac{1}{2} \begin{pmatrix} \kappa & -1 & \kappa - 1 \\ -1 & 1 - \kappa & \kappa \\ \kappa - 1 & \kappa & 1 \end{pmatrix} \equiv U_{RC}. \quad (\text{B.4})$$

We can extract the mixing angles: $\sin^2 \theta_{12} = (3 - \kappa)/5 \simeq 0.276$, $\sin^2 \theta_{23} = (2 + \kappa)/5 \simeq 0.724$ and $\sin^2 \theta_{13} = (2 - \kappa)/4 \simeq 0.0955$. Both θ_{13} and θ_{23} are too large to be acceptable. This mixing pattern has also been found in Ref. [49]. In summary, no mixing matrix in agreement with experimental data can be obtained if the full Klein symmetry is preserved by the neutrino mass matrix. In the following, we consider the situation with a single residual Z_2 flavor symmetry in the neutrino sector or in the charged lepton sector.

B.2 $G_\nu = Z_2$ or $G_l = Z_2$

In this case, only one column or one row of the PMNS matrix would be determined up to permutations and phases of its elements by the remnant flavor symmetries G_l and

G_l	G_ν	Fixed column or row	
Z_5^T	Z_2^S	$(-\sqrt{\frac{\kappa}{\sqrt{5}}}, \frac{1}{\sqrt{2\sqrt{5}\kappa}}, \frac{1}{\sqrt{2\sqrt{5}\kappa}})^T$	✓
	$Z_2^{T^3ST^2ST^3}$	$(\sqrt{\frac{1}{\sqrt{5}\kappa}}, \sqrt{\frac{\kappa}{2\sqrt{5}}}, \sqrt{\frac{\kappa}{2\sqrt{5}}})^T$	✓
	$Z_2^{T^3ST^2ST^3S}$	$(0, -\frac{1}{\sqrt{2}}, \frac{1}{\sqrt{2}})^T$	✗
$Z_3^{T^3ST^2S}$	Z_2^S	$(0, -\frac{1}{\sqrt{2}}, \frac{1}{\sqrt{2}})^T$	✗
	$Z_2^{T^3ST^2ST^3}$	$(\frac{1-\kappa}{\sqrt{3}}, \frac{\kappa}{\sqrt{6}}, \frac{\kappa}{\sqrt{6}})^T$	✗
	$Z_2^{T^3ST^2ST^3S}$	$(\frac{\kappa}{\sqrt{3}}, \frac{\kappa-1}{\sqrt{6}}, \frac{\kappa-1}{\sqrt{6}})^T$	✗
$Z_3^{T^3ST^2S}$	$Z_2^{ST^2ST^3S}$	$(\frac{1}{\sqrt{3}}, \frac{1}{\sqrt{3}}, \frac{1}{\sqrt{3}})^T$	✓
$K_4^{(ST^2ST^3S, TST^4)}$	Z_2^S	$(\frac{\kappa}{2}, -\frac{1}{2}, \frac{\kappa-1}{2})^T$	✓
$K_4^{(ST^2ST^3S, TST^4)}$	$Z_2^{TST^4}$	$(1, 0, 0)^T$	✗
Z_2^S	$K_4^{(ST^2ST^3S, TST^4)}$	$(\frac{\kappa}{2}, \frac{1}{2}, \frac{\kappa-1}{2})$	✗
$Z_2^{TST^4}$	$K_4^{(ST^2ST^3S, TST^4)}$	$(1, 0, 0)$	✗

Table 4: The possible form of one column (row) of the PMNS matrix determined by the residual flavor symmetry $G_\nu = Z_2$ ($G_l = Z_2$) within the framework of A_5 flavor symmetry. The notation “✓” denotes that the relevant lepton mixing is compatible with the experimental data at 3σ level [5]. The notation “✗” implies the resulting mixing is not viable.

G_ν [34, 52]. This method generally allows us to obtain relations between mixing parameters and a non-zero θ_{13} . We have scanned all independent combinations of G_l and G_ν , and the corresponding explicit forms of the fixed column or row vector are presented in Table 4. Comparing with the present 3σ confidence level ranges of the moduli of the elements of the leptonic mixing matrix [5]

$$|U_{PMNS}|_{3\sigma} = \begin{pmatrix} 0.789 \rightarrow 0.853 & 0.501 \rightarrow 0.594 & 0.133 \rightarrow 0.172 \\ 0.194 \rightarrow 0.558 & 0.408 \rightarrow 0.735 & 0.602 \rightarrow 0.784 \\ 0.194 \rightarrow 0.558 & 0.408 \rightarrow 0.735 & 0.602 \rightarrow 0.784 \end{pmatrix}, \quad (\text{B.5})$$

we find that neither of the two possible row vectors can be accommodated by the data, and only four cases are viable. The remnant symmetries can be chosen to be $(G_l, G_\nu) = (Z_5^T, Z_2^S)$, $(Z_5^T, Z_2^{T^3ST^2ST^3})$, $(Z_3^{T^3ST^2S}, Z_2^{ST^2ST^3S})$ and $(K_4^{(ST^2ST^3S, TST^4)}, Z_2^S)$ without loss of generality, and the fixed column are $(-\sqrt{\frac{\kappa}{\sqrt{5}}}, \frac{1}{\sqrt{2\sqrt{5}\kappa}}, \frac{1}{\sqrt{2\sqrt{5}\kappa}})^T$, $(\sqrt{\frac{1}{\sqrt{5}\kappa}}, \sqrt{\frac{\kappa}{2\sqrt{5}}}, \sqrt{\frac{\kappa}{2\sqrt{5}}})^T$, $\frac{1}{\sqrt{3}}(1, 1, 1)^T$ and $\frac{1}{2}(\kappa, -1, \kappa - 1)^T$ respectively. These column vectors can fit the first or the second column of the PMNS matrix. The resulting lepton mixing matrix can be obtained from U_{GR} , U_{DM} and U_{RC} by multiplying a unitary matrix U_{23} or U_{13} from the right-hand side with

$$U_{13} = \begin{pmatrix} \cos \theta & 0 & \sin \theta e^{-i\delta} \\ 0 & 1 & 0 \\ -\sin \theta e^{i\delta} & 0 & \cos \theta \end{pmatrix}, \quad U_{23} = \begin{pmatrix} 1 & 0 & 0 \\ 0 & \cos \theta & \sin \theta e^{-i\delta} \\ 0 & -\sin \theta e^{i\delta} & \cos \theta \end{pmatrix}, \quad (\text{B.6})$$

where θ and δ are real, and a arbitrary phase matrix in the right-hand side of U_{13} and U_{23} is omitted, since they can be absorbed into the Majorana phases which are not constrained by flavor symmetry. The multiplication of U_{13} (U_{23}) corresponds to performing a unitary linear transformation of the 1st (2nd) and 3rd columns. In the following, we shall discuss the predictions for the PMNS matrix and lepton mixing parameters in each case.

B.2.1 $G_l = Z_5^T, G_\nu = Z_2^S$

The lepton mixing matrix U_{PMNS} is predicted to have one column $(-\sqrt{\frac{\kappa}{5}}, \frac{1}{\sqrt{2\sqrt{5}\kappa}}, \frac{1}{\sqrt{2\sqrt{5}\kappa}})^T$, which coincides with the first column of the GR mixing. The other two columns should be orthogonal to it, and they can be obtained by making a unitary rotation of the 2nd and 3rd columns of U_{GR} .

$$U_{PMNS} = U_{GR}U_{23} = \begin{pmatrix} -\sqrt{\frac{\kappa}{5}} & \sqrt{\frac{1}{5\kappa}} \cos \theta & \sqrt{\frac{1}{5\kappa}} \sin \theta e^{-i\delta} \\ \frac{1}{\sqrt{2\sqrt{5}\kappa}} & \sqrt{\frac{\kappa}{2\sqrt{5}}} \cos \theta + \frac{\sin \theta}{\sqrt{2}} e^{i\delta} & \sqrt{\frac{\kappa}{2\sqrt{5}}} \sin \theta e^{-i\delta} - \frac{\cos \theta}{\sqrt{2}} \\ \frac{1}{\sqrt{2\sqrt{5}\kappa}} & \sqrt{\frac{\kappa}{2\sqrt{5}}} \cos \theta - \frac{\sin \theta}{\sqrt{2}} e^{i\delta} & \sqrt{\frac{\kappa}{2\sqrt{5}}} \sin \theta e^{-i\delta} + \frac{\cos \theta}{\sqrt{2}} \end{pmatrix}. \quad (\text{B.7})$$

This form of modification to the GR mixing has been discussed in a phenomenological way in Ref. [53–55]. Here we show that this mixing pattern can be naturally reproduced from the A_5 flavor symmetry. The mixing angles can be straightforwardly extracted as follows,

$$\begin{aligned} \sin^2 \theta_{13} &= \frac{3 - \kappa}{5} \sin^2 \theta, \quad \sin^2 \theta_{12} = \frac{2 \cos^2 \theta}{3 + 2\kappa + \cos 2\theta}, \\ \sin^2 \theta_{23} &= \frac{1}{2} - \frac{\sqrt{3 + 4\kappa} \sin 2\theta \cos \delta}{3 + 2\kappa + \cos 2\theta}. \end{aligned} \quad (\text{B.8})$$

We see that the solar and reactor mixing angles are related by

$$5 \cos^2 \theta_{12} \cos^2 \theta_{13} = 2 + \kappa. \quad (\text{B.9})$$

Given the 3σ ranges $1.76 \times 10^{-2} \leq \sin^2 \theta_{13} \leq 2.95 \times 10^{-2}$ and $0.259 \leq \sin^2 \theta_{12} \leq 0.359$ from global analysis [5], θ_{13} and θ_{12} are further constrained to be in the intervals of $1.76 \times 10^{-2} \leq \sin^2 \theta_{13} \leq 2.35 \times 10^{-2}$ and $0.259 \leq \sin^2 \theta_{12} \leq 0.263$ by this correlation. The well-known Jarlskog invariant J_{CP} [56], which measures the size of the CP violation, is written as

$$J_{CP} = -\frac{\sqrt{3 - \kappa}}{20} \sin 2\theta \sin \delta. \quad (\text{B.10})$$

The Dirac CP violating phase δ_{CP} is expressed in terms of θ and δ as

$$\sin \delta_{CP} = -\frac{\sqrt{2}(3 + 2\kappa + \cos 2\theta) \text{sign}(\sin 2\theta) \sin \delta}{\sqrt{4(3 + 2\kappa) \cos 2\theta + (7 + 8\kappa)(3 + \cos 4\theta) - 4(3 + 4\kappa) \cos 2\delta \sin^2 2\theta}}, \quad (\text{B.11})$$

In order to see how well the lepton mixing angles can be described by this mixing pattern and its prediction for δ_{CP} , we perform a numerical analysis. The free parameters θ and δ are scattered in their whole allowed ranges of $0 \leq \theta < 2\pi$ and $0 \leq \delta < 2\pi$. The correlations and the possible values of the mixing parameters are plotted in Fig. 6. Furthermore, the experimental data of three mixing angles θ_{12} , θ_{13} and θ_{23} at 3σ level [5] are considered, accordingly the allowed values of the mixing parameters would generically be constrained in small regions. Here and hereafter, we perform numerical analysis and present results only for normal ordering neutrino mass spectrum. The results would change a little bit for the inverted ordering case. From Fig. 6, we can read that $\sin^2 \theta_{12}$ is predicted to be around 0.26, any value of θ_{23} within the 3σ range can be achieved and δ_{CP} is restricted in the range of $[0.990, 2.152] \cup [4.131, 5.293]$. Recalling that if both A_5 family symmetry and generalized CP are imposed, as discussed in section 3.1, the parameter δ can only be $\pi/2$ (case II) rather than free. Note that case I is not viable. As a consequence, the Dirac CP δ_{CP} would be maximal. Therefore we conclude that the generalized CP symmetry is a quite effective method of predicting the CP violating phases.

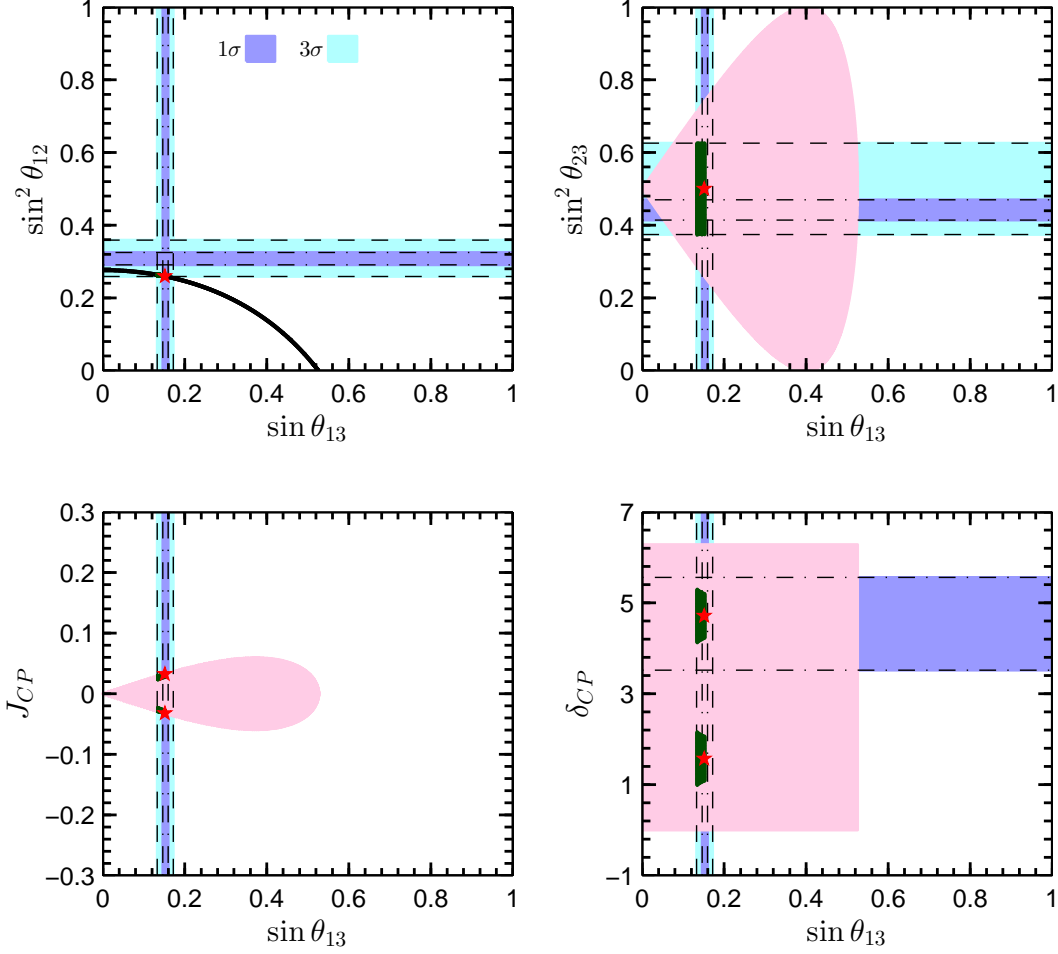


Figure 6: Predictions for the mixing parameters $\sin^2 \theta_{12}$, $\sin^2 \theta_{23}$, J_{CP} and δ_{CP} with respect to $\sin \theta_{13}$ when the remnant flavor symmetries are $G_l = Z_5^T$ and $G_\nu = Z_2^S$. The corresponding PMNS matrix is given by Eq. (B.7). The pink regions denote the possible values of the parameters when both θ and δ freely vary in the whole region of $[0, 2\pi]$. The dark green areas represent the regions allowed by the current experimental data for three neutrino mixing angles at 3σ level [5]. The red pentagrams refer to the best fitting values of case II discussed in section 3.1, after the generalized CP is imposed.

B.2.2 $G_l = Z_5^T, G_\nu = Z_2^{T^3 ST^2 ST^3}$

In this case, one column of U_{PMNS} is determined to be $(\sqrt{\frac{1}{\sqrt{5}\kappa}}, \sqrt{\frac{\kappa}{2\sqrt{5}}}, \sqrt{\frac{\kappa}{2\sqrt{5}}})^T$ which is exactly the second column of the GR mixing. The corresponding PMNS matrix can be obtained from U_{GR} by multiplying U_{13} from right-hand side,

$$U_{PMNS} = U_{GR} U_{13} = \begin{pmatrix} -\sqrt{\frac{\kappa}{\sqrt{5}}} \cos \theta & \sqrt{\frac{1}{\sqrt{5}\kappa}} & -\sqrt{\frac{\kappa}{\sqrt{5}}} \sin \theta e^{-i\delta} \\ \frac{\cos \theta}{\sqrt{2\sqrt{5}\kappa}} + \frac{\sin \theta}{\sqrt{2}} e^{i\delta} & \sqrt{\frac{\kappa}{2\sqrt{5}}} & -\frac{\cos \theta}{\sqrt{2}} + \frac{\sin \theta}{\sqrt{2\sqrt{5}\kappa}} e^{-i\delta} \\ \frac{\cos \theta}{\sqrt{2\sqrt{5}\kappa}} - \frac{\sin \theta}{\sqrt{2}} e^{i\delta} & \sqrt{\frac{\kappa}{2\sqrt{5}}} & \frac{\cos \theta}{\sqrt{2}} + \frac{\sin \theta}{\sqrt{2\sqrt{5}\kappa}} e^{-i\delta} \end{pmatrix}. \quad (\text{B.12})$$

The lepton mixing parameters read

$$\sin^2 \theta_{13} = \frac{2 + \kappa}{5} \sin^2 \theta, \quad \sin^2 \theta_{12} = \frac{2}{3 + \kappa + (1 + \kappa) \cos 2\theta},$$

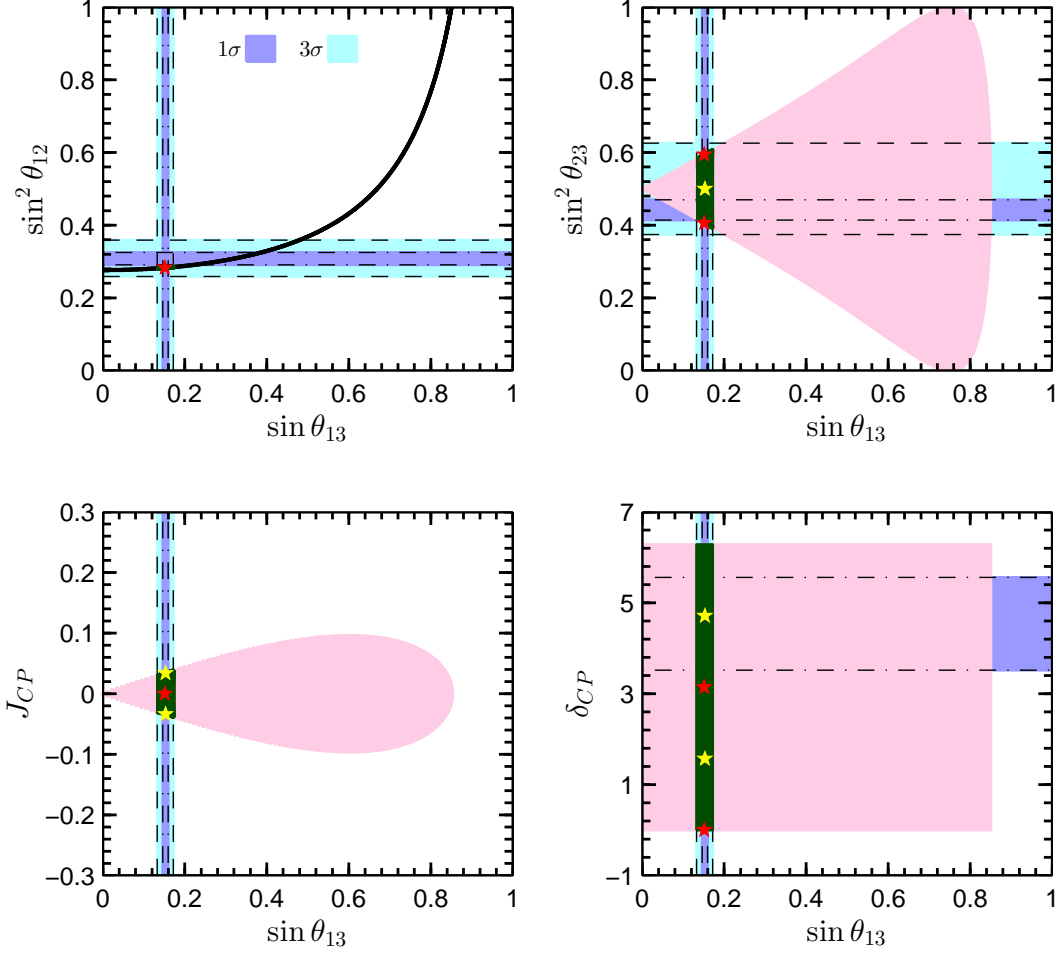


Figure 7: Predictions for the mixing parameters $\sin^2 \theta_{12}$, $\sin^2 \theta_{23}$, J_{CP} and δ_{CP} with respect to $\sin \theta_{13}$ when the remnant flavor symmetries are $G_l = Z_5^T$ and $G_\nu = Z_2^{T^3 ST^2 ST^3}$. The corresponding PMNS matrix is given by Eq. (B.12). The pink regions denote the possible values of the parameters when both θ and δ freely vary in the whole region of $[0, 2\pi]$. The dark green areas represent the regions allowed by the current experimental data for three neutrino mixing angles at 3σ level [5]. The red and yellow pentagrams denote the best fitting values of case III and case IV discussed in section 3.2, where the generalized CP symmetry is considered. Notice that the red pentagrams almost coincides with the yellow one in the first panel, since the best fitting values of $\sin^2 \theta_{12}$ and $\sin \theta_{13}$ are nearly the same in case III and case IV.

$$\begin{aligned} \sin^2 \theta_{23} &= \frac{1}{2} - \frac{\sqrt{2+\kappa} \sin 2\theta \cos \delta}{3+\kappa+(1+\kappa) \cos 2\theta}, & J_{CP} &= \frac{\sqrt{2+\kappa}}{20} \sin 2\theta \sin \delta, \\ \sin \delta_{CP} &= \frac{\sqrt{2(2+\kappa)} (3\kappa-2+\kappa \cos 2\theta) \text{sign}(\sin 2\theta) \sin \delta}{\sqrt{(13+4\kappa)(3+\cos 4\theta)+4(7+6\kappa) \cos 2\theta-20 \sin^2 2\theta \cos 2\delta}}. \end{aligned} \quad (\text{B.13})$$

We have a relation between θ_{12} and θ_{13} ,

$$5 \sin^2 \theta_{12} \cos^2 \theta_{13} = 3 - \kappa. \quad (\text{B.14})$$

The solar mixing angle θ_{12} is restricted by the observed value of θ_{13} such as $0.281 \leq \sin^2 \theta_{12} \leq 0.285$ which is in the 3σ range [5]. We display the allowed regions of the mixing angles, J_{CP} and δ_{CP} in Fig. 7. No dependence of δ_{CP} on $\sin \theta_{13}$ is observed, and δ_{CP} can take any value in the whole range of $[0, 2\pi]$. However, δ_{CP} can only be conserved or maximally broken

if generalized CP is considered, as shown in section 3.2. Note that the mixing pattern in Eq. (B.12) has been discussed in Ref. [53, 55].

B.2.3 $G_l = Z_3^{T^3 ST^2 S}, G_\nu = Z_2^{ST^2 ST^3 S}$

The chosen remnant symmetry leads to a trimaximal column $\frac{1}{\sqrt{3}}(1, 1, 1)^T$, and U_{PMNS} takes the form

$$U_{PMNS} = U_{DC} U_{13} = \frac{1}{\sqrt{3}} \begin{pmatrix} \cos \theta - e^{i\delta} \sin \theta & 1 & \cos \theta + e^{-i\delta} \sin \theta \\ e^{\frac{2\pi i}{3}} \cos \theta + e^{i(\frac{\pi}{3} + \delta)} \sin \theta & 1 & e^{i(\frac{2\pi}{3} - \delta)} \sin \theta - e^{\frac{\pi i}{3}} \cos \theta \\ -e^{\frac{\pi i}{3}} \cos \theta - e^{i(\frac{2\pi}{3} + \delta)} \sin \theta & 1 & e^{\frac{2\pi i}{3}} \cos \theta - e^{i(\frac{\pi}{3} - \delta)} \sin \theta \end{pmatrix}. \quad (\text{B.15})$$

Such a mixing pattern as a minimal modification to the tri-bimaximal has been widely discussed in the literature [53, 55, 57], and it can also be naturally reproduced from simple flavor symmetries A_4 [23, 58] and S_4 [20, 24, 58]. The predictions for the lepton mixing parameters are given by

$$\begin{aligned} \sin^2 \theta_{13} &= \frac{1}{3}(1 + \sin 2\theta \cos \delta), & \sin^2 \theta_{12} &= \frac{1}{2 - \sin 2\theta \cos \delta}, \\ \sin^2 \theta_{23} &= \frac{1}{2} - \frac{\sqrt{3} \sin 2\theta \sin \delta}{4 - 2 \sin 2\theta \cos \delta}, & J_{CP} &= -\frac{\cos 2\theta}{6\sqrt{3}}, \\ \sin \delta_{CP} &= \frac{-\sqrt{2} \cos 2\theta (2 - \sin 2\theta \cos \delta)}{\sqrt{(1 - \sin 2\theta \cos \delta)(5 + 3 \cos 4\theta + 2 \sin^3 2\theta \cos 3\delta)}}. \end{aligned} \quad (\text{B.16})$$

As expected, the following relation is fulfilled,

$$3 \sin^2 \theta_{12} \cos^2 \theta_{13} = 1, \quad (\text{B.17})$$

which generically holds true for trimaximal mixing. Inserting the experimental bound of θ_{13} [5], we obtain $0.339 \leq \sin^2 \theta_{12} \leq 0.343$. A numerical analysis similar to previous cases is performed, as shown in Fig. 8. We see that no prediction for δ_{CP} can be made. Recalling that δ_{CP} would be constrained to be maximal by generalized CP symmetry discussed in section 3.3.

B.2.4 $G_l = K_4^{(ST^2 ST^3 S, TST^4)}, G_\nu = Z_2^S$

One column is fixed to be $\frac{1}{2}(\kappa, -1, \kappa - 1)^T$ in this case, and it can only be the first column of the PMNS matrix in order to be consistent with the experimental data. As a result, U_{PMNS} is of the form

$$U_{PMNS} = U_{RC} U_{23} = \frac{1}{2} \begin{pmatrix} \kappa & -\cos \theta - \kappa^{-1} \sin \theta e^{i\delta} & \kappa^{-1} \cos \theta - \sin \theta e^{-i\delta} \\ -1 & -\kappa^{-1} \cos \theta - \kappa \sin \theta e^{i\delta} & \kappa \cos \theta - \kappa^{-1} \sin \theta e^{-i\delta} \\ \kappa - 1 & \kappa \cos \theta - \sin \theta e^{i\delta} & \cos \theta + \kappa \sin \theta e^{-i\delta} \end{pmatrix}. \quad (\text{B.18})$$

Then the three mixing angles read

$$\begin{aligned} \sin^2 \theta_{13} &= \frac{\kappa - 1}{8}(\sqrt{5} - \cos 2\theta - 2 \sin 2\theta \cos \delta), \\ \sin^2 \theta_{12} &= \frac{3 - \kappa + (\kappa - 1)(\cos 2\theta + 2 \sin 2\theta \cos \delta)}{5 + \kappa + (\kappa - 1)(\cos 2\theta + 2 \sin 2\theta \cos \delta)}, \\ \sin^2 \theta_{23} &= \frac{3 + \sqrt{5} \cos 2\theta - 2 \sin 2\theta \cos \delta}{5 + \kappa + (\kappa - 1)(\cos 2\theta + 2 \sin 2\theta \cos \delta)}. \end{aligned} \quad (\text{B.19})$$

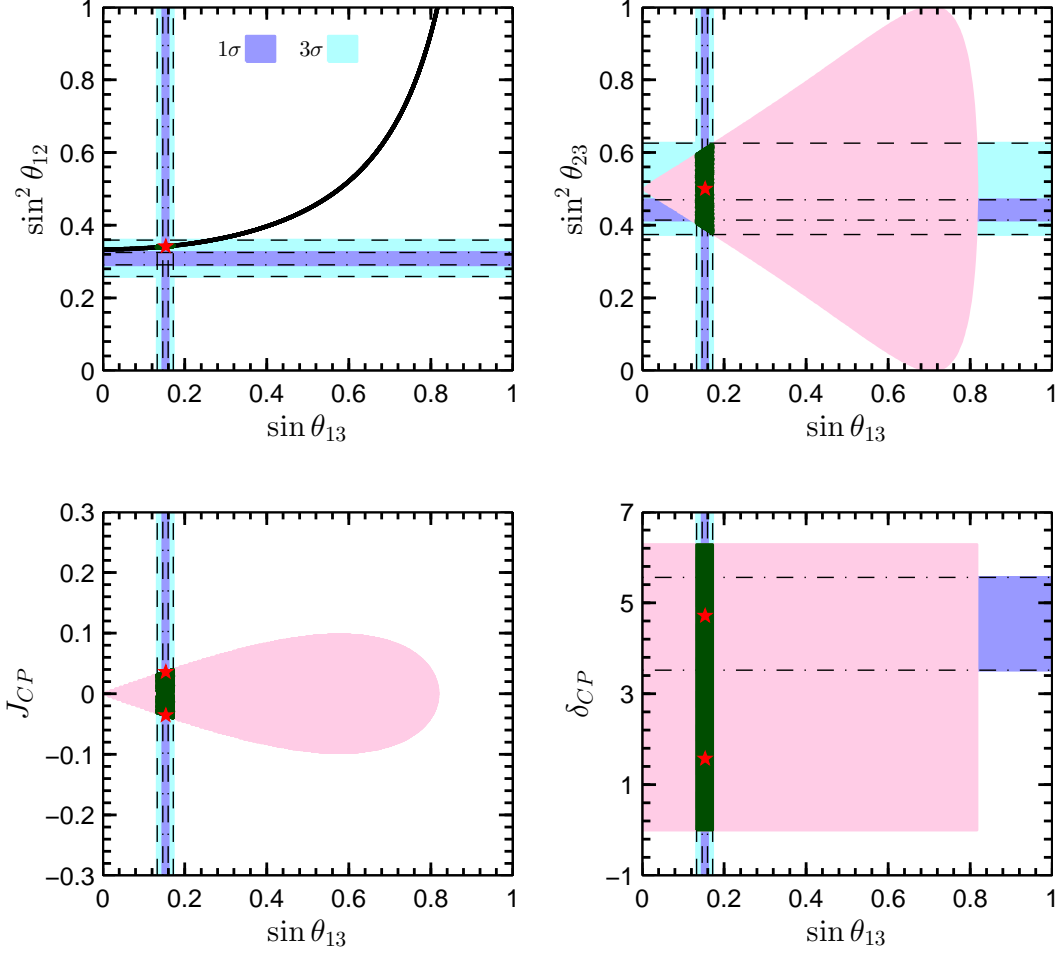


Figure 8: Predictions for the mixing parameters $\sin^2 \theta_{12}$, $\sin^2 \theta_{23}$, J_{CP} and δ_{CP} with respect to $\sin \theta_{13}$ when the remnant flavor symmetries are $G_l = Z_3^{T^3 ST^2 S}$ and $G_\nu = Z_2^{ST^2 ST^3 S}$. The corresponding PMNS matrix is given by Eq. (B.15). The pink regions denote the possible values of the parameters when both θ and δ freely vary in the whole region of $[0, 2\pi]$. The dark green areas represent the regions allowed by the current experimental data for three neutrino mixing angles at 3σ level [5]. The red pentagrams refer to the best fitting values of case V discussed in section 3.3, after the generalized CP is imposed.

A relation between θ_{12} and θ_{13} follows immediately

$$4 \cos^2 \theta_{12} \cos^2 \theta_{13} = 1 + \kappa. \quad (\text{B.20})$$

The solar mixing angle is predicted as $0.326 \leq \sin^2 \theta_{12} \leq 0.334$ which is in the experimental 3σ bound [5]. The Jarlskog invariant J_{CP} is given by

$$J_{CP} = -\frac{1}{16} \sin 2\theta \sin \delta. \quad (\text{B.21})$$

The Dirac CP violating phase δ_{CP} is

$$\sin \delta_{CP} = \frac{-\sqrt{2\kappa - 3}(6\kappa + 1 + \cos 2\theta + 2 \sin 2\theta \cos \delta) \sin 2\theta \sin \delta}{\sqrt{[5 - (\cos 2\theta + 2 \sin 2\theta \cos \delta)^2] (\sqrt{5} - \cos 2\theta + 2 \sin 2\theta \cos \delta) (3 + \sqrt{5} \cos 2\theta - 2 \sin 2\theta \cos \delta)}}. \quad (\text{B.22})$$

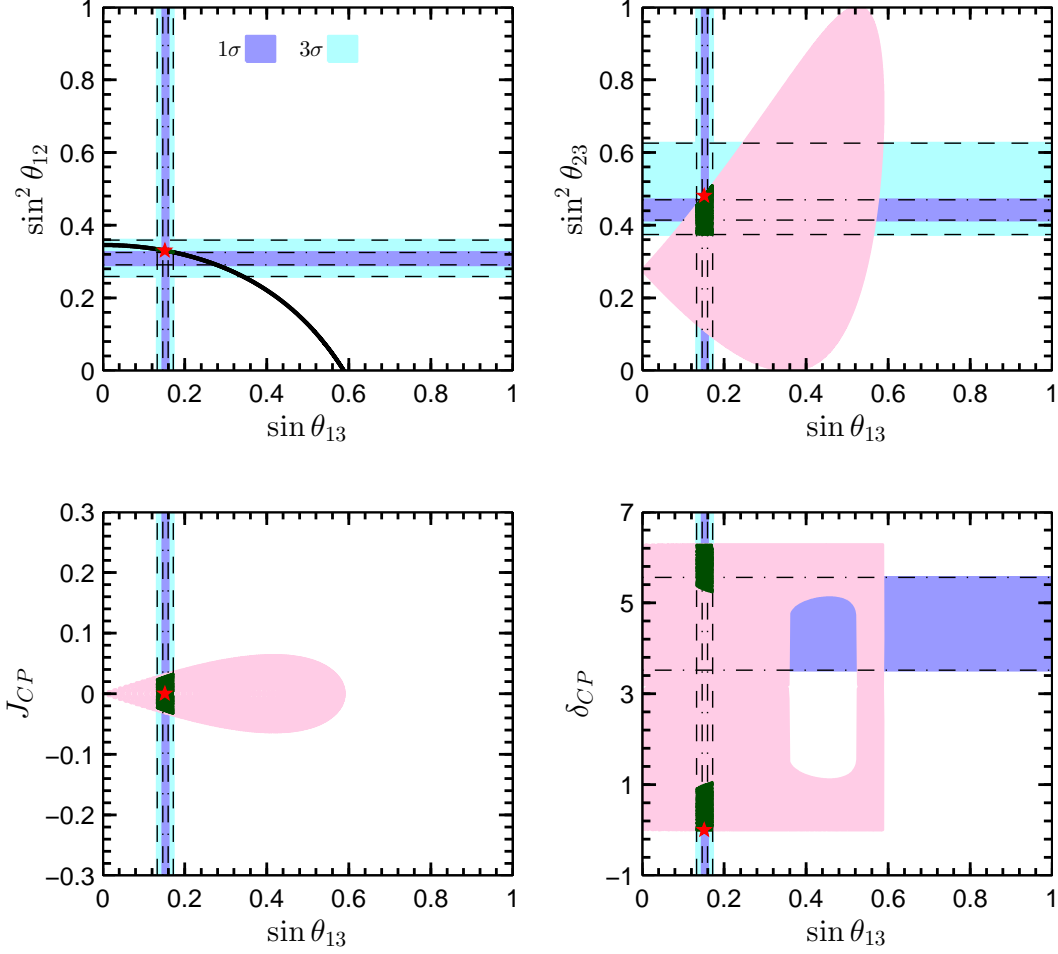


Figure 9: Predictions for the mixing parameters $\sin^2 \theta_{12}$, $\sin^2 \theta_{23}$, J_{CP} and δ_{CP} with respect to $\sin \theta_{13}$ when the remnant flavor symmetries are $G_l = K_4^{(ST^2 ST^3 S, TST^4)}$ and $G_\nu = Z_2^S$. The corresponding PMNS matrix is given by Eq. (B.18). The pink regions denote the possible values of the parameters when both θ and δ freely vary in the whole region of $[0, 2\pi]$. The dark green areas represent the regions allowed by the current experimental data for three neutrino mixing angles at 3σ level [5]. The red pentagrams refer to the best fitting values of case VII with $\theta_{23}(\theta_{bf}) < 45^\circ$ discussed in section 3.4, after the generalized CP is imposed.

The numerical results are displayed in Fig. 9. We see that δ_{CP} is predicted to be in the range of $[0, 1.043] \cup [5.240, 2\pi]$, and the atmospheric mixing angle θ_{23} mostly is less than 45° (i.e., in the first octant) in order to be compatible with experimental data of θ_{13} . The scenario of θ_{23} in the second octant can be achieved, if the second and third rows of the PMNS matrix in Eq. (B.18) are exchanged. Then the predictions for the solar and reactor mixing angles in Eq. (B.19) remain, δ_{CP} becomes $\pi + \delta_{CP}$, and θ_{23} becomes $\pi/2 - \theta_{23}$. Consequently both J_{CP} and $\sin \delta_{CP}$ change into their opposite, and the expression of $\sin^2 \theta_{23}$ in Eq. (B.19) is replaced by

$$\sin^2 \theta_{23} = \frac{\kappa(\sqrt{5} - \cos 2\theta + 2 \sin 2\theta \cos \delta)}{5 + \kappa + (\kappa - 1)(\cos 2\theta + 2 \sin 2\theta \cos \delta)}. \quad (\text{B.23})$$

The predictions for $\sin^2 \theta_{23}$ and δ_{CP} versus $\sin \theta_{13}$ are shown in Fig. 10. As expected, θ_{23} is really larger than 45° to accommodate the measured values of θ_{13} , and the CP phase δ_{CP} is in the range of $[2.099, 4.185]$. Notice that generalized CP would constrain δ_{CP} to be trivial,

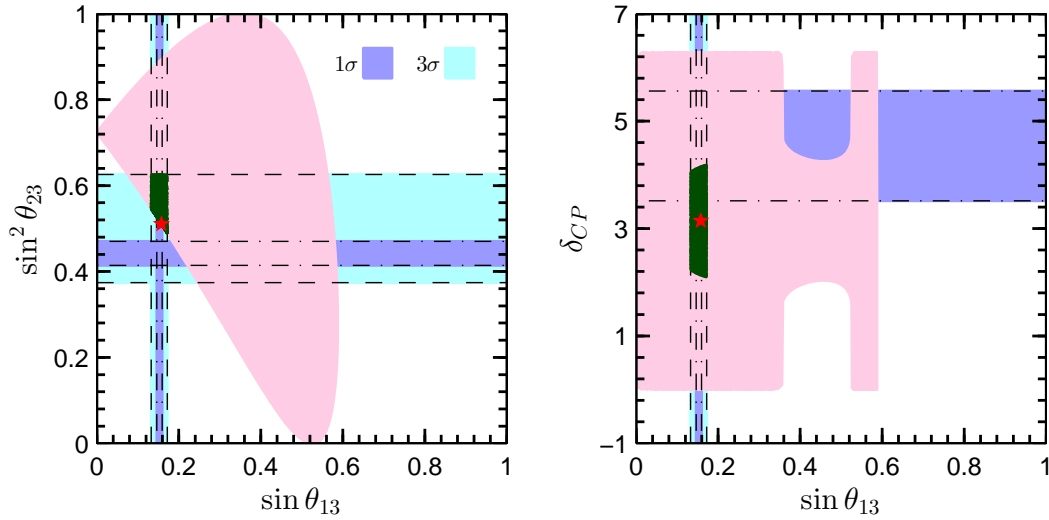


Figure 10: The correlations of $\sin^2 \theta_{23}$ and δ_{CP} with respect to $\sin \theta_{13}$, where the PMNS matrix arises from an exchange of the second and third rows in the pattern in Eq.(B.18). The pink regions denote the possible values of the parameters when both θ and δ freely vary in the whole region of $[0, 2\pi]$. The dark green areas represent the regions allowed by the current experimental data for three neutrino mixing angles at 3σ level [5]. The red pentagrams refer to the best fitting values of case VII with $\theta_{23}(\theta_{bf}) > 45^\circ$ discussed in section 3.4, after the generalized CP is imposed.

as studied in section 3.4. In summary, if a single Z_2 subgroup of the A_5 flavor symmetry is preserved by the neutrino mass matrix, only one column of the PMNS matrix can be determined and agreement with experimental data can be achieved. However, the Majorana phases cannot be predicted by flavor symmetry, and the Dirac phase δ_{CP} is constrained very weakly. On the other hand, if we extend the A_5 family symmetry to include the generalized CP, δ_{CP} is predicted to be trivial or maximal and Majorana phases are trivial.

References

- [1] K. A. Olive *et al.* [Particle Data Group Collaboration], Chin. Phys. C **38**, 090001 (2014).
- [2] F. P. An *et al.* [DAYA-BAY Collaboration], Phys. Rev. Lett. **108**, 171803 (2012) [arXiv:1203.1669 [hep-ex]]; F. P. An *et al.* [Daya Bay Collaboration], Chin. Phys. C **37**, 011001 (2013) [arXiv:1210.6327 [hep-ex]].
- [3] J. K. Ahn *et al.* [RENO Collaboration], Phys. Rev. Lett. **108**, 191802 (2012) [arXiv:1204.0626 [hep-ex]].
- [4] Y. Abe *et al.* [DOUBLE-CHOOZ Collaboration], Phys. Rev. Lett. **108**, 131801 (2012) [arXiv:1112.6353 [hep-ex]]; Y. Abe *et al.* [Double Chooz Collaboration], Phys. Rev. D **86**, 052008 (2012) [arXiv:1207.6632 [hep-ex]].
- [5] F. Capozzi, G. L. Fogli, E. Lisi, A. Marrone, D. Montanino and A. Palazzo, Phys. Rev. D **89**, 093018 (2014) [arXiv:1312.2878 [hep-ph]].
- [6] D. V. Forero, M. Tortola and J. W. F. Valle, Phys. Rev. D **90**, no. 9, 093006 (2014) [arXiv:1405.7540 [hep-ph]].
- [7] M. C. Gonzalez-Garcia, M. Maltoni and T. Schwetz, JHEP **1411**, 052 (2014) [arXiv:1409.5439 [hep-ph]].

- [8] K. Abe *et al.* [T2K Collaboration], Phys. Rev. Lett. **112**, 061802 (2014) [arXiv:1311.4750 [hep-ex]]; K. Abe *et al.* [T2K Collaboration], Phys. Rev. Lett. **112**, 181801 (2014) [arXiv:1403.1532 [hep-ex]].
- [9] C. Adams *et al.* [LBNE Collaboration], arXiv:1307.7335 [hep-ex]; M. Bass *et al.* [LBNE Collaboration], arXiv:1311.0212 [hep-ex].
- [10] S. K. Agarwalla *et al.* [LAGUNA-LBNO Collaboration], JHEP **1405**, 094 (2014) [arXiv:1312.6520 [hep-ph]]; L. Agostino, B. Andrieu, R. Asfandiyarov, D. Autiero, O. Bsida, F. Bay, R. Bayes and A. M. Blebea-Apostu *et al.*, arXiv:1409.4405 [physics.ins-det]; S. K. Agarwalla *et al.* [LAGUNA-LBNO Collaboration], arXiv:1412.0593 [hep-ph]; S. K. Agarwalla *et al.* [LAGUNA-LBNO Collaboration], arXiv:1412.0804 [hep-ph].
- [11] E. Kearns *et al.* [Hyper-Kamiokande Working Group Collaboration], arXiv:1309.0184 [hep-ex].
- [12] C. S. Lam, Phys. Lett. B **656**, 193 (2007) [arXiv:0708.3665 [hep-ph]]; C. S. Lam, Phys. Rev. Lett. **101**, 121602 (2008) [arXiv:0804.2622 [hep-ph]]; C. S. Lam, Phys. Rev. D **78**, 073015 (2008) [arXiv:0809.1185 [hep-ph]].
- [13] G. Altarelli and F. Feruglio, Rev. Mod. Phys. **82**, 2701 (2010) [arXiv:1002.0211 [hep-ph]]; H. Ishimori, T. Kobayashi, H. Ohki, Y. Shimizu, H. Okada and M. Tanimoto, Prog. Theor. Phys. Suppl. **183**, 1 (2010) [arXiv:1003.3552 [hep-th]]; S. F. King and C. Luhn, Rept. Prog. Phys. **76**, 056201 (2013) [arXiv:1301.1340 [hep-ph]]; S. F. King, A. Merle, S. Morisi, Y. Shimizu and M. Tanimoto, New J. Phys. **16**, 045018 (2014) [arXiv:1402.4271 [hep-ph]].
- [14] R. M. Fonseca and W. Grimus, JHEP **1409**, 033 (2014) [arXiv:1405.3678 [hep-ph]].
- [15] P. Chen, C. C. Li and G. J. Ding, Phys. Rev. D **91**, no. 3, 033003 (2015) [arXiv:1412.8352 [hep-ph]].
- [16] L. L. Everett, T. Garon and A. J. Stuart, arXiv:1501.04336 [hep-ph].
- [17] P. F. Harrison and W. G. Scott, Phys. Lett. B **535**, 163 (2002) [hep-ph/0203209]; P. F. Harrison and W. G. Scott, Phys. Lett. B **547**, 219 (2002) [hep-ph/0210197]; W. Grimus and L. Lavoura, Phys. Lett. B **579**, 113 (2004) [hep-ph/0305309]; P. F. Harrison and W. G. Scott, Phys. Lett. B **594**, 324 (2004) [hep-ph/0403278]; Y. Farzan and A. Y. Smirnov, JHEP **0701**, 059 (2007) [hep-ph/0610337]; W. Grimus and L. Lavoura, Fortsch. Phys. **61**, 535 (2013) [arXiv:1207.1678 [hep-ph]].
- [18] G. Ecker, W. Grimus and W. Konetschny, Nucl. Phys. B **191**, 465 (1981); G. Ecker, W. Grimus and H. Neufeld, Nucl. Phys. B **247**, 70 (1984); G. Ecker, W. Grimus and H. Neufeld, J. Phys. A **20**, L807 (1987); H. Neufeld, W. Grimus and G. Ecker, Int. J. Mod. Phys. A **3**, 603 (1988).
- [19] W. Grimus and M. N. Rebelo, Phys. Rept. **281**, 239 (1997) [hep-ph/9506272].
- [20] F. Feruglio, C. Hagedorn and R. Ziegler, JHEP **1307**, 027 (2013) [arXiv:1211.5560 [hep-ph]].
- [21] M. Holthausen, M. Lindner and M. A. Schmidt, JHEP **1304**, 122 (2013) [arXiv:1211.6953 [hep-ph]].

- [22] S. F. King and T. Neder, Phys. Lett. B **736**, 308 (2014) [arXiv:1403.1758 [hep-ph]].
- [23] G. J. Ding, S. F. King and A. J. Stuart, JHEP **1312**, 006 (2013) [arXiv:1307.4212 [hep-ph]].
- [24] G. J. Ding, S. F. King, C. Luhn and A. J. Stuart, JHEP **1305**, 084 (2013) [arXiv:1303.6180 [hep-ph]].
- [25] F. Feruglio, C. Hagedorn and R. Ziegler, Eur. Phys. J. C **74**, 2753 (2014) [arXiv:1303.7178 [hep-ph]].
- [26] C. Luhn, Nucl. Phys. B **875**, 80 (2013) [arXiv:1306.2358 [hep-ph]].
- [27] C. C. Li and G. J. Ding, Nucl. Phys. B **881**, 206 (2014) [arXiv:1312.4401 [hep-ph]].
- [28] C. C. Li and G. J. Ding, arXiv:1408.0785 [hep-ph].
- [29] I. Girardi, A. Meroni, S. T. Petcov and M. Spinrath, JHEP **1402**, 050 (2014) [arXiv:1312.1966 [hep-ph]].
- [30] G. J. Ding and Y. L. Zhou, Chin. Phys. C **39**, 021001 (2015) [arXiv:1312.5222 [hep-ph]]; G. J. Ding and Y. L. Zhou, JHEP **1406**, 023 (2014) [arXiv:1404.0592 [hep-ph]].
- [31] G. J. Ding and S. F. King, Phys. Rev. D **89**, no. 9, 093020 (2014) [arXiv:1403.5846 [hep-ph]].
- [32] C. Hagedorn, A. Meroni and E. Molinaro, Nucl. Phys. B **891**, 499 (2015) [arXiv:1408.7118 [hep-ph]].
- [33] G. J. Ding, S. F. King and T. Neder, JHEP **1412**, 007 (2014) [arXiv:1409.8005 [hep-ph]].
- [34] D. Hernandez and A. Y. Smirnov, Phys. Rev. D **86**, 053014 (2012) [arXiv:1204.0445 [hep-ph]]; D. Hernandez and A. Y. Smirnov, Phys. Rev. D **87**, no. 5, 053005 (2013) [arXiv:1212.2149 [hep-ph]].
- [35] D. L. Johnson, Presentations of Groups, 2nd ed., 1997, Cambridge Univ. Press.
- [36] M. C. Chen, M. Fallbacher, K. T. Mahanthappa, M. Ratz and A. Trautner, Nucl. Phys. B **883**, 267 (2014) [arXiv:1402.0507 [hep-ph]].
- [37] G. C. Branco, I. de Medeiros Varzielas and S. F. King, arXiv:1502.03105 [hep-ph].
- [38] A. Datta, F. S. Ling and P. Ramond, Nucl. Phys. B **671**, 383 (2003) [hep-ph/0306002]; Y. Kajiyama, M. Raidal and A. Strumia, Phys. Rev. D **76**, 117301 (2007) [arXiv:0705.4559 [hep-ph]].
- [39] L. L. Everett and A. J. Stuart, Phys. Rev. D **79**, 085005 (2009) [arXiv:0812.1057 [hep-ph]]; F. Feruglio and A. Paris, JHEP **1103**, 101 (2011) [arXiv:1101.0393 [hep-ph]]; G. J. Ding, L. L. Everett and A. J. Stuart, Nucl. Phys. B **857**, 219 (2012) [arXiv:1110.1688 [hep-ph]]; I. K. Cooper, S. F. King and A. J. Stuart, Nucl. Phys. B **875**, 650 (2013) [arXiv:1212.1066 [hep-ph]]; J. Gehrlein, J. P. Oppermann, D. Schäfer and M. Spinrath, Nucl. Phys. B **890**, 539 (2015) [arXiv:1410.2057 [hep-ph]].
- [40] M. Auger *et al.* [EXO Collaboration], Phys. Rev. Lett. **109**, 032505 (2012) [arXiv:1205.5608 [hep-ex]].

- [41] J. B. Albert *et al.* [EXO-200 Collaboration], Nature **510** (2014) 229-234 [arXiv:1402.6956 [nucl-ex]].
- [42] A. Gando *et al.* [KamLAND-Zen Collaboration], Phys. Rev. Lett. **110** (2013) 062502 [arXiv:1211.3863 [hep-ex]].
- [43] P. A. R. Ade *et al.* [Planck Collaboration], Astron. Astrophys. **571**, A16 (2014) [arXiv:1303.5076 [astro-ph.CO]].
- [44] JUNO experiment, <http://english.ihep.cas.cn/rs/fs/juno0815/>.
- [45] G. Altarelli and F. Feruglio, Nucl. Phys. B **741**, 215 (2006) [hep-ph/0512103].
- [46] L. L. Everett and A. J. Stuart, Phys. Lett. B **698**, 131 (2011) [arXiv:1011.4928 [hep-ph]].
- [47] G. J. Ding, L. L. Everett and A. J. Stuart, Nucl. Phys. B **857**, 219 (2012) [arXiv:1110.1688 [hep-ph]].
- [48] R. d. A. Toorop, F. Feruglio and C. Hagedorn, Phys. Lett. B **703**, 447 (2011) [arXiv:1107.3486 [hep-ph]].
- [49] R. de Adelhart Toorop, F. Feruglio and C. Hagedorn, Nucl. Phys. B **858**, 437 (2012) [arXiv:1112.1340 [hep-ph]].
- [50] N. Cabibbo, Phys. Lett. B **72**, 333 (1978); L. Wolfenstein, Phys. Rev. D **18**, 958 (1978).
- [51] C. S. Lam, Phys. Rev. D **83**, 113002 (2011) [arXiv:1104.0055 [hep-ph]].
- [52] S. F. Ge, D. A. Dicus and W. W. Repko, Phys. Lett. B **702**, 220 (2011) [arXiv:1104.0602 [hep-ph]]; S. F. Ge, D. A. Dicus and W. W. Repko, Phys. Rev. Lett. **108**, 041801 (2012) [arXiv:1108.0964 [hep-ph]].
- [53] B. Wang, J. Tang and X. Q. Li, Phys. Rev. D **88**, 073003 (2013) [arXiv:1303.1592 [hep-ph]].
- [54] I. de Medeiros Varzielas and L. Lavoura, J. Phys. G **41**, 055005 (2014) [arXiv:1312.0215 [hep-ph]].
- [55] S. T. Petcov, Nucl. Phys. B **892**, 400 (2015) [arXiv:1405.6006 [hep-ph]].
- [56] C. Jarlskog, Phys. Rev. Lett. **55**, 1039 (1985).
- [57] C. H. Albright and W. Rodejohann, Eur. Phys. J. C **62**, 599 (2009) [arXiv:0812.0436 [hep-ph]]; C. H. Albright, A. Dueck and W. Rodejohann, Eur. Phys. J. C **70**, 1099 (2010) [arXiv:1004.2798 [hep-ph]]; X. G. He and A. Zee, Phys. Lett. B **645**, 427 (2007) [hep-ph/0607163]; X. G. He and A. Zee, Phys. Rev. D **84**, 053004 (2011) [arXiv:1106.4359 [hep-ph]]; Y. Shimizu and M. Tanimoto, Mod. Phys. Lett. A **30**, 0002 (2015) [arXiv:1405.1521 [hep-ph]].
- [58] S. F. King and C. Luhn, JHEP **1109**, 042 (2011) [arXiv:1107.5332 [hep-ph]].